Capillary-based Microreactor System Integrated with UHPLC/GC for High Throughput Screening of Catalysts for Organic Reactions

by

Hui Fang

Bachelor of Science, Nankai University, 2001

Master of Science, Nankai University, 2004

Master of Science, University of Pittsburgh, 2008

Submitted to the Graduate Faculty of

Arts and Sciences in partial fulfillment

of the requirements for the degree of

Doctor of Philosophy

University of Pittsburgh

2009

UNIVERSITY OF PITTSBURGH

THE SCHOOL OF ARTS AND SCIENCES

This dissertation was presented

by

Hui Fang

It was defended on

May 13th, 2009

and approved by

Billy W. Day, Professor, Department of Pharmaceutical Sciences

Paul E. Floreancig, Associate Professor, Departmental Chemistry

Scott G. Nelson, Associate Professor, Department of Chemistry

Dissertation Advisor: Stephen G. Weber, Professor, Department of Chemistry

Capillary-based Microreactor System Integrated with UHPLC/GC for High Throughput Screening of Catalysts for Organic Reactions

Hui Fang, Ph.D.

University of Pittsburgh, 2009

Catalyst discovery through high throughput screening can greatly take advantage of automated microreactor technology. Quantitative analysis of reaction outcomes is necessary for evaluating catalyst activities and GC and/or LC are common tools. Few microfluidic systems, however, have the capability of automatically screening catalysts in slow reactions with in situ chromatography analysis. Thus, a novel microreactor was developed that integrated sample loading, reaction and online analysis functions in a totally automated format. An autosampler and syringe pump load homogeneous catalysts and reagents. The chemicals are mixed and reacted in a long capillary followed by online analysis, either by GC or UHPLC. The approach of parallel reactions in a flow stream is good for either slow reactions or fast reactions depending on the operation mode. Some palladium and ligand complex catalysts for the Stille reaction were chosen and screened by a stop-flow approach with GC analysis for validation. The screening results were in good accordance with the literature.

The first application of this microreactor was to discover peptidic catalysts for the direct aldol reaction. A major difficulty was the poor solubility of peptidic catalysts. This was solved by allowing catalysts to react with one of the aldol substrates to form soluble catalyst adduct, which was then loaded into the microreactor to complete the reaction. This two-step approach was used to screen a diverse set of amino acids and short peptidic catalysts, in which two groups of peptides containing γ-Glu and β-Asp residues showed higher activities than other catalysts.

The second application was to screen Brønsted or Lewis acid catalysts for an internal cyclization reaction. This reaction can be used to prepare large libraries of amide compounds for drug discovery. A continuous flow approach with online UHPLC analysis was applied to study this relatively fast reaction. The experimental throughput can reach 9 reactions/h. Results showed that strong acids are generally good for conversion and yield. Lanthanide triflate compounds, although having weak acidity, had better conversion and selectivity than other acids. Side reaction analysis by GC-MS and LC-MS indicated that strong and weak Brønsted acids can lead to the formation of different major byproducts.

TABLE OF CONTENTS

LIST OF TABLES

LIST OF FIGURES

LIST OF SCHEMES

LIST OF ABBREVIATIONS

GC	Gas chromatography
UHPLC	Ultra-high pressure liquid chromatography
HRMS	High resolution mass spectrum
IR	Infrared spectroscopy
CE	Capillary electrophoresis
THF	Tetrahydrofuran
DMSO	Dimethyl sulfoxide
DMF	Dimethylformamide
AN	Acetonitrile
MeOH	Methanol
IS	Internal standard

PREFACE (ACKNOWLEDGEMENT)

“Genius only means hard-working all one's life.”- Dmitri Mendeleev

First of all, I would like to express my deep gratitude to my supervisor, Prof. Stephen G Weber. I really enjoyed working with him in the past five years. He is not only a distinguished scientist but also an excellent teacher. His broad knowledge and deep insight often inspired my research a lot. I am truly honored to pursue my Ph.D. degree under the guidance of Prof. Weber.

Second, I want to thank all of our project collaborators including Prof. Scott Nelson, Prof. Paul Floreancig, Prof. Peter Wipf, Prof. Stephane Petoud and Prof. Nathaniel Rosi. I gained a great deal of knowledge and expertise in multiple fields of chemistry from them, which contributed to my research accomplishments very much. Besides, I am also grateful to Prof. Billy Day who mentored my proposal and served on my dissertation committee. Prof. Kay Brummond and Prof. Shiregu Amemiya are also greatly appreciated for their guidance on my comprehensive exam.

Third, I want to thank all of my lab colleagues for their generous help on my research. The Weber group is just like a big family to me. I have been thriving in this family to become an independent and creative researcher.

Finally, I would like to genuinely thank my wife Manyan Wang, who is also my lab colleague, and my parents for their long-lasting selfless support of my education and research. I could not achieve the success without their love.

1.0 INTRODUCTION

Microfluidics is a new science and technology field that generally processes very small amounts of liquids, gases or fluidized solids/particles within micron-dimensioned channels either on chips or in tubes. It originated from some popular capillary microanalytical methods such as capillary GC/HPLC and capillary CE in the 1980s. The channel dimension usually ranges from several micrometers to some hundreds of micrometers and sample volumes range from a few nanoliters to several microliters. The fundamental advantages of miniaturization for biology and chemistry enabled microfluidics to undergo tremendous growth in the last two decades, in which 'lab-on-a-chip' and 'microreactor', two closely related microfluidic technologies, have shown great potential in bioanalytical chemistry and synthetic chemistry, with great promise to revolutionize the traditional macroscale approaches that have been performed for decades.

1.1 LAB-ON-A-CHIP

1.1.1 Introduction

Lab-on-a-chip is one of the most popular microfluidic technologies. It has been widely used in a variety of fields such as biology, chemistry and medicine with major contributions to biological analyses and cell-based assays. The name of 'lab-on-a-chip' derives from its basic format and

function, which is the use of miniaturized devices to perform chemical or biological processes in a highly automated and integrated manner. The merits of lab-on-a-chip include high-throughput analysis capability, minimal sample usage, high integration of functionalities, automated processing and excellent portability.

Micro Total Analysis Systems (μTAS) are often referred to as lab-on-a-chip. However, they are not exactly the same concept. Generally, μTAS refers to specific systems that are able to carry out whole stage of analyses such as sampling, sample pretreatment, mixing, transport, reaction, separation, detection and data processing in a fully integrated fashion, whereas lab-on-a-chip is a broader term that can apply to any kind of technology that miniaturizes chemical or biological processes on microfluidic devices. Some systems such as sensors or arrays, which are often termed as biochips, are also categorized as lab-on-a-chip technology.

1.1.2 Chip fabrication

Most lab-on-a-chip or microreactor applications are carried out on chips. Currently, there is a great variety of microfabrication techniques suitable for fabricating diverse types of microfluidic chips on materials like glass, silicon, quartz, metal, biomaterials and polymeric materials. Glass is well known for its chemical compatibility and mechanical strength, and so it is predominantly used to make chips that have to perform chemical or biochemical processes involved with significant amounts of organic solvents, or under harsh conditions such as high temperature, high pressure, corrosive solvents, and so on. Microreactors, commonly used for synthetic chemistry, are usually fabricated on glass chips. The general method for glass fabrication is photolithography combined with chemical etching. Various channel patterns on can be

constructed. Some newly developed methods do not need special expertise or expensive clean facilities to fabricated complicated small-dimension channels on glass chips.

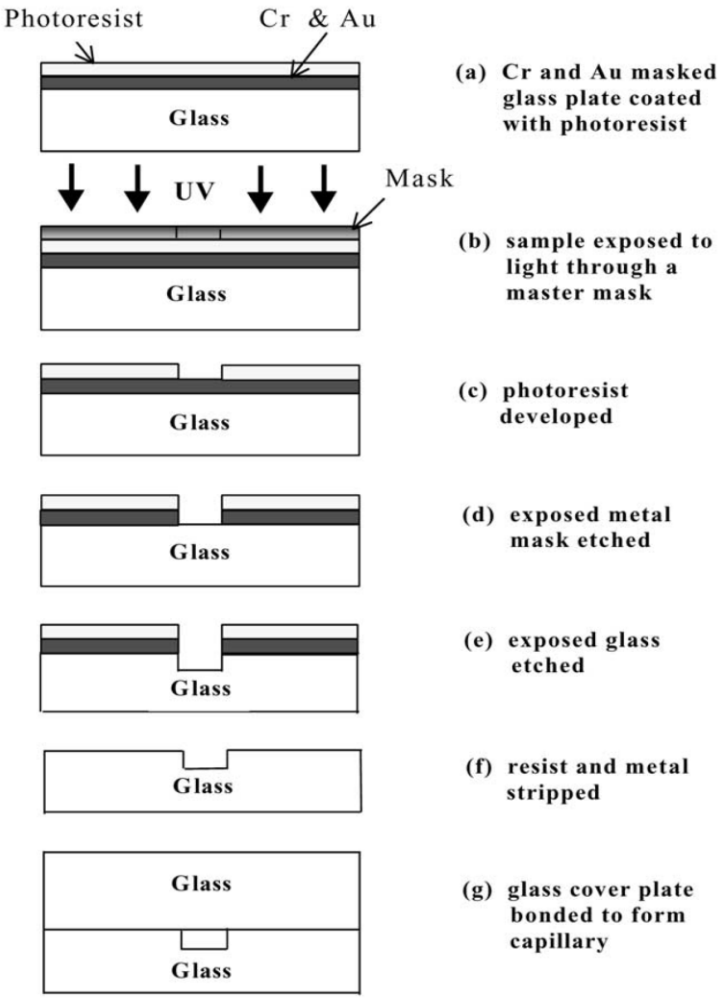

Figure 1. Typical procedures of photolithography and wet etching fabrication of channels on a glass chip.

(Photograph is reproduced with permission from Elsevier.[1])

The typical fabrication process of a glass chip is schematically shown in Figure 1[1]. The commercially-sold photolithographic glass plates (ca. 3 mm thickness) generally have two precoated layers, a positive photoresist (0.5-2.0 μm) layer above a thin metal etch mask

(normally chromium). The design of channel network is produced and printed with the aid of some computer softwares like Corel Draw or CAD programs. The printed drawing produces the optical mask that is placed on the photoresist layer. The negative mask (clear lines with a black background) is typically used in glass fabrication. The pattern of the channels on chip follows the optical mask. Through UV exposure, the photoresist develops at the place of clear lines. After evaporating the solvents, chemical etching is performed on the patterned glass plates using a mixture of aqueous 1% HF and 5% NH_4F with ultrasound agitation. Once the plate is etched for the required time, post-etch cleaning is then carried out to remove the remaining photoresist and metal. The base plate containing the channel network is sealed by thermally bonding to an upper glass plate containing pre-drilled holes. These holes act as reservoirs or connectors to outer pumps or capillaries.

A drawback of this method is the time-consuming process. Therefore researchers developed another more efficient method called soft lithography to fabricate chips. This method usually works on polymeric materials like polydimethylsiloxane (PDMS). PDMS chips are mostly used for biological applications such as biomolecule analysis or cell assays[2-4], due to its excellent gas permeability, good biocompatibility and no toxicity. By using soft lithography, complex microstructures on PDMS chips like 3-D or multi-layer patterns can be made in a rather efficient and cost-effective way. PDMS is not compatible with organic solvents, however, limiting its uses for microreactor construction for synthetic chemistry applications.

1.1.3 Fluid control of microfluidics

Electrokinetic or hydrodynamic pumping is generally used to motivate liquid flow in microchannels. Electroosmotic flow (EOF) offers a very convenient pumping mechanism for

fluid manipulation, particularly for aqueous solutions, with minimal hydrodynamic dispersion.[2-6] Electrodes are placed in the appropriate reserviors to which specific voltage sequences can be delivered under automated computer control. No external pumps or moving parts are needed, allowing EOF to work well on complicated channel structures.

Pressure-driven flow (PD), on the other hand, takes advantage of conventional micro-scale pumps to maneuver solutions around the channel network.[7-11] Those pumps like HPLC or syringe pumps are usually commercially-sold and easily connected to chip ports. In addition, there are several important theoretical advantages of PD over EOF pumping: (i) the control of flow velocity is more accurate by PD than EOF because PD is independent of factors such as pH, electrolyte concentration, channel material, surface adsorption, and composition of sample matrix. (ii) PD has a better solvent compatibility. EOF has to pump solvents with certain polarity, which limits its use in pumping non-polar organic liquids. (iii) When electrochemical detection method is preferred, there would be little interference for PD because the electric field generating EOF can interfere with the electrical field for detection. (iv) PD has a broader choice of chip materials too. It is necessary that the channel constructing materials should have a very low electrical conductivity to insulate the electric field, then, some common materials like silicon have to be excluded by EOF method.[12]

1.1.4 Applications of lab-on-a-chip/μTAS

Lab-on-a-chip or μTAS systems are primarily developed for biochemical analyses, clinical diagnostics and cell biology studies, in which one of the focuses is the high efficient analysis of nucleic acids or proteins in support of biological and pharmaceutical researches.

DNA or RNA sequence analysis involves polymerase chain reaction processes (PCR) which can be incorporated onto glass or PDMS chips by microfabrication. To have a complete analysis, a single chip usually integrates multiple functionalities such as sample loading and mixing, PCR heating and temperature control, electrophoresis separation, fluorescence detection and collection of eluted samples. The process is highly automated and efficient. Typical sample volume is several to hundreds of nanoliters and the processing time is less than a few minutes.[13, 14] Recently, high-throughput μTAS systems that can carry out parallel analysis have aroused a lot of attention.[15-17] A typical example is the chip platform developed by Ottensen[17] who used microfluidic digital PCR to amplify and analyze multiple, different genes obtained from single bacterial cells. This device contained 12 sample panels and each panel can be partitioned into 1176 chambers. The system was very efficient for simultaneous multigene analysis.

In addition to nucleic acids, lab-on-a-chip technologies have also been widely used for analyses of proteins or other biomolecules, a common approach for understanding the cell mechanisms.[18-20] Two-dimensional electrophoretic separation of protein mixtures or sequence analysis of amino acids can be dramatically accelerated by miniaturization technology.[21, 22] Huang developed an automated single-cell analysis chip by complicated integration.[23] The system consisted of serial sections including single cell manipulation, cell lysis, generic labeling of proteins, CE separation of proteins and single-molecule counting by high efficiency fluorescence method.

Crystallization is an important technique for protein characterization. High-throughput lab-on-a-chip systems can significantly reduce the time and effort for screening protein crystallization conditions.[24] Zhou used degassed PDMS microchannels to dispense nanoliters of liquids into a 3 × 52 array of microwells (156 wells) for studies of four protein crystallizing

conditions.[25] This dispensing system can also work on commerically-available microplates like 96-well or 384-well formats, allowing the general laboratory to use it for diverse applications.

Lab-on-a-chip devices have also been used for cell cultivation and research. A novel micro-bioreactor developed by Figallo showed the high potential of using microfluidic devices for parallel cultivation of a large amount of cells.[26] The bioreactor integrated the microchannels with small-dimensioned cell culture wells on a PDMS chip, overcoming the difficulty of putting large-sized cells directly into the microchannels. An array of wells was constructed to cultivate diverse cells in a high-throughput and independent manner. Nutrients and media were supplied in a continuous flow from the microchannels. The cultivation of human embryonic stem cells (hESCs), which is often challenging in traditional methods, seemed to be easier. It demonstrated the benefits of microfluidic approach for cell growth and studies.

1.2 MICROREACTORS

While most of 'lab-on-a-chip' applications have been directed toward chemical or biological analyses, another microfluidic technology called 'microreactor' or 'micro reaction technology' has been exclusively studied for synthetic chemistry.[27, 28] In a similar constructing format and fluid control mechanism to μTAS, microreactors are often built on glass chips containing a series of interconnecting micro-dimensioned channels in which organic reactions are usually carried out in a flow stream. Microreactors are often flow devices manipulated by electroosmotic flow or pressure-driven flow. Although microreactors are still at the early development stage, this new technology has shown great impact on synthetic chemistry and related fields like combinatorial chemistry and pharmaceutical chemistry. A broad range of applications have been studied so far,

in both academia and industry.[29-37] The research of microreactors is still growing at a tremendous speed.

1.2.1 Merits of microreactors

The reason that microreactors acquire so much attention is due to their fundamental advantages over traditional macroscale batch reactors such as round-bottom flasks or tubes. The advantages exhibit in many aspects, e.g., mixing, heat transfer, safety, cost, environmental effect, and scalability, and so on.

1.2.1.1 Mixing

Microfluidic transport is basically different from macroscale transport. The Reynolds number (*Re*) can be used to evaluate the degree of flow turbulence in tubes. It is generally defined by Eq. (1). The channel dimension contributes significantly to the magnitude of *Re*.

$$Re = \frac{\rho V D}{\mu} \qquad (1)$$

ρ: $fluid\ density$; V: $fluid\ velocity$; D: $tube\ diameter$; μ: $fluid\ viscosity$.

In large reactors like round-bottom flasks and test tubes, due to the large dimension, Reynolds number is typically high and turbulence is usually dominant. In microchannels, however, turbulence is almost unattainable and laminar flow is dominant with a characteristic of mass transfer primarily controlled by molecular diffusion.[38]

In batch reactors, mixing process generally involves two steps: first, turbulence generated by mechanical stirring creates a highly-dispersed heterogeneous mixture; second, molecules

located in adjacent regions diffuse to form a homogeneous solution. Thus mechanical stirring is indispensable for creation of strong turbulence to rapidly bring reagent or catalyst molecules close enough to allow efficient mixing by diffusion. The time-scale of turbulent mixing is much longer than that of diffusion. If batch reactors are downsized to the dimension near micrometers, mixing can be well done by only diffusion, a very rapid process that reaction rates are probably only limited by inherent reaction kinetics rather than the time for homogenizing reagents.[31] Therefore, many reactions carried out in microreactors often produce good yield within seconds/minutes in contrast to hours/days taken by batch reactions. Greenway[39] studied the synthesis of 4-cyanobiphenyl at room temperature in a flow microreactor, achieving a yield of 67.7% within 25 seconds, whereas under other identical conditions, bench-top synthesis can only give 10% yield in 8 hours. Besides reaction rates, better mixing can also contribute to higher product yield by minimizing the extent of side reactions due to the inhomogeneity of reaction solutions.

1.2.1.2 Heat transfer efficiency

Microreactors are also good at heat transfer. Temperature is an important factor for organic reactions. Due to the large surface-to-volume ratio of microchannels, heat transfer efficiency in microreactors may be higher several orders of magnitude than that of conventional vessels or heat exchangers.[40] Efficient heat transfer can result in fast and accurate heating and cooling of reactions, allowing researchers to exert precise control on process temperature. This can largely minimize some side reactions due to uneven temperature distribution. Moreover, to extremely exothermic processes, rapid heat dissipation and close temperature control can maximumly lower the chance of explosion or side reaction occurrence.

1.2.1.3 Safety

Safety is a major concern in synthetic chemistry. Compared to larger reaction vessels, microreactors are much safer for organic reactions involved with toxic, hazardous or radioactive chemicals due to their small chemical usage and totally enclosed reaction environment. The high efficiency of heat transfer makes microreactors very suitable for investigating extremely exothermic reactions. For example, Fortt[41] used a continuous-flow microreactor to generate diazonium reactive intermediates, a notorious industrial process as diazonium salts are sensitive to the environment and rapidly uncontrollable explosion can happen as induced by heat, light, shock, static electricity, and dehydration. The industry usually applies stringent safety procedures; however, the authors demonstrated this reaction runs very efficiently and safely in the microreactor. Yield was also increased a lot compared to traditional approaches.

1.2.1.4 Automated process control

Thanks to microfabrication techniques, microreactors can be integrated with a variety of on-chip or off-chip components like pumps, valves, heaters or detectors. The whole reaction process in microreactors can be automatically controlled by computer programs or instruments in a similar way to μTAS, allowing very efficient and precise control of chemical processing. Besides, by employing flow-through concept, microreactors are capable of integrating synthesis and analysis by coupling versatile detection systems like UV-Vis, fluorescence, GC-MS and LC-MS to the reaction channel for online analysis of synthetic outcomes. This can greatly improve the processing efficiency which would be very beneficial for high-throughput screening or process optimization.

1.2.1.5 Scaling-up and numbering-up

Since most microreactors are flow devices using continuous flow processes, many researchers state that reaction conditions studied in microreactors can be directly transferred to large flow reactors in the production site with no need to reoptimize those conditions.[42] The usual scaling-up process is very time-consuming and costly. Some researchers state that 50% of industrially interested reactions can benefit from continuous flow processes and 44% of these reactions can take advantage of this benefit of microreactors.[33] The major limitation is that microreactors are not suitable for reactions involved with solids which indeed occupy a large portion of organic transformations processed by industry.

In addition to scaling-up, it is also reasonable to argue that when microreactors are parallelized, a large number of microreactors can directly transform laboratory scale into production scale. Numbering-up of synthetic processes has been applied in industry. Cytos® Lab System, a microreactor with a channel width of less than 100 μm, can be parallelized to form Cytos® Pilot System that includes 10 reactors with a cumulative product mass flow of 0.6 kg/h, comparable to the conventional pilot production vessels.[43]

1.2.2 Construction of microreactors

A majority of microreactors are built on chips. Glass is the most popular material due to its chemical inertness and mechanical strength, but other materials such as silicon, metals and polymers are also widely used for specific reaction demands. Figure 2 shows some typical microreactors built on chips.[44]

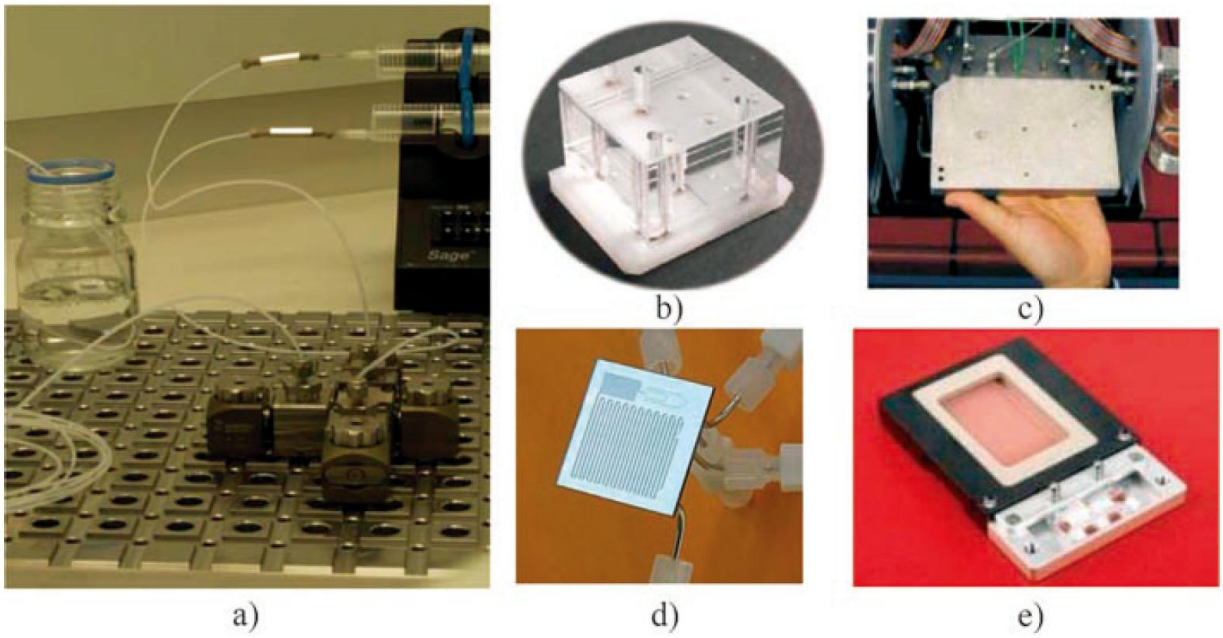

Figure 2. Images of various types of microreactors.

a. Stainless steel microreactor system with pressure-driven flow; b. Glass microreactor with EOF pumping; c. Stainless steel microreactor of the CYTOS Lab system; d. Silicon-based microreactor; e. Glass microreactor of the AFRICA System.

(Photograph is reproduced with permission from Wiley InterScience.[44])

The complicated fabrication process and expensive fabrication facilities limits the use of chip-based microreactors in ordinary synthetic laboratories. Consequently, some researchers have developed capillary-based microreactors by connecting a series of commercially available, micrometer-sized capillaries to form the fluid microchannels, while integrating other components such as mixers, heaters, and detectors just like lab-on-a-chip approach. The commercially-sold capillaries generally include metal tubing (nickel and stainless steel tubing), fused-silica tubing, Teflon tubing and PEEK tubing, among which fused-silica capillary has a great variety of dimensions, good chemical stability, high temperature and pressure tolerance, high maneuver

flexibility and low cost, making it very appropriate to construct microreactors. Actually, fused-silica capillaries have long been used in CE and capillary LC, and they work similarly to microchannels on chips in terms of high fluid conservation, isolation from the atmosphere, inert capillary surface, and ease of transport of species by using EOF or pressure induced flow. Thus, microreactors built from fused-silica capillaries are important alternatives to chips.

Comer and Organ[45] have developed a single-capillary-based flow reactor coupled with microwave irradiation (MW). Microwave has become a very popular heating method for synthetic chemistry. However, no one has tried to use microwave to heat reactions on chips because it is difficult to interface small chips with large microwave generators and heating efficiency is usually low due to the large thickness of chip plates. The capillary wall is much thinner and heating efficiency is very high. A variety of organic reactions have been done in capillary-based reactors by the authors. The more recent work by Comer and Organ[46] also demonstrated the feasibility to develop a multiple capillary reactor for parallel synthesis.

1.2.3 Synthetic applications of microreactors

Due to the significant advantages of microreactors, the applications of microreactors for synthetic chemistry are wide, covering most types of reaction types. Liquid-, gas- and even some solid-phased reactions have been successfully performed in microreactors. Not only small organic molecules, but polymers and nanomaterials can be synthesized under various microfluidic approaches.

1.2.3.1 Stoichiometric reactions

Up to now, microreactors have been tested to carry out a large number of stoichiometric transformations, including: 1) Carbon-carbon formation reactions, e.g., aldol reactions[47], Michael additions[48], Wittig reactions[49], cyclization reactions[50], enolate[51] or enamine[52] formation reactions, Ugi four component coupling[53] and other multicomponent reactions[54]. 2) Heterocyclization reactions, e.g., generation of pyrazoles[55], thiazoles[56], imidazoles[57] and pyridones[58]. 3) Oxidation and reduction reactions, e.g., sodium borohydride reductions[58], Swern oxidations[59]. 4) Fluorination[60] and nitration reactions[61, 62]. 5) Carbon-nitrogen and Carbon-oxygen formation reactions, e.g., esterification reactions[63], peptide synthesis[64-67]. 6) Phase transfer reactions, e.g., diazo coupling reactions[68].

Chambers and Spink[60] first reported the use of a nickel microreactor for direct fluorination and perfluorination of organic compounds by elemental fluorine. In bulk scale, it is always troublesome to handle corrosive gaseous fluorine and control reaction conditions exactly due to the extreme exothermic nature of fluorination. Microreactors are advantageous for this dangerous process due to its sealed compartment, small volume and close control, enabling high efficiency with great safety.

Wiles[47] used a borosilicate glass microreactor to carry out an aldol reaction of silyl enol ethers of acetophenone and cyclohexanone with 4-bromobenzaldehyde. The conversion of silyl enol ethers to β-hydroxyketones was completely done in 20 min in the microreactor, while it required 24 h for a typical batch reactor to achieve the similar conversion. Reaction rate and yield were significantly increased by using the microreactor.

Watts[69] demonstrated microreactors can not only improve reaction conversion but also the diastereoselectivity due to better mixing and heat exchange in micron-dimensioned channels.

They studied the alkylation of enolates in a flow glass microreactor at -100 ^{o}C with a yield of 41% and a diastereometric ratio of 47:3. In a batch reaction under the same temperature, the best yield was 31% and the diastereometric ratio of 15:3. The authors estimated that higher yield and selectivity are possible in the microreactor through reaction optimization.

Peptide synthesis is a well-known multi-step process involving a series of protection and deprotection procedures along with the addition of amino acids. Solid-phase synthesis based on polymer supports is traditionally used for peptide construction. This method needs expensive polymer supports, however, requires tedious procedures to couple and decouple protecting groups repeatedly, which is particularly time-consuming and costly for preparing long peptides.[70, 71] Watts and coworkers[66] demonstrated the efficacy to assemble β-peptides in solution-phase reactions in a continuous-flow glass microreactor using electroosmotic pumping. Through microfabrication, a network of reagent reservoirs and channels can be produced on chip and multi-step syntheses of dipeptides or tripeptides proved that microfluidic approach can achieve higher atom efficiency than solid-phase synthesis. It was also possible to remove protecting agents from peptides downstream in microchannels.

1.2.3.2 Catalytic reactions

A large number of organic transformations are involved with catalysts, either metal-based catalysts or organocatalysts derived from amino acids, peptides or enzymes. Some catalysts are soluble in reaction solvents to perform homogeneous catalysis while a lot of catalysts that have poor solubility in certain solvents have to catalyze the reaction heterogeneously. Many catalytic reactions have been performed in microreactors including both homogeneous and heterogeneous processes.[72-82]

Homogeneous catalysis

Catalysts that are soluble in reaction solutions can be easily loaded into microchannels and reactions proceed just like ordinary stoichiometric reactions. For example, Mikami[83] investigated a Baeyer–Villiger oxidation reactions catalyzed by fluorous lanthanide catalysts in a nanoflow reactor system. The Baeyer–Villiger reaction was complete in a few seconds with excellent yield and regioselectivity.

Heterogeneous catalysis

Microreactors are incompatible with chemical processes containing insoluble solids or particulates because they can easily clog microchannels and hinder the flow stream. Therefore, most microreactors that work on heterogeneous catalysis either immobilize insoluble catalysts onto the channel surface or embed solid-supported catalysts into microchannels like packed-bed reactors. Microreactors are particularly advantageous for surface-based catalysis of gas-liquid, gas-solid or liquid-solid reactions due to their large surface-to-volume ratio, which can greatly enhance contacting between catalysts and reagents. As for packed-bed catalysis, since the common solid supports are polymers such as Merrifield resins, there is always a danger for microchannels being clogged by swelling resins in organic solvents.[84] Non-swelling supports like silica or alumina have been used as catalyst carriers;[80] however, their applications are limited to wide reactor channels (usually larger than millimeters) because of high backpressure produced in narrow reaction channels just like typical packed column for liquid chromatography.

Haswell[10] immobilized nickel catalysts onto Merrifield resins and loaded beads into polypropylene tubing (2 mm i.d.) and/or glass tubing (1 mm i.d.) to catalyze a Kumada-Corriu reaction by a pressure-driven flow. Compared to bench-top reactions, reaction rates in the

microreactor can be dramatically increased to over three orders of magnitude. The usual 24 h batch reaction can be done in a few minutes by the flow microreactor.

Organ and coworkers[82] studied Suzuki–Miyama and Heck reactions in a borosilicate capillary reactor (1.1 mm i.d.) coated with Pd film on its inner surface as catalyst. Reactions were carried out in a pressure-driven flow at high temperature under microwave irradiation. The authors characterized Pd films (approximately 6 μm in thickness) by SEM, which consist of clusters of highly porous nanometer grains. The films have excellent mechanical strength to withstand constant fast flow and high temperature. Reactions with a variety of substrates can range from a few minutes to several days.

Enzyme bioreactor can also take advantage of surface immobilization techniques.[5, 85, 86] Enzyme biocatalysts can be immobilized onto the inner wall of microchannels to perform heterogeneous catalysis in a flow stream. Ho[87] developed a long-lived capillary-based enzyme microreactor coated with glucose oxidase on its inner surface, which can determine glucose concentration with higher sensitivity and better stability than regular packed columns.

1.2.3.3 Precipitate-forming reactions

Immobilization techniques can circumvent the clogging problem of heterogeneous catalysis in microreactors; however, for some reactions that are prone to form precipitating products or byproducts, immobilization techniques might not work well. McQuade[88] developed a two-phase droplet flow approach to handle insoluble solid particles in precipitate-forming reactions. The synthesis of indigo, which can form small solid particles during the reaction, was successfully carried out in a monodisperse droplet flow in mineral oil without causing channel blockage at all. Mineral oil was very effective to stop particles from sticking to the channel wall. However, this approach, while clever and effective, is not really microfluidic in nature since it requires large

reactor tubing (1.68 mm i.d.) and high flow rate (0.3 mL/min) to prevent particle sticking and clogging in microchannels. Basically, reactor channels less than hundreds of micrometers may be hard to take advantage of this approach due to high channel backpressure when using viscous liquids like mineral oil.

1.2.3.4 Photochemistry and microwave-assistant reactions

Photochemistry is a powerful technique for organic synthesis. However, batch reactions are often limited by the size and power of lamps. Flow reactors are more suitable for photochemical reactions due to its scalability to large-scale production. Microreactors are an excellent tool to carry out photochemical synthesis because their small dimensions and fast mass transfer rates. Small lamp is good enough to produce good conversion. So far, a number of photochemical reactions have been studied in microreactors, including oxygen oxidations,[89] pinacol formation reactions,[90] photocyanation reactions,[91] cyclization reactions.[92] An example chip-based photochemical reactor is shown in Figure 3.[90] The chip was made by bonding quartz wafers to patterned silicon wafers at low temperature. Under the fiber optic UV illumination, the pinacolation process of benzophenone was highly efficient.

Just like photochemistry, microwave irradiation is also very suitable for flow reactors. Capillaries or tubes are often used to carry out microwave-assisted continuous-flow organic synthesis (MACOS).[82, 93, 94] Reaction rate and conversion can be significantly enhanced by microfluidic approach. Moreover, heated by a single microwave source, it is likely to carry out sequential reactions in a single capillary or parallel reactions in multiple capillaries simultaneously.[45, 46] Both ways are very efficient towards the synthesis of a large collection of compounds.

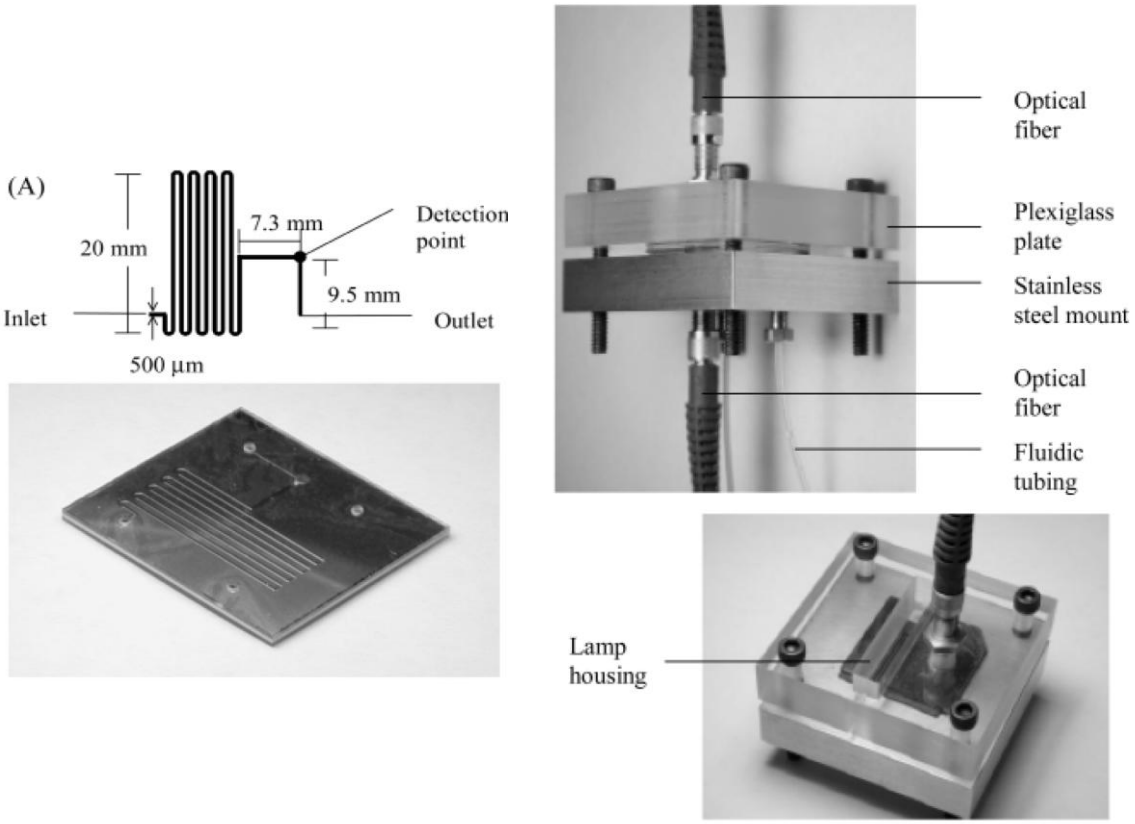

Figure 3. Photographs of an integrated chip reactor (silicon-quartz) interfaced with chuck, tubing and UV fiber optics.

(Photograph is reproduced with permission from RSC Publishing.[90])

1.2.3.5 Electrochemical reactions and flash chemistry

Electrosynthesis is a fast and powerful method to make complex compounds from simple molecules. Very reactive anion, cation or free radical intermediates are generated electro-chemically and reactions are usually complete in a very short time ranging from milliseconds to seconds. This process is similar to a concept called flash chemistry, which was recently defined by Yashida[95] as "a field of chemical synthesis where extremely fast reactions are conducted in a highly controlled manner to produce desired compounds with high selectivity". Due to the nature of flash chemistry, batch reactors are not appropriate because they cannot provide precise

monitoring of reaction conditions that play a key role in the reactivity and selectivity of reactive species. Microreactors are highly desirable for investigating fast electrochemical reactions or flash chemical processes.[96-101] Efficient mixing, fast heat dissipation and accurate condition control all contribute to the ease of controlling highly reactive, short-lived intermediates.

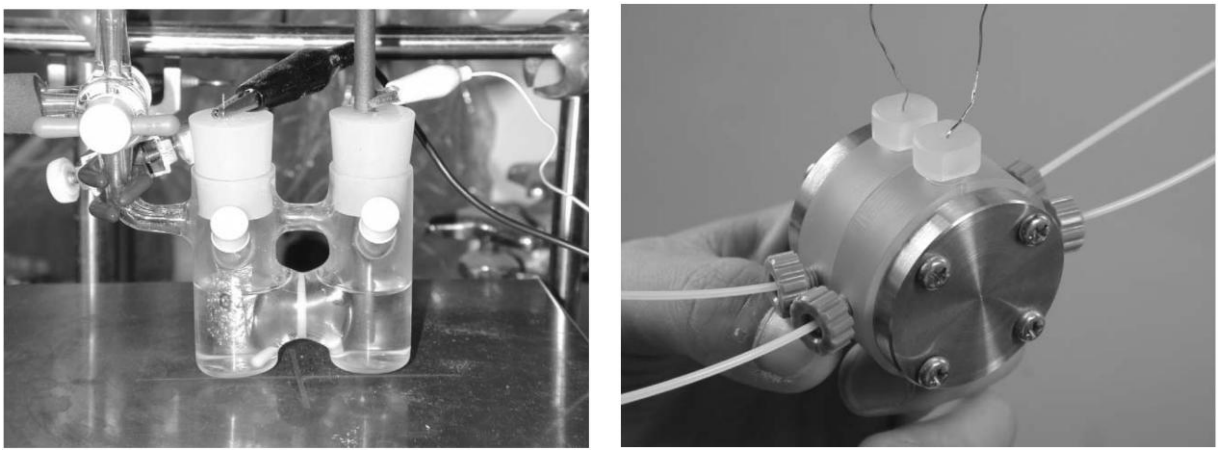

Figure 4. Photographs of a H-type cell (L) and a microflow reactor (R) for electrosynthesis and flash chemistry.

(Photographs are reproduced with permission from RSC Publishing.[105])

Yoshida's group is very active in the field of electrochemical synthesis and flash chemistry using microfluidics.[102, 103] They first developed the "cation pool" method using an H-type electrochemical cell (as shown in Figure 4, left image) to electrolyze the substrate at low temperature to prevent side reactions. The generated cations in the cation chamber can then react with the subsequently-added nucleophiles to complete the reaction in a batch mode. His group used this method to perform [4+2] cycloaddition reactions, in which a *N*-acyliminium ion pool generated by low temperature electrolysis is able to react with different dienophiles, e.g., alkenes or alkynes, to produce high yield of products. In addition to the cell-type reactor, his group also developed a flow electrochemical system (Figure 4, right image) that can generate a continuous-

flow stream of cations by low temperature electrolysis. This “cation flow” method is more like a typical microfluidic approach, allowing scaling-up to the production scale. Both above systems are useful for fast synthesis of either small molecules or large polymers.

1.2.3.6 Macromolecular synthesis

Many polymerization processes are highly exothermic and very fast. Therefore, in principle, polymer synthesis could benefit from microfluidic technology. Efficient reagent mixing can promote homogenization and fast heat transfer can reduce temperature distribution. Moreover, close control of conditions like time, temperature, concentration is good for monitoring polymerization extent. However, applications of microfluidic technology are still very limited so far. The major issue is that a lot of polymerization reactions are involved with solid or highly viscous substances that might induce very high backpressure in microchannels or completely disrupt the flow. Thus, reaction conditions for polymer synthesis have to be screened with great care. Currently, a number of polymerization reactions have been successfully studied, most of which are fast reactions.[104-110] For example, Wilms[108] studied synthesis of hyperbranched polyglycerols by a continuous flow microreactor. Results showed that not only reaction time can be largely shortened, but molecular weight dispersion of different fractions of polyglycerols can all be significantly narrowed, particularly for some high molecular weight fractions that usually have much broader distribution in bench-top synthesis.

1.2.3.7 Nanomaterial synthesis

In a similar manner to polymer synthesis, synthesis of nanomaterials, such as nanoparticles or nanocrystals, often involves the accumulation of a large amount of building atoms or molecules within a short time period. Batch reactors may suffer from solution inhomogeneity and

temperature variation in reaction vessels, leading to huge variation of sizes and shapes of nanomaterials. Microreactors, on the contrary, provide powerful mixing and heating that can lead to better yield and more uniform particle size and shape. The early work by Wagner and Kohler[111], who investigated the process of continuous direct synthesis of gold nanoparticles in a microreactor, demonstrated that the microreactor was able to give more uniformed-shape nanoparticles than batch method. Currently, many researchers are focusing on combining microfluidic technology with nanotechnology to advance their applications.[111-114] Some typical synthesis modes include continuous-flow synthesis,[115-118] segmented-flow synthesis where reactions take place in large liquid slugs,[119-121] and nanoscale droplet-flow synthesis where precursors and solvents are encapsulated in small droplets.[122-124] Those methods are applicable for various types of nanomaterial synthesis in microreactors.

1.3 MICROREACTORS FOR HIGH-THROUGHPUT CATALYST DISOCVERY

1.3.1 Traditional approach for catalyst discovery

Many organic transformations need catalysts. Synthetic chemists have long been endeavoring to discover new catalysts that possess high catalytic efficiency and selectivity, low cost, and green to the environment. The best natural catalysts, enzymes, capable of catalyzing the formation of diverse organic molecules or biomolecules under mild and benign conditions, are refined and optimized by nature over millions of years evolution following “a survival of the fittest approach”. This natural process involves millions of times of repetition of enzyme synthesis and modification in order to make the best catalysts. It is basically a natural screening process.

Scientists have been trying to find useful catalysts for synthetic chemistry by mimicking this natural catalyst discovery approach. Combinatorial chemistry is a very valuable tool for catalyst discovery. After generating a large collection of catalysts with different structures and properties through combinatorial synthesis, active catalysts can be rapidly identified through certain high-throughput screening (HTS) methods. Therefore, the efficiency of catalyst discovery depends on both synthesis and screening processes.[125-128]

In a traditional batch approach, combinatorial synthesis and high-throughput screening are usually done on solid supports because this solid-phase method requires fewer amounts of reagents and solvents than solution-phase reactions. The procedures of post-reaction purification and characterization are also much simpler. A well-known combinatorial approach called 'one-bead-one-compound' has been widely used for simultaneous generation and screening of large 'split-and-mix'[129] libraries of catalysts based on solid-phase synthesis and screening.[130-132]

Wennemers[130] developed a "catalyst-substrate coimmobilization" method that works with 'one-bead-one-compound' synthesis to generate and identify large libraries of peptidic catalysts for the aldol reaction. The authors prepared an encoded[133] 'split-and-mix' library of 15^3 (3375) different tripeptides synthesized from 15 D- and L-amino acids for each of the three residues in a tripeptide molecule on the TentaGel resin. Then one of the substrate was immobilized onto the resins. While the other substrate tagged with dye was added in the solution, the reaction of two substrates catalyzed by immobilized peptides will lead to the colorization of some beads that can be observed by a microscope. The extent of color depends on reaction conversion. Colored beads were then isolated and peptides were cleaved followed by sequence analysis to identify their structures. This combinatorial method is depicted in Figure 5[130]. It combines combinatorial synthesis and high-throughput screening in a highly efficient way.

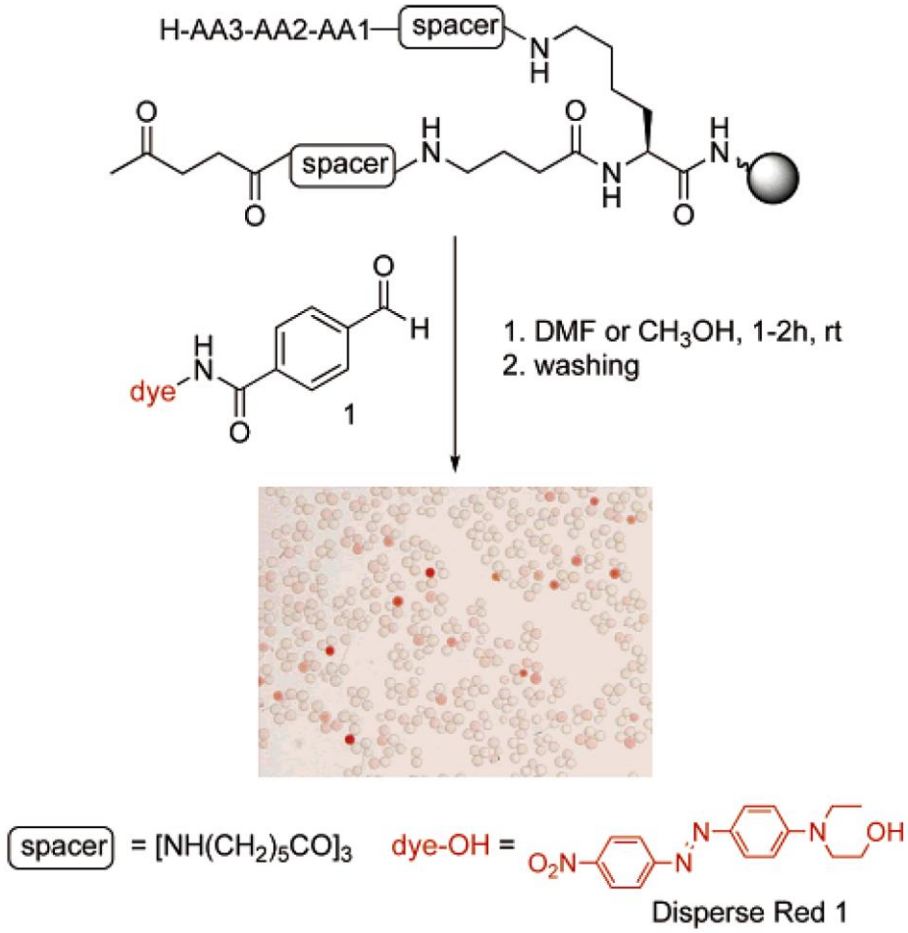

Figure 5. Substrate-Catalyst coimmobilization method for high-throughput screening of tripeptide catalysts.

(Image is reproduced with permission from ACS.[130])

1.3.2 Parallelization of chemical reactions in microreactors

Solid-phase synthesis is a straightforward method; however, a lot of additional effort is usually needed, e.g., preparing polymer supports, immobilizing and demobilizing catalysts/reagents on solid supports, chemically or physically encoding and decoding the supports in order to track synthesized compounds. Deactivation of catalysts/reagents during immobilization is also a

potential problem. Besides, reactions on solid supports are usually slower than solution-phase reactions due to the hindrance of mass transfer by bulky supports, leading to lower synthesis and screening efficiency. Therefore, solution-phase reaction is of still great interest for combinatorial chemistry.[134]

Microreactor technology is deemed as a very promising approach for solution-phase combinatorial chemistry.[135, 136] To synthesize and screen a large library of compounds, parallelization of reactions is necessary to achieve high efficiency and throughput. Microreactors are excellent for conducting simultaneous reactions under close process control. The cost and effort for synthesis and screening can also be minimized in terms of atom efficiency and chemical consumption in microreactors. Moreover, flow-through process makes it easy for microreactors to combine parallel synthesis and analysis in a highly integrated and automated manner.[55, 137] A representative system is the Miniaturised-SYNthesis and Total Analysis System (μSYNTAS) developed by Mitchell[138] This system is capable of conducting continuous-flow reactions in a silicon chip microreactor which is interfaced with a time-of-flight mass spectrometer (TOF-MS) for online product analysis. An Ugi multicomponent reaction (MCR) carried out in μSYNTAS demonstrated the efficiency of this system for sequence synthesis of a large number of compounds. In fact, in addition to MS detectors, a variety of online analytical techniques have been studied, including IR[139], UV-Vis[8, 140], fluorescence[141], X-ray[142], mass spectrometry[7, 143, 144], NMR[145], GC-MS[146] and LC-MS[147, 148]. GC-MS and LC-MS are excellent tools because they are particularly useful to identify unknown compounds for library generation.

Currently, there are a number of ways to conduct parallelized reactions in microreactors. For instance, parallel reactions are conducted in an array of microreactors; a single reactor with multiple layers of microchannels performs parallel reactions; sequential reactions are conducted

in slugs or droplets in a single microchannel; or microreactor array like 96-well plate performs parallel reactions in an array of micron-dimensioned chambers.

Reactions in parallel microreactors

A simple model of combinatorial synthesis on different chips is shown in Figure 6.[149] Two reagents from one library mixed with two in another library in 2×2 combination delivered by four syringe pumps. Four reactions take place on individual single-channel chips. This approach is very straightforward; however, many chips, pumps, tubing and connectors have to be used to carry out large numbers of reactions, requiring considerable effort of chip fabrication and high cost of instruments and apparatus.

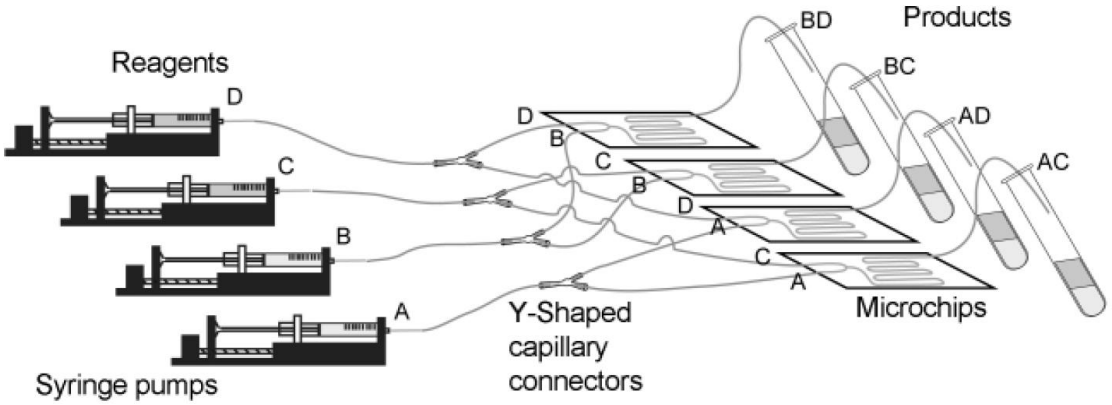

Figure 6. Schematic view of 2×2 parallel synthesis on four chips.

(Photograph is reproduced with permission from RSC Publishing.[149])

Kikutani[149] reported an example of glass chip microreactor consisting of two layers of microchannels on a single chip (Figure 7). By using the regular photolithography method, several layers of microchannels can be fabricated on a glass chip to form a three-dimensioned microchannel network. The efficacy of this two-layer microreactor was demonstrated by a 2×2 parallel synthesis of amide compounds. In principle, more layers can be constructed on a single

chip; however, the fabrication process will become more and more complicated with the increasing complexity of channel networks.

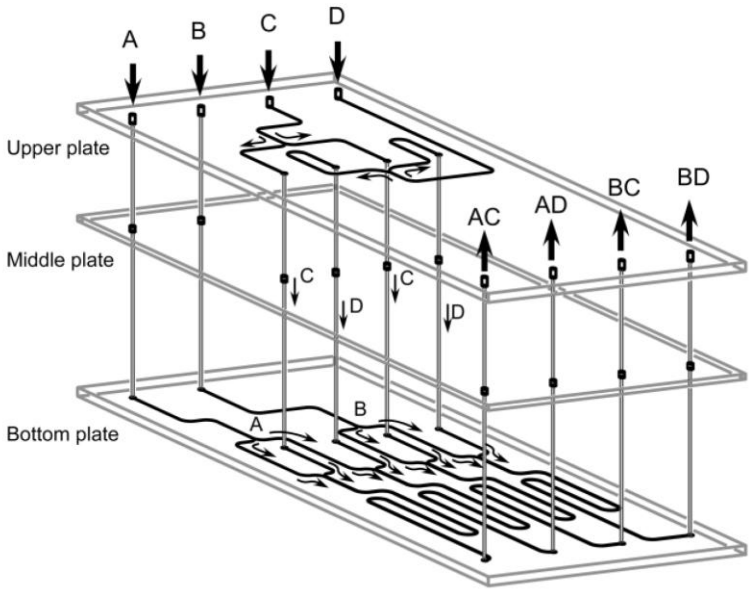

Figure 7. Schematic view of three dimensional microchannels on a two-layer glass chip for 2×2 parallel synthesis.

(Photograph is reproduced with permission from RSC Publishing.[149])

A simple and economical way to run chemical reactions on parallel reactors is to use cheap, commercially-sold capillaries rather than expensive glass chips. Each capillary works just like a microchannel. Comer and Organ[46] proved the efficacy of parallel capillary system (Figure 8) for combinatorial synthesis by carrying out 2×2 parallel reactions in a four-capillary microreactor, which can also be heated by microwave irradiation.

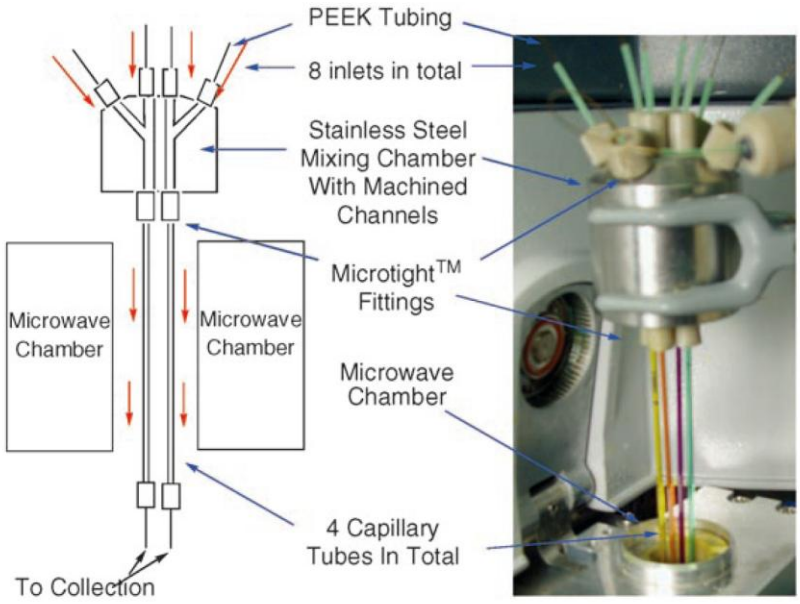

Figure 8. Schematic view and image of the multi-capillary microreactor.

(Photograph is reproduced with permission from Wiley InterScience.[46])

Serial reactions in slugs or droplets

Multiphase slug flow (also called segmented flow) or droplet flow is a common microfluidic method to conduct dynamic sequential reactions for combinatorial synthesis.[150, 151] The general method usually involves two immiscible phases, e.g., gas/liquid phases or liquid/liquid phases such as organic, aqueous, or fluorous phases. Both phases are injected simultaneously into a microchannel on chip or a capillary tube via a mixer. Continuous flow is usually employed and parallel reactions take place in a train of separate slugs or droplets that behave just like individual reactors. Slugs or droplets can have very small volumes from microliters down to picoliters, allowing extremely fast mass and heat transfer within one phase or between adjacent phases when used for phase transfer reactions.[121, 152, 153]

The droplet flow approach is good for a variety of reactions, not only homogeneous reactions, but some solid-involving reactions such as heterogeneous catalysis[154], precipitate-

forming reactions[88] or nanoparticle synthesis.[155] Solutions containing solids or particulates are incorporated into droplets and suspended in the carrier liquid, completely stopping them sticking to the channel surface to induce blockage. This is a potential solution to solve the clogging problem of microreactors; however, it does need optimization of a number of factors before running, such as size of droplets, channel dimensions, flow rates, injection modes and so on, in order to generate stable and uniform droplets for good reaction reproducibility and minimal clogging danger.

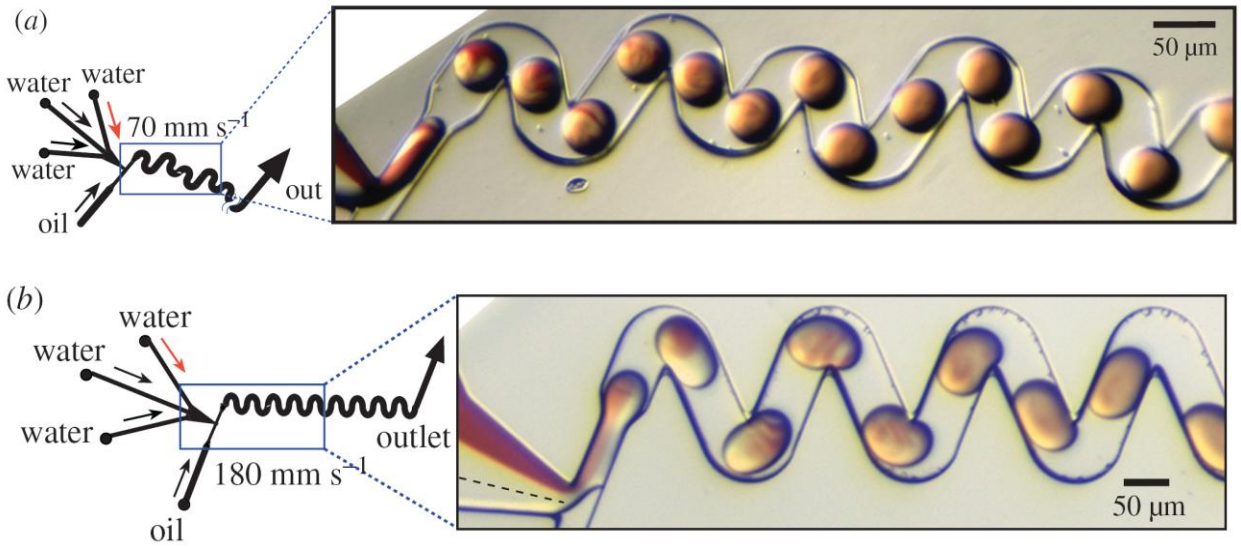

Figure 9. Photographs of microdroplets formed in microchannels.

(a) formation of small droplets under a slow flow velocity of water; (b) large droplets formed in a fast flow stream of water.

(Photograph is reproduced with permission from Royal Society Publishing.[156])

The aforementioned research work by McQuade's group[88] demonstrated the principle of carrying out precipitate-forming reactions in a droplet flow. Figure 9 shows an example of serial droplets of picoliter volumes formed and delivered through a winding microchannel.[156] Three

streams of aqueous solutions are simultaneously injected into a narrow channel and mixed together at the junction site to form a laminar flow stream which then rapidly transforms into tiny droplets pushed by constant flow oil. Each droplet is surrounded by the carrier liquid oil without touching the wall. Fast mixing is achieved by both convection and diffusion, and red dye can quickly fill the whole droplet after only walking a short length along the channel. The droplet shape and size can be precisely controlled by flow rates and channel diameter. High flow rate of aqueous solution leads to the formation of large droplets while slow rate results in small droplets.

Microreactor arrays

Commercialized automated or semi-automated synthesis systems based on micro well plates are popular tools for combinatorial synthesis and screening.[157] Reaction solutions are serially loaded by robotic dispensing systems and reacted in parallel chambers like 96- or 384-deep-well reactors. Reaction outcomes can be either collected for offline analysis or analyzed by some in-situ instruments like HPLC or GC. This approach is still in batch nature and usually requires lots of samples (hundreds of microliters to some milliliters) and external shaking to facilitate reagent mixing. Thus, some researchers developed micro reactor arrays on glass or PDMS chips,[158-161] which can have very high-density format through delicate microfabrication techniques. Compared to regular micro well plates, microreactor arrays can downsize volume of reaction chambers to nanoliters.

Gross[159] designed a glass microreactor array with 1563 parallel nanoliter-volume wells, which is also assembled with robot-controlled bead loading and liquid dispensing systems (Figure 10). A model combinatorial approach to generate a multiple core structure library for diversity-oriented synthesis was carried out on this microreactor array with a “split-and-mix” solid-phase synthesis strategy. An individual bead in each well was encoded by its spacial

position in the array instead of tedious chemical or physical coding. The history of each synthesized compound can be easily tracked by this one-bead-one-well approach, which is impossible for traditional "split-and-mix" method that can only track a group of beads since individual bead information is lost during a split-and-recombine process.

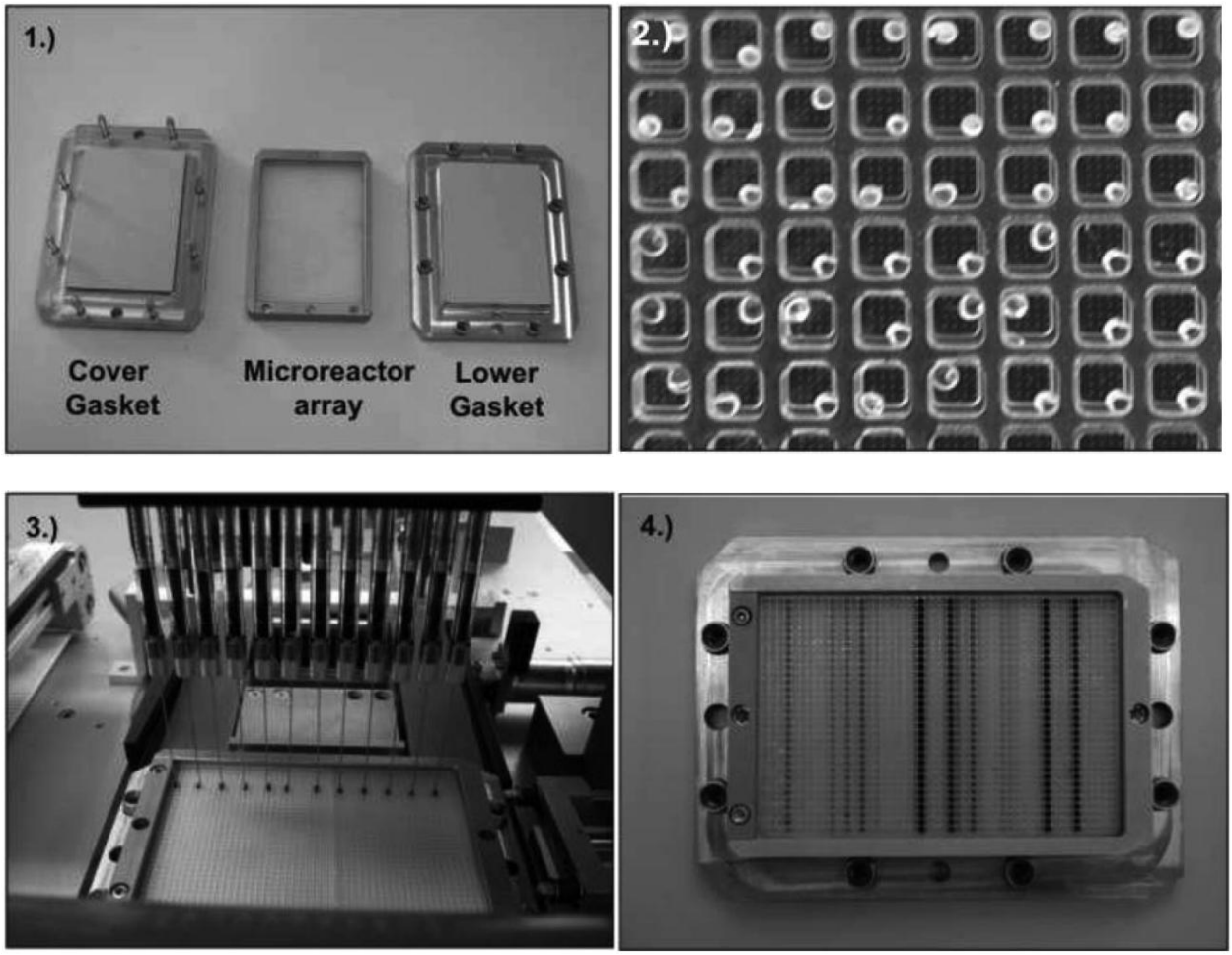

Figure 10. Images of a microreactor array and its assembly.

1) Reactor module with the gasket bearing plates. 2) Beads in the chambers. 3) Robot Syringe for solution dispensing. 4) Microreactor array filled with beads and reaction solution, before enclosing.

(Photograph is reproduced with permission from Wiley InterScience.[159])

Microreactor arrays are good at throughput and automation; however, it does have certain drawbacks. For example, solution loss by evaporation is a common problem for 96-deep-well reactors especially when high temperature or long period of time is needed. It becomes more serious for microreactor arrays since solution volume inside a well is too little. Unlike flow reactors that have closed channels, microreactor arrays have open wells sealed by removable covers. Thus, tight sealing is very important to prevent evaporation. However, evaporation can happen during solution dispense or reagent transfer when there is no cover on top of wells. Chemical crosstalk in close chambers is also a potential threat to reaction reproducibility. Besides, microreactor arrays with robotic dispensing systems are expensive and complicated, which are not very applicable for ordinary synthetic laboratories.

1.3.3 Flow microreactor systems for catalyst screening

Currently, most microreactors are developed aiming for synthesis rather than screening. But it is apparent that high-throughput screening can benefit a lot from microreactor technology, especially automated reactor technology. Catalyst screening usually requires the accumulation of large amounts of reaction data and the whole discovery process can be significantly simplified and economized by using automated microreactor systems integrating both synthesis and analysis functionalities.

However, catalyst screening in microreactors is still limited so far. Most of the studies are focused on screening packed-bed solid metal catalysts for gas-phase reactions,[135, 162-167] e.g., hydrogenation over Pd catalysts coated in capillaries or tubes. Typically, reaction is faster and screening throughput is higher in microreactors. For example, Yi[168] developed a 64-channel (8×8 parallel channels) tubing microreactor that can screen 64 fixed-bed catalysts simultaneously. The

authors screened some metal catalysts for oxidation of propylene and the product acrolein can be analyzed by an efficient online colorimetric imaging method.

Few researchers have built microreactors specifically for liquid-phase catalyst screening. A main limitation is the threat of catalyst precipitating or formation of insoluble byproducts in microchannels when unknown catalysts are screened with different substrates or under varied conditions. Most current microreactors are developed for proof-of-purpose. Reaction process and conditions are usually well understood or have been studied in batch reactions previously. Therefore, it will be very significant to build a practical microreactor system specifically for high-throughput catalyst screening in liquid phase, which could greatly facilitate catalyst discovery for synthetic chemistry.

1.4 RESEARCH MOTIVATION AND PLAN

In view of the inadequacy of current microreactor technology for high-throughput catalyst screening, I decided to develop a new type of microreactor system that can fill this application gap. The design idea was to make this system useful and practical for ordinary synthetic laboratories and organic chemists. Thus, besides screening efficiency, I also wanted this system to have a straightforward design and economic construction. Capillary is preferred to build this microreactor due to its good adaptability, high flexibility and low cost. Considering most current microreactors are limited to work on fast reactions, I want to extend the scope to slow reactions, allowing more organic reactions applicable for this microreactor. The ultimate goal of my research is to provide the synthetic community with a powerful and flexible prototype microreactor system possessing the capability of synthesis with in-situ analysis. The major

application focus of this microreactor will be high-throughput screening of catalysts, but it may also find applications in combinatorial chemistry such as diversity-oriented organic synthesis or biological chemistry such as biochemical analyses or enzyme reactors.

The planned research will include: 1. Construct the microreactor system with capillaries and some commonly used instruments; 2. Validate the system's performance by a well-studied organic reaction with known catalysts to test its screening efficacy; 3. Extend the application scope to some important organic reactions: optimize reaction conditions, screen new catalysts and study reaction mechanisms by the microreactor. The detailed research work will be described in the next several chapters.

BIBLIOGRAPHY

1. Fletcher, P. D. I.; Haswell, S. J.; Pombo-Villar, E.; Warrington, B. H.; Watts, P.; Wong, S. Y. F.; Zhang, X., Micro reactors: principles and applications in organic synthesis. *Tetrahedron* **2002,** 58, 4735-4757.

2. Salimi-Moosavi, H.; Tang, T.; Harrison, D. J., Electroosmotic pumping of organic solvents and reagents in microfabricated reactor chips. *J. Am. Chem. Soc.* **1997,** 119, 8716-8717.

3. Fletcher, P. D.; Haswell, S. J.; Zhang, X., Electrical currents and liquid flow rates in micro-reactors. *Lab Chip* **2001,** 1, 115-21.

4. Fletcher, P. D. I.; Haswell, S. J.; Zhang, X., Electrokinetic control of a chemical reaction in a lab-on-a-chip micro-reactor: measurement and quantitative modelling. *Lab Chip* **2002,** 2, 102-112.

5. Kohlheyer, D.; Besselink, G. A. J.; Lammertink, R. G. H.; Schlautmann, S.; Unnikrishnan, S.; Schasfoort, R. B. M., Electroosmotically controllable multi-flow microreactor. *Microfluid Nanofluid* **2005,** 1, 242-248.

6. Jacobson, S. C.; McKnight, T. E.; Ramsey, J. M., Microfluidic devices for electrokinetically driven parallel and serial mixing. *Anal. Chem.* **1999,** 71, 4455-4459.

7. Brivio, M.; Fokkens, R. H.; Verboom, W.; Reinhoudt, D. N.; Tas, N. R.; Goedbloed, M.; van den Berg, A., Integrated microfluidic system enabling (Bio)chemical reactions with on-line MALDI-TOF mass spectrometry. *Anal. Chem.* **2002,** 74, 3972-3976.

8. Benito-Lopez, F.; Verboom, W.; Kakuta, M.; Gardeniers, J. G. E.; Egberink, R. J. M.; Oosterbroek, E. R.; van den Berg, A.; Reinhoudt, D. N., Optical fiber-based on-line UV/Vis spectroscopic monitoring of chemical reaction kinetics under high pressure in a capillary microreactor. *Chem. Commun.* **2005**, 2857-2859.

9. Fernandez-Suarez, M.; Wong, S. Y. F.; Warrington, B. H., Synthesis of a three-member array of cycloadducts in a glass microchip under pressure driven flow. *Lab Chip* **2002,** 2, 170-174.

10. Haswell, S. J.; O'Sullivan, B.; Styring, P., Kumada-Corriu reactions in a pressure-driven microflow reactor. *Lab Chip* **2001,** 1, 164-166.

11. Kashid, M. N.; Gerlach, I.; Goetz, S.; Franzke, J.; Acker, J. F.; Platte, F.; Agar, D. W.; Turek, S., Internal circulation within the liquid slugs of a liquid-liquid slug-flow capillary microreactor. *Ind. Eng. Chem. Res.* **2005,** 44, 5003-5010.

12. Kutter, J. P.; Fintschenko, Y., *Separation Methods in Microanalytical Systems*. 2006; p 165-207.

13. Jakeway, S. C.; de Mello, A. J.; Russell, E. L., Miniaturized total analysis systems for biological analysis. *Fresenius. J. Anal. Chem.* **2000,** 366, 525-539.

14. Burns, M. A.; Johnson, B. N.; Brahmasandra, S. N.; Handique, K.; Webster, J. R.; Krishnan, M.; Sammarco, T.; Man, P. M.; Jones, D.; Heldsinger, D.; Mastrangelo, C. H.; Burke, D. T., An integrated nanoliter DNA analysis device. *Science* **1998,** 282, 484-487.

15. Marcus, J. S.; Anderson, W. F.; Quake, S. R., Microfluidic single-cell mrna isolation and analysis. *Anal. Chem.* **2006,** 78, 3084-3089.

16. Marcy, Y.; Ouverney, C.; Bik, E. M.; Loesekann, T.; Ivanova, A.; Martin, H. G.; Szeto, E.; Platt, D.; Hugenholtz, P.; Relman, D. A.; Quake, S. R., Dissecting biological "dark matter" with single-cell genetic analysis of rare and uncultivated TM7 microbes from the human mouth. *Proc. Natl. Acad. Sci. U. S. A.* **2007,** 104, 11889-11894.

17. Ottesen, E. A.; Hong, J. W.; Quake, S. R.; Leadbetter, J. R., Microfluidic digital PCR enables multigene analysis of individual environmental bacteria. *Science* **2006,** 314, 1464-1467.

18. Ochsner, M.; Dusseiller, M. R.; Grandin, H. M.; Luna-Morris, S.; Textor, M.; Vogel, V.; Smith, M. L., Micro-well arrays for 3D shape control and high resolution analysis of single cells. *Lab Chip* **2007,** 7, 1074-1077.

19. Yi, C.; Li, C.-W.; Ji, S.; Yang, M., Microfluidics technology for manipulation and analysis of biological cells. *Anal. Chim. Acta* **2006,** 560, 1-23.

20. McClain, M. A.; Culbertson, C. T.; Jacobson, S. C.; Allbritton, N. L.; Sims, C. E.; Ramsey, J. M., Microfluidic devices for the high-throughput chemical analysis of cells. *Anal. Chem.* **2003,** 75, 5646-5655.

21. Emrich, C. A.; Medintz, I. L.; Chu, W. K.; Mathies, R. A., Microfabricated two-dimensional electrophoresis device for differential protein expression profiling. *Anal. Chem.* **2007,** 79, 7360-7366.

22. Fan, H.; Chen, G., Fiber-packed channel bioreactor for microfluidic protein digestion. *Proteomics* **2007,** 7, 3445-3449.

23. Huang, B.; Wu, H.; Bhaya, D.; Grossman, A.; Granier, S.; Kobilka, B. K.; Zare, R. N., Counting low-copy number proteins in a single cell. *Science* **2007,** 315, 81-84.

24. Shim, J.-u.; Cristobal, G.; Link, D. R.; Thorsen, T.; Fraden, S., Using microfluidics to decouple nucleation and growth of protein crystals. *Cryst. Growth Des.* **2007,** 7, 2192-2194.

25. Zhou, X.; Lau, L.; Lam, W. W. L.; Au, S. W. N.; Zheng, B., Nanoliter Dispensing Method by Degassed Poly(dimethylsiloxane) Microchannels and its application in protein crystallization. *Anal. Chem.* **2007,** 79, 4924-4930.

26. Figallo, E.; Cannizzaro, C.; Gerecht, S.; Burdick, J. A.; Langer, R.; Elvassore, N.; Vunjak-Novakovic, G., Micro-bioreactor array for controlling cellular microenvironments. *Lab Chip* **2007,** 7, 710-719.

27. Watts, P.; Wiles, C., Recent advances in synthetic micro reaction technology. *Chem. Commun.* **2007**, 443-467.

28. Wiles, C.; Watts, P., Continuous flow reactors, a tool for the modern synthetic chemist. *Eur. J. Org. Chem.* **2008**, 1655-1671.

29. Cullen, C. J.; Wootton, R. C. R.; de Mello, A. J., Microfluidic systems for high-throughput and combinatorial chemistry. *Curr. Opin. Drug Discovery Dev.* **2004,** 7, 798-806.

30. Doku, G. N.; Verboom, W.; Reinhoudt, D. N.; van den Berg, A., On-microchip multiphase chemistry-a review of microreactor design principles and reagent contacting modes. *Tetrahedron* **2005,** 61, 2733-2742.

31. Haswell, S. J., Miniaturization - What's in it for chemistry? *Micro Total Analysis Systems 2001, Proceedings mTAS 2001 Symposium, 5th, Monterey, CA, United States, Oct. 21-25, 2001* **2001**, 637-639.

32. Jas, G.; Kirschning, A., Continuous flow techniques in organic synthesis. *Chem. Eur. J.* **2003,** 9, 5708-5723.

33. Roberge, D. M.; Ducry, L.; Bieler, N.; Cretton, P.; Zimmermann, B., Microreactor technology: a revolution for the fine chemical and pharmaceutical industries? *Chem. Eng. Technol.* **2005,** 28, 318-323.

34. Watts, P.; Haswell, S. J., Continuous flow reactors for drug discovery. *Drug Discov. Today* **2003,** 8, 586-593.

35. Watts, P.; Haswell, S. J., Microfluidic combinatorial chemistry. *Curr. Opin. Chem. Biol.* **2003,** 7, 380-387.

36. Watts, P.; Haswell, S. J., The application of microreactors for small scale organic synthesis. *Chem. Eng. Technol.* **2005,** 28, 290-301.

37. Zech, T.; Klein, J.; Schunk, S. A.; Johann, T.; Schueth, F.; Kleditzsch, S.; Deutschmann, O., Miniaturized reactor concepts and advanced analytics for primary screening in high-throughput experimentation. *High-Throughput Analysis* **2003**, 491-523.

38. Bessoth, F. G.; deMello, A. J.; Manz, A., Microstructure for efficient continuous flow mixing. *Anal. Commun.* **1999,** 36, 213-215.

39. Greenway, G. M.; Haswell, S. J.; Morgan, D. O.; Skelton, V.; Styring, P., The use of a novel microreactor for high throughput continuous flow organic synthesis. *Sens. Actuators, B* **2000,** B63, 153-158.

40. Haswell, S. J.; Middleton, R. J.; O'Sullivan, B.; Skelton, V.; Watts, P.; Styring, P., The application of micro reactors to synthetic chemistry. *Chem. Commun.* **2001**, 391-398.

41. Fortt, R.; Wootton, R. C. R.; de Mello, A. J., Continuous-Flow Generation of Anhydrous Diazonium Species: Monolithic microfluidic reactors for the chemistry of unstable intermediates. *Org. Process Res. Dev.* **2003,** 7, 762-768.

42. Mason, B. P.; Price, K. E.; Steinbacher, J. L.; Bogdan, A. R.; McQuade, D. T., Greener approaches to organic synthesis using microreactor technology. *Chem. Rev.* **2007,** 107, 2300-2318.

43. Kralisch, D.; Kreisel, G., Assessment of the ecological potential of microreaction technology. *Chem. Eng. Sci.* **2007,** 62, 1094-1100.

44. Geyer, K.; Codee, J. D. C.; Seeberger, P. H., Microreactors as tools for synthetic chemists - the chemists' round-bottomed flask of the 21st century? *Chem. Eur. J.* **2006,** 12, 8434-8442.

45. Comer, E.; Organ, M. G., A microreactor for microwave-assisted capillary (continuous flow) organic synthesis. *J. Am. Chem. Soc.* **2005,** 127, 8160-8167.

46. Comer, E.; Organ, M. G., A microcapillary system for simultaneous, parallel microwave-assisted synthesis. *Chem. Eur. J.* **2005,** 11, 7223-7227.

47. Wiles, C.; Watts, P.; Haswell, S. J.; Pombo-Villar, E., The aldol reaction of silyl enol ethers within a micro reactor. *Lab Chip* **2001,** 1, 100-101.

48. Wiles, C.; Watts, P.; Haswell Stephen, J.; Pombo-Villar, E., 1,4-addition of enolates to alpha,beta-unsaturated ketones within a micro reactor. *Lab Chip* **2002,** 2, 62-4.

49. Skelton, V.; Greenway, G. M.; Haswell, S. J.; Styring, P.; Morgan, D. O.; Warrington, B.; Wong, S. Y., The preparation of a series of nitrostilbene ester compounds using micro reactor technology. *Analyst* **2001,** 126, 7-10.

50. Acke, D. R. J.; Stevens, C. V.; Roman, B. I., Microreactor technology: continuous synthesis of *1H*-isochromeno[3,4-d]imidazol-5-ones. *Org. Process Res. Dev.* **2008,** 12, 921-928.

51. Wiles, C.; Watts, P.; Haswell, S. J.; Pombo-Villar, E., The preparation and reaction of enolates within micro reactors. *Tetrahedron* **2005,** 61, 10757-10773.

52. Sands, M.; Haswell, S. J.; Kelly, S. M.; Skelton, V.; Morgan, D. O.; Styring, P.; Warrington, B., The investigation of an equilibrium dependent reaction for the formation of enamines in a microchemical system. *Lab Chip* **2001,** 1, 64-65.

53. Skelton, V.; Haswell, S. J.; Styring, P.; Warrington, B.; Wong, S., A microreactor device for the Ugi four component condensation (4CC) reaction. *Micro Total Anal. Syst. 2001, Proc. micro TAS 2001 Symp., 5th* **2001**, 589-590.

54. Acke, D. R. J.; Stevens, C. V., A HCN-based reaction under microreactor conditions: industrially feasible and continuous synthesis of 3,4-diamino-1*H*-isochromen-1-ones. *Green Chem.* **2007,** 9, 386-390.

55. Garcia-Egido, E.; Spikmans, V.; Wong Stephanie, Y. F.; Warrington Brian, H., Synthesis and analysis of combinatorial libraries performed in an automated micro reactor system. *Lab Chip* **2003,** 3, 73-6.

56. Garcia-Egido, E.; Wong Stephanie, Y.; Warrington Brian, H., A Hantzsch synthesis of 2-aminothiazoles performed in a heated microreactor system. *Lab Chip* **2002,** 2, 31-3.

57. Acke, D. R. J.; Orru, R. V. A.; Stevens, C. V., Continuous synthesis of tri- and tetrasubstituted imidazoles via a multicomponent reaction under microreactor conditions. *QSAR Comb. Sci.* **2006,** 25, 474-483.

58. Schwalbe, T.; Autze, V.; Wille, G., Chemical synthesis in microreactors. *Chimia* **2002,** 56, 636-646.

59. Kawaguchi, T.; Miyata, H.; Ataka, K.; Mae, K.; Yoshida, J.-i., Room-temperature Swern oxidations by using a microscale flow system. *Angew. Chem., Int. Ed.* **2005,** 44, 2413-2416.

60. Chambers, R. D.; Spink, R. C. H., Microreactors for elemental fluorine. *Chem. Commun.* **1999**, 883-884.

61. Doku, G. N.; Haswell, S. J.; McCreedy, T.; Greenway, G. M., Electric field-induced mobilisation of multiphase solution systems based on the nitration of benzene in a micro reactor. *Analyst* **2001,** 126, 14-20.

62. Panke, G.; Schwalbe, T.; Stirner, W.; Taghavi-Moghadam, S.; Wille, G., A practical approach of continuous processing to high energetic nitration reactions in microreactors. *Synthesis* **2003**, 2827-2830.

63. Brivio, M.; Edwin Oosterbroek, R.; Verboom, W.; Goedbloed, M. H.; van den Berg, A.; Reinhoudt, D. N., Surface effects in the esterification of 1-pyrenebutyric acid within a glass micro reactor. *Chem. Commun.* **2003**, 1924-1925.

64. George, V.; Watts, P.; Haswell, S. J.; Pombo-Villar, E., On-chip separation of peptides prepared within a micro reactor. *Chem. Commun.* **2003**, 2886-2887.

65. Watts, P.; Wiles, C.; Haswell, S. J.; Pombo-Villar, E., Investigation of racemization in peptide synthesis within a micro reactor. *Lab Chip* **2002,** 2, 141-144.

66. Watts, P.; Wiles, C.; Haswell, S. J.; Pombo-Villar, E., Solution phase synthesis of beta -peptides using micro reactors. *Tetrahedron* **2002,** 58, 5427-5439.

67. Floegel, O.; Codee, J. D. C.; Seebach, D.; Seeberger, P. H., Microreactor synthesis of beta -peptides. *Angew. Chem., Int. Ed.* **2006,** 45, 7000-7003.

68. Hisamoto, H.; Saito, T.; Tokeshi, M.; Hibara, A.; Kitamori, T., Fast and high conversion phase-transfer synthesis exploiting the liquid-liquid interface formed in a microchannel chip. *Chem. Commun.* **2001**, 2662-2663.

69. Wiles, C.; Watts, P.; Haswell, S. J.; Pombo-Villar, E., Stereoselective alkylation of an Evans auxiliary derivative within a pressure-driven micro reactor. *Lab Chip* **2004,** 4, 171-173.

70. Merrifield, R. B., Solid phase peptide synthesis. I. The synthesis of a tetrapeptide. *J. Am. Chem. Soc.* **1963,** 85, 2149-54.

71. Whitney, D. B.; Tam, J. P.; Merrifield, R. B., A new base-catalyzed cleavage reaction for the preparation of protected peptides. *Tetrahedron* **1984,** 40, 4237-44.

72. Desai, B.; Kappe, C. O., Heterogeneous hydrogenation reactions using a continuous flow high pressure device. *J. Comb. Chem.* **2005,** 7, 641-643.

73. Haswell, S. J.; O'Sullivan, B.; Styring, P., Kumada-Corriu reactions in a pressure-driven microflow reactor. *Lab Chip* **2001,** 1, 164-166.

74. Jones, R. V.; Godorhazy, L.; Varga, N.; Szalay, D.; Urge, L.; Darvas, F., Continuous-flow high pressure hydrogenation reactor for optimization and high-throughput synthesis. *J. Comb. Chem.* **2006,** 8, 110-116.

75. Kiwi-Minsker, L.; Renken, A., Microstructured reactors for catalytic reactions. *Catal. Today* **2005,** 110, 2-14.

76. Kobayashi, J.; Mori, Y.; Okamoto, K.; Akiyama, R.; Ueno, M.; Kitamori, T.; Kobayashi, S., A microfluidic device for conducting gas-liquid-solid hydrogenation reactions. *Science* **2004,** 304, 1305-1308.

77. Nikbin, N.; Watts, P., Solid-supported continuous flow synthesis in microreactors using electroosmotic flow. *Org. Process Res. Dev.* **2004,** 8, 942-944.

78. Baxendale, I. R.; Griffiths-Jones, C. M.; Ley, S. V.; Tranmer, G. K., Microwave-assisted Suzuki coupling reactions with an encapsulated palladium catalyst for batch and continuous-flow transformations. *Chem. Eur. J.* **2006,** 12, 4407-4416.

79. He, P.; Haswell, S. J.; Fletcher, P. D. I., Microwave heating of heterogeneously catalyzed Suzuki reactions in a micro reactor. *Lab Chip* **2004,** 4, 38-41.

80. Phan, N. T. S.; Brown, D. H.; Styring, P., A facile method for catalyst immobilisation on silica: nickel-catalysed Kumada reactions in mini-continuous flow and batch reactors. *Green Chem.* **2004,** 6, 526-532.

81. Phan, N. T. S.; Khan, J.; Styring, P., Polymer-supported palladium catalyzed Suzuki-Miyaura reactions in batch and a mini-continuous flow reactor system. *Tetrahedron* **2005,** 61, 12065-12073.

82. Shore, G.; Morin, S.; Organ, M. G., Catalysis in capillaries by Pd thin films using microwave-assisted continuous-flow organic synthesis (MACOS). *Angew. Chem., Int. Ed.* **2006,** 45, 2761-2766.

83. Mikami, K.; Islam, M. N.; Yamanaka, M.; Itoh, Y.; Shinoda, M.; Kudo, K., Nanoflow system for perfect regiocontrol in the Baeyer-Villiger oxidation by aqueous hydrogen peroxide using lowest concentration of a fluorous lanthanide catalyst. *Tetrahedron Lett.* **2004,** 45, 3681-3683.

84. Ahmed-Omer, B.; Brandt, J. C.; Wirth, T., Advanced organic synthesis using microreactor technology. *Org. Biomol. Chem.* **2007,** 5, 733-740.

85. Bossi, A.; Guizzardi, L.; D'Acunto, M. R.; Righetti, P. G., Controlled enzyme-immobilisation on capillaries for microreactors for peptide mapping. *Anal. Bioanal. Chem.* **2004,** 378, 1722-1728.

86. Mersal, G. A. M.; Bilitewski, U., Development of monolithic enzymatic reactors in glass microchips for the quantitative determination of enzyme substrates using the example of glucose determination via immobilized glucose oxidase. *Electrophoresis* **2005,** 26, 2303-2312.

87. Ho, J.-a. A.; Wu, L.-c.; Fan, N.-C.; Lee, M.-S.; Kuo, H.-Y.; Yang, C.-S., Development of a long-life capillary enzyme bioreactor for the determination of blood glucose. *Talanta* **2007,** 71, 391-396.

88. Poe, S. L.; Cummings, M. A.; Haaf, M. P.; McQuade, D. T., Solving the clogging problem: precipitate-forming reactions in flow. *Angew. Chem. Int. Ed.* **2006,** 45, 1544-1548.

89. Wootton, R. C. R.; Fortt, R.; de Mello, A. J., A microfabricated nanoreactor for safe, continuous generation and use of singlet oxygen. *Org. Process Res. Dev.* **2002,** 6, 187-189.

90. Lu, H.; Schmidt, M. A.; Jensen, K. F., Photochemical reactions and on-line UV detection in microfabricated reactors. *Lab Chip* **2001,** 1, 22-28.

91. Ueno, K.; Kitagawa, F.; Kitamura, N., Photocyanation of pyrene across an oil/water interface in a polymer microchannel chip. *Lab Chip* **2002,** 2, 231-234.

92. Hook, B. D. A.; Dohle, W.; Hirst, P. R.; Pickworth, M.; Berry, M. B.; Booker-Milburn, K. I., A practical flow reactor for continuous organic photochemistry. *J. Org. Chem.* **2005,** 70, 7558-7564.

93. Shore, G.; Organ, M. G., Gold-film-catalyzed hydrosilylation of alkynes by microwave-assisted, continuous-flow organic synthesis (MACOS). *Chem. Eur. J.* **2008,** 14, 9641-9646.

94. Shore, G.; Organ, M. G., Diels-Alder cycloadditions by microwave-assisted, continuous flow organic synthesis (MACOS): the role of metal films in the flow tube. *Chem. Commun.* **2008**, 838-840.

95. Yoshida, J.-i.; Nagaki, A.; Yamada, T., Flash chemistry: fast chemical synthesis by using microreactors. *Chem. Eur. J.* **2008,** 14, 7450-7459.

96. Matsumoto, K.; Ueoka, K.; Fujie, S.; Suga, S.; Yoshida, J.-i., Synthesis of thiochromans based on indirect cation pool method. *Heterocycles* **2008,** 76, 1103-1119.

97. Nagaki, A.; Tomida, Y.; Yoshida, J.-i., Microflow-system-controlled anionic polymerization of styrenes. *Macromolecules* **2008,** 41, 6322-6330.

98. Nokami, T.; Shibuya, A.; Yoshida, J.-i., Electrochemical conversion of thioglycosides to glycosyl triflates. *Trends Glycosci. Glycotechnol.* **2008,** 20, 175-185.

99. Nokami, T.; Tsuyama, H.; Shibuya, A.; Nakatsutsumi, T.; Yoshida, J.-i., Oligosaccharide synthesis based on a one-pot electrochemical glycosylation-Fmoc deprotection sequence. *Chem. Lett.* **2008,** 37, 942-943.

100. Suga, S.; Shimizu, I.; Ashikari, Y.; Mizuno, Y.; Maruyama, T.; Yoshida, J.-i., Electro-initiated coupling reactions of N-acyliminium ion pools with arylthiomethylsilanes and aryloxymethylsilanes. *Chem. Lett.* **2008,** 37, 1008-1009.

101. Yoshida, J.-i.; Editor, *Flash Chemistry: Fast Organic Synthesis in Microsystems*. 2008; p 234 pp.

102. Yoshida, J.-I.; Suga, S., Basic concepts of "cation pool" and "cation flow" methods and their applications in conventional and combinatorial organic synthesis. *Chem. Eur. J.* **2002,** 8, 2650-2658.

103. Yoshida, J.-I., Flash chemistry using electrochemical method and microsystems. *Chem. Commun.* **2005**, 4509-16.

104. Honda, T.; Miyazaki, M.; Nakamura, H.; Maeda, H., Controllable polymerization of N-carboxy anhydrides in a microreaction system. *Lab Chip* **2005,** 5, 812-818.

105. Iwasaki, T.; Nagaki, A.; Yoshida, J.-i., Microsystem controlled cationic polymerization of vinyl ethers initiated by CF3SO3H. *Chem. Commun.* **2007**, 1263-1265.

106. Ouchi, M.; Inagaki, N.; Ando, T.; Sawamoto, M., Living cationic polymerization of vinyl ethers in a continuous flow system with micromixers. *Polym. Prepr. (Am. Chem. Soc., Div. Polym. Chem.)* **2005,** 46, 939-940.

107. Rosenfeld, C.; Serra, C.; Brochon, C.; Hadziioannou, G., High-temperature nitroxide-mediated radical polymerization in a continuous microtube reactor: Towards a better control of the polymerization reaction. *Chem. Eng. Sci.* **2007,** 62, 5245-5250.

108. Wilms, D.; Nieberle, J.; Klos, J.; Loewe, H.; Frey, H., Synthesis of hyperbranched polyglycerol in a continuous flow microreactor. *Chem. Eng. Technol.* **2007,** 30, 1519-1524.

109. Xu, C.; Wu, T.; Drain, C. M.; Batteas, J. D.; Beers, K. L., Microchannel Confined Surface-Initiated Polymerization. *Macromolecules* **2005,** 38, 6-8.

110. Wilms, D.; Klos, J.; Frey, H., Microstructured reactors for polymer synthesis: a renaissance of continuous flow processes for tailor-made macromolecules? *Macromol. Chem. Phys.* **2008,** 209, 343-356.

111. Koehler, J. M.; Held, M.; Huebner, U.; Wagner, J., Formation of Au/Ag nanoparticles in a two step micro flow-through process. *Chem. Eng. Technol.* **2007,** 30, 347-354.

112. Chang, C.-H.; Paul, B. K.; Remcho, V. T.; Atre, S.; Hutchison, J. E., Synthesis and post-processing of nanomaterials using microreaction technology. *J. Nanopart. Res.* **2008,** 10, 965-980.

113. Schabas, G.; Yusuf, H.; Moffitt, M. G.; Sinton, D., Controlled self-assembly of quantum dots and block copolymers in a microfluidic device. *Langmuir* **2008,** 24, 637-643.

114. Yang, H.; Luan, W.; Tu, S.-t.; Wang, Z. M., Synthesis of nanocrystals via microreaction with temperature gradient: towards separation of nucleation and growth. *Lab Chip* **2008,** 8, 451-455.

115. Jahn, A.; Reiner, J. E.; Vreeland, W. N.; DeVoe, D. L.; Locascio, L. E.; Gaitan, M., Preparation of nanoparticles by continuous-flow microfluidics. *J. Nanopart. Res.* **2008,** 10, 925-934.

116. Karnik, R.; Gu, F.; Basto, P.; Cannizzaro, C.; Dean, L.; Kyei-Manu, W.; Langer, R.; Farokhzad, O. C., Microfluidic platform for controlled synthesis of polymeric nanoparticles. *Nano Lett.* **2008,** 8, 2906-2912.

117. Luan, W.; Yang, H.; Tu, S.-t.; Wang, Z., Open-to-air synthesis of monodisperse CdSe nanocrystals via microfluidic reaction and its kinetics. *Nanotechnology* **2007,** 18, 175603/1-6.

118. Winterton, J. D.; Myers, D. R.; Lippmann, J. M.; Pisano, A. P.; Doyle, F. M., A novel continuous microfluidic reactor design for the controlled production of high-quality semiconductor nanocrystals. *J. Nanopart. Res.* **2008,** 10, 893-905.

119. Li, S.; Xu, J.; Wang, Y.; Luo, G., Controllable preparation of nanoparticles by drops and plugs flow in a microchannel device. *Langmuir* **2008,** 24, 4194-4199.

120. Grodrian, A.; Metze, J.; Henkel, T.; Martin, K.; Roth, M.; Kohler, J. M., Segmented flow generation by chip reactors for highly parallelized cell cultivation. *Biosens. Bioelectron.* **2004,** 19, 1421-1428.

121. Burns, J. R.; Ramshaw, C., The intensification of rapid reactions in multiphase systems using slug flow in capillaries. *Lab Chip* **2001,** 1, 10-15.

122. Chan, E. M.; Alivisatos, A. P.; Mathies, R. A., High-temperature microfluidic synthesis of cdse nanocrystals in nanoliter droplets. *J. Am. Chem. Soc.* **2005,** 127, 13854-13861.

123. Song, H.; Chen, D. L.; Ismagilov, R. F., Reactions in droplets in microfluidic channels. *Angew. Chem., Int. Ed.* **2006,** 45, 7336-7356.

124. Teh, S.-Y.; Lin, R.; Hung, L.-H.; Lee, A. P., Droplet microfluidics. *Lab Chip* **2008,** 8, 198-220.

125. Revell, J. D.; Wennemers, H., Identification of catalysts in Combinatorial libraries. *Top. Curr. Chem.* **2007,** 277, 251-266.

126. Revell, J. D.; Wennemers, H., Peptidic catalysts developed by combinatorial screening methods. *Curr. Opin. Chem. Biol.* **2007,** 11, 269-278.

127. Schmuck, C.; Dudaczek, J., Screening of a combinatorial library reveals peptide-based catalysts for phosphorester cleavage in water. *Org. Lett.* **2007,** 9, 5389-5392.

128. Fonseca, M. H.; List, B., Combinatorial chemistry and high-throughput screening for the discovery of organocatalysts. *Curr. Opin. Chem. Biol.* **2004,** 8, 319-326.

129. Pescarmona, P. P.; Van der Waal, J. C.; Maxwell, I. E.; Maschmeyer, T., Combinatorial chemistry, high-speed screening and catalysis. *Catal. Lett.* **1999,** 63, 1-11.

130. Krattiger, P.; Kovasy, R.; Revell, J. D.; Ivan, S.; Wennemers, H., Increased structural complexity leads to higher activity: peptides as efficient and versatile catalysts for asymmetric aldol reactions. *Org. Lett.* **2005,** 7, 1101-1103.

131. Krattiger, P.; Kovasy, R.; Revell, J. D.; Wennemers, H., Using catalyst-substrate coimmobilization for the discovery of catalysts for asymmetric aldol reactions in split-and-mix libraries. *QSAR Comb. Sci.* **2005,** 24, 1158-1163.

132. Wennemers, H., Combinatorial methods for the discovery of catalysts. *Highlights Bioorg. Chem.* **2004**, 436-445.

133. Ohlmeyer, M. H. J.; Swanson, R. N.; Dillard, L.; Reader, J. C.; Asouline, G.; Kobayashi, R.; Wigler, M.; Still, W. C., Complex synthetic chemical libraries indexed with molecular tags. *Proc. Natl. Acad. Sci. U. S. A.* **1993,** 90, 10922-6.

134. Maier, W. F., Combinatorial chemistry-challenge and chance for the development of new catalysts and materials. *Angew. Chem., Int. Ed.* **1999,** 38, 1216-1218.

135. Trapp, O.; Weber, S. K.; Bauch, S.; Hofstadt, W., High-throughput screening of catalysts by combining reaction and analysis. *Angew. Chem., Int. Ed.* **2007,** 46, 7307-7310.

136. Murphy, V.; Volpe, A. F.; Weinberg, W. H., High-throughput approaches to catalyst discovery. *Curr. Opin. Chem. Biol.* **2003,** 7, 427-433.

137. Schwalbe, T.; Kadzimirsz, D.; Jas, G., Synthesis of a library of Ciprofloxacin analogues by means of sequential organic synthesis in microreactors. *QSAR Comb. Sci.* **2005,** 24, 758-768.

138. Mitchell, T. N., Palladium-catalyzed reactions of organotin compounds. *Synthesis* **1992**, 803-15.

139. Silverwood, I.; McDougall, G.; Whittaker, G., Comparison of conventional versus microwave heating of the platinum catalysed oxidation of carbon monoxide over EUROPT-1 in a novel infrared microreactor cell. *J. Mol. Catal. A: Chem.* **2007,** 269, 1-4.

140. Tsukagoshi, K.; Jinno, N.; Nakajima, R., Development of a micro total analysis system incorporating chemiluminescence detection and application to detection of cancer markers. *Anal. Chem.* **2005,** 77, 1684-1688.

141. Marchand, G.; Dubois, P.; Delattre, C.; Vinet, F.; Blanchard-Desce, M.; Vaultier, M., Organic synthesis in soft wall-free microreactors: real-time monitoring of fluorogenic reactions. *Anal. Chem.* **2008,** 80, 6051-6055.

142. Hansen, C. L.; Classen, S.; Berger, J. M.; Quake, S. R., A microfluidic device for kinetic optimization of protein crystallization and in situ structure determination. *J. Am. Chem. Soc.* **2006,** 128, 3142-3143.

143. Krenkova, J.; Bilkova, Z.; Foret, F., Characterization of a monolithic immobilized trypsin microreactor with on-line coupling to ESI-MS. *J. Sep. Sci.* **2005,** 28, 1675-1684.

144. Korenaga, T., Development of a micro time-of-flight mass spectrometer suitable for micro total analysis system (micro TAS). *Nippon Nogei Kagaku Kaishi* **2003,** 77, 876-879.

145. Bouchard, L.-S.; Burt, S. R.; Anwar, M. S.; Kovtunov, K. V.; Koptyug, I. V.; Pines, A., NMR imaging of catalytic hydrogenation in microreactors with the use of para-hydrogen. *Science* **2008,** 319, 442-445.

146. Bonnet, E.; White, R. L., Catalytic microreactor with repetitive injection GC/MS effluent analysis. *Instrum. Sci. Technol.* **2001,** 29, 317-327.

147. Duan, J.; Liang, Z.; Yang, C.; Zhang, J.; Zhang, L.; Zhang, W.; Zhang, Y., Rapid protein identification using monolithic enzymatic microreactor and LC-ESI-MS/MS. *Proteomics* **2006,** 6, 412-419.

148. Shi, G.; Hong, F.; Liang, Q.; Fang, H.; Nelson, S.; Weber, S. G., Capillary-based, serial-loading, parallel microreactor for catalyst screening. *Anal. Chem.* **2006,** 78, 1972-1979.

149. Kikutani, Y.; Horiuchi, T.; Uchiyama, K.; Hisamoto, H.; Tokeshi, M.; Kitamori, T., Glass microchip with three-dimensional microchannel network for 2 * 2 parallel synthesis. *Lab Chip* **2002,** 2, 188-192.

150. de Mello, A. J., Control and detection of chemical reactions in microfluidic systems. *Nature* **2006,** 442, 394-402.

151. Kashid, M. N.; Rivas, D. F.; Agar, D. W.; Turek, S., On the hydrodynamics of liquid-liquid slug flow capillary microreactors. *Asia-Pac. J. Chem. Eng.* **2008,** 3, 151-160.

152. Dummann, G.; Quittmann, U.; Groschel, L.; Agar, D. W.; Worz, O.; Morgenschweis, K., The capillary-microreactor: a new reactor concept for the intensification of heat and mass transfer in liquid-liquid reactions. *Catal. Today* **2003,** 79-80, 433-439.

153. Kashid, M. N.; Agar, D. W., Hydrodynamics of liquid-liquid slug flow capillary microreactor: Flow regimes, slug size and pressure drop. *Chem. Eng. J.* **2007,** 131, 1-13.

154. De Bellefon, C.; Tanchoux, N.; Caravieilhes, S.; Grenoullet, P.; Hessel, V., Microreactors for dynamic, high-throughput screening of fluid/liquid molecular catalysis. *Angew. Chem., Int. Ed.* **2000,** 39, 3442-3445.

155. Yen, B. K. H.; Gunther, A.; Schmidt, M. A.; Jensen, K. F.; Bawendi, M. G., A microfabricated gas-liquid segmented flow reactor for high-temperature synthesis: The case of CdSe quantum dots. *Angew. Chem., Int. Ed.* **2005,** 44, 5447-5451.

156. Bringer, M. R.; Gerdts, C. J.; Song, H.; Tice, J. D.; Ismagilov, R. F., Microfluidic systems for chemical kinetics that rely on chaotic mixing in droplets. *Philos. Trans. R. Soc. London, Ser. A* **2004,** 362, 1087-1104.

157. Sucholeiki, I.; Editor, *High-Throughput Synthesis: Principles and Practices*. 2001; p 366.

158. Gross, G. A.; Mayer, G.; Albert, J.; Riester, D.; Osterodt, J.; Wurziger, H.; Schober, A., Spatially encoded single-bead Biginelli synthesis in a microstructured silicon array. *Angew. Chem., Int. Ed.* **2006,** 45, 3102-3106.

159. Gross, G. A.; Wurziger, H.; Schlingloff, G.; Schober, A., Microreactor array assembly, designed for diversity oriented synthesis using a multiple core structure library on solid support. *QSAR Comb. Sci.* **2006,** 25, 1055-1062.

160. Srivannavit, O. Design, fabrication and modeling of microreactor arrays for biochips and discovery research. *PhD Thesis,* University of Michigan, **2002**.

161. Yamamoto, T.; Hino, M.; Kakuhata, R.; Nojima, T.; Shinohara, Y.; Baba, Y.; Fujii, T., Evaluation of cell-free protein synthesis using PDMS-based microreactor arrays. *Anal. Sci.* **2008,** 24, 243-246.

162. Allwardt, A.; Holzmueller-Laue, S.; Wendler, C.; Stoll, N., A high parallel reaction system for efficient catalyst research. *Catal. Today* **2008,** 137, 11-16.

163. Cao, C.; Palo, D. R.; Tonkovich, A. L. Y.; Wang, Y., Catalyst screening and kinetic studies using microchannel reactors. *Catal. Today* **2007,** 125, 29-33.

164. Mies, M. J. M.; Rebrov, E. V.; Deutz, L.; Kleijn, C. R.; de Croon, M. H. J. M.; Schouten, J. C., Experimental Validation of the Performance of a microreactor for the high-throughput screening of catalytic coatings. *Ind. Eng. Chem. Res.* **2007,** 46, 3922-3931.

165. Mies, M. J. M.; Rebrov, E. V.; Schiepers, C. J. B. U.; de Croon, M. H. J. M.; Schouten, J. C., High-throughput screening of Co-BEA and Co-ZSM-5 coatings in the ammoxidation of ethylene to acetonitrile in a microstructured reactor. *Chem. Eng. Sci.* **2007,** 62, 5097-5101.

166. Quaade, U. J.; Hansen, O.; Johansson, S. M.; Jensen, S.; Thorsteinsson, S. Microreactor for controlling and studying chemical reactions. 2006-120135, 1897612, 20060905. 2008.

167. Zech, T.; Bohner, G.; Klein, J., High-throughput screening of supported catalysts in massively parallel single-bead microreactors: workflow aspects related to reactor bonding and catalyst preparation. *Catal. Today* **2005,** 110, 58-67.

168. Yi, J. P.; Fan, Z. G.; Jiang, Z. W.; Li, W. S.; Zhou, X. P., High-throughput parallel reactor system for propylene oxidation catalyst investigation. *J. Comb. Chem.* **2007,** 9, 1053-1059.

2.0 MICROREACTOR CONSTRUCTION AND VALIDATION BY THE STILLE REACTION

Some work in this section has been published in *Analytical Chemistry* **2006,** 78, (6), 1972-1979. Photographs are reproduced with permission from American Chemical Society (ACS).

2.1 INTRODUCTION

I aim to develop a novel microreactor system that is good for high-throughput screening of catalysts for either slow reactions or fast reactions. The prototype design of this microreactor[1], which was initialized by some previous lab colleagues, Guoyue Shi, Quansheng Liang and Feng Hong, was based on the simple idea of combining standard flow injection and continuous slug flow approach together with chromatography for quantitative online analysis. This microreactor is an integrated system including serial injection of reagents and catalysts by pumps, reacting in parallel in a long capillary and *in situ* analysis by GC or LC. All instruments and parts like pumps, capillaries, valves and detectors are commercially available and inexpensive, which makes this system very suitable for ordinary synthetic laboratory uses.

The Stille reaction is a well-known carbon-carbon bond formation process.[2-6] Soluble metal-ligand complexes catalysts are commonly used to catalyze the reaction. The large number of metal precatalysts and ligands suggests a combinatorial approach for catalyst discovery. Thus,

this reaction will be a good model to test the efficacy of the microreactor for homogeneous catalyst screening. The preliminary validation work was mostly done by Guoyue Shi and other colleagues. I collaborated with them on some testing experiments that will be described in this context.

2.2 EXPERIMENTAL SECTION

2.2.1 Chemicals and Materials

HPLC grade methanol, tetrahydrofuran, Tributyl (vinyl) tin, iodobenzene, dodecane and styrene were purchased from Sigma (St.Louis, MO). Neutral red was purchased from J. T. Baker Chemical Co. (Phillipsburg, NJ). The ligands, $AsPh_3$, PPh_3, $(2\text{-furyl})_3P$, $(4\text{-}FC_6H_4)_3P$ and $(4\text{-}ClC_6H_4)_3P$ were also purchased from Sigma. The palladium precatalysts, Pd_2dba_3, $Pd[(C_6H_5)_3P]_4$, $Pd[(C_6H_5)_3P]_4$, $PdCl_2[(C_6H_5)_3P]_2$, $Pd(OAC)_2$ were purchased from Strem Chemicals (Newburyport, MA). $PdCl_2(CH_3CN)_2$ was locally synthesized in Dr. Nelson's lab. Nitrogen, argon, hydrogen and air were obtained from Valley National Gases Inc. (Washington, PA)

2.2.2 Instrumentation

Syringe pumps were purchased from Harvard Apparatus Inc. (Holliston, MA). The Waters M-45 pump was from Waters Corp. (Milford, MA). The HP 1050 autosampler was purchased from Agilent (Palo Alto, CA). VICI six-port injector (Model E60), VICI 10-port valve (model EPCA-CE) and M6 pump were purchased from Valco Instruments Co, Inc. (Houston, TX). A USB

2000 optical fiber UV-visible absorbance detector was purchased from Ocean Optics, Inc. (Dunedin, FL). The heater for the reactor capillary was constructed locally. The temperature controller and standard round mica heater were from Minco Products Inc. (Minneapolis, MN). The fused-silica capillary with 75-μm i.d., 360-μm o.d. was purchased from Polymicro Technologies, L.L.C (Phoenix, AZ). The Focus GC was purchased from Thermo-Electron. It has a single column (RTX-5, 7 m × 0.32 mm (0.25-μm thick phase), Restek Corporation) and detector (FID).

2.2.3 Microreactor construction

This microreactor system, which is schematically shown in Figure 11, includes three basic modules: sample loading section, parallel reaction section and online analysis section. A standard HPLC autosampler loads vials of catalysts. Catalysts sampled by the autosampler are combined with reagents pushed by a syringe pump (SP1) at equal flow rates (15 μL/min) in a locally-made nano-volume tee mixer.[7, 8] The combined fluids pass through and fill a loop (750 nL) in a 6-port nano-volume injector (L1). Then the injector is switched to the 'inject' position triggered by the autosampler program and the contents of the loop are injected into the reaction capillary by another syringe pump (SP2) filled with THF solvent operating at a constant rate of 250 nL/min. Following injection, the injector is returned to the 'load' position. The 750 nL loop is then filled with a solution containing the next catalyst and reagents. The cycling of autosampler injection and injector turning will push a serial of reaction solutions containing same reagents and different catalysts into the reaction capillary that are defined as parallel reaction zones. Individual zone contains 750 nL of reaction solution and separated by THF solvent from SP2. The original reactor design does not include filters in the flow stream between the autosampler

and the 750 nL loop;[1] however, in order to prevent any particulates entering the nano-volume injector and reaction capillary, an ultra-low-volume precolumn filters with 0.5 µm stainless steel frits (Upchurch Scientific, Inc., Oak Harbor, WA) is installed at four positions in the flow stream, which are shown in Scheme 2 depicted as green bars.

The reaction capillary is a 75-µm-i.d., 6.7-m-long piece of fused-silica capillary tube. It is directly connected to the injector L1. When all reaction zones are loaded into it, a digitally-controlled heater can warm the capillary to the required temperature and the flow from SP2 can be stopped for a defined reaction time. Then all reactions take place in individual zones in a static mode just like batch reactor.

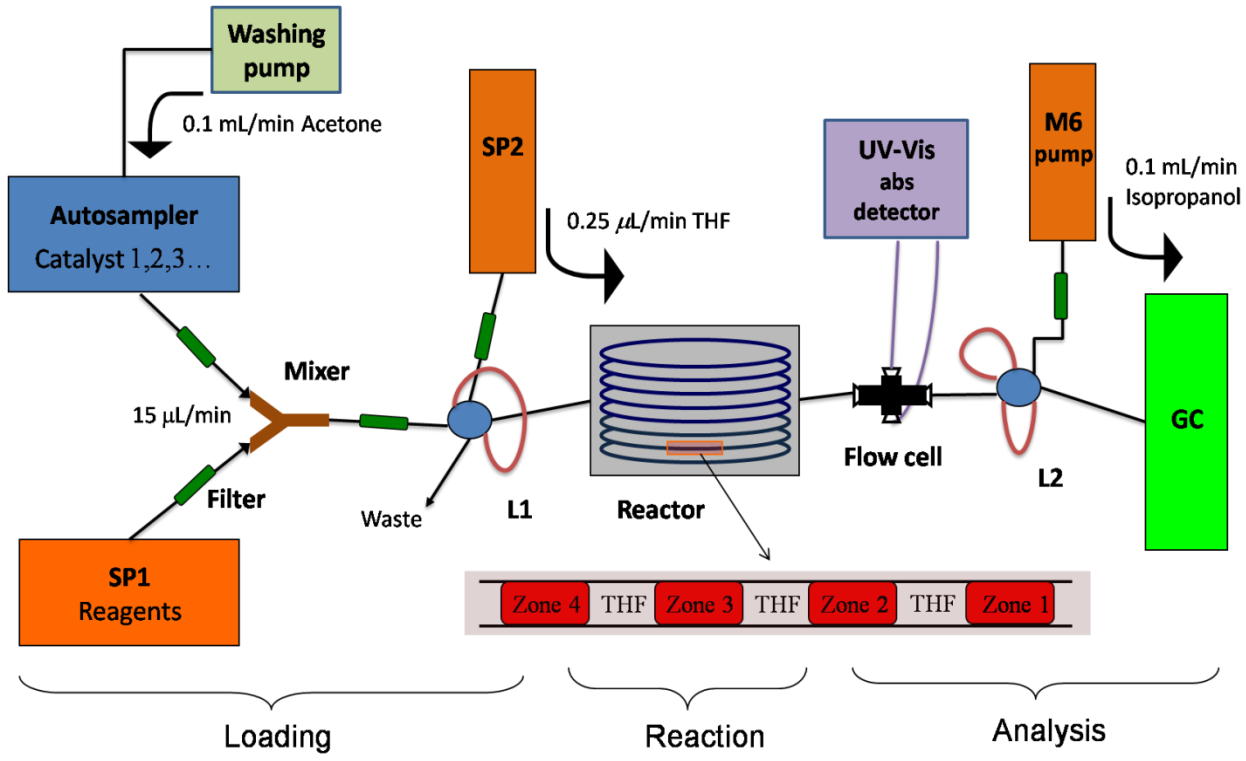

Figure 11. Schematic view of the microreactor screening system.

When the reactions are completed, the flow from SP2 is turned on again to push the zones continuously out of the reaction capillary. The zones first go through a cross-shaped flow cell monitored by a UV-Vis, fiber optic-based detector which captures the absorbance signal from zones and send signals to the computer to trigger the online injection process. A 10-port double-loop (750 nL) nano-volume injector (L2) enables the loading of one loop from the capillary while the contents of the other loop are chromatographed. The contents of the 750 nL loop are pushed into the GC with a low-pressure, refillable M6 pump that can deliver a short pulse flow at high rate 100 μL/min. The whole chromatographic injection and analysis process is under automated control by a self-written screening software.

2.2.4 Online analysis by GC

The initial oven temperature of 85 ℃ was held for 0.8 min. The temperature was then increased from 85 ℃ to 200 ℃ at 100 ℃/min. Two minutes was allowed for cooling. Typically, flow-splitting was used to inject 10% of the 1.0-μL loop contents. A programmed M6 pump filled with isopropanol pushed the contents in the loop into the GC inlet at a flow rate of 100 μL/min for a duration time of 3 seconds. GC was triggered to start running at the same time of sample injection by the M6 pump.

2.2.5 Screening of catalysts for the Stille reaction

The Stille reaction was carried out in the microreactor at 50˚C in anhydrous THF solvent. A group of precatalysts, Pd_2dba_3, $Pd[(C_6H_5)_3P]_4$, $Pd[(C_6H_5)_3P]_4$, $PdCl_2[(C_6H_5)_3P]_2$, $Pd(OAC)_2$ and $PdCl_2(CH_3CN)_2$, and a group of ligands, $AsPh_3$, PPh_3, $(2\text{-furyl})_3P$, $(4\text{-}FC_6H_4)_3P$ and $(4\text{-}ClC_6H_4)_3P$

were selected to create the model catalyst library for the screening experiment. Various molar equivalents of palladium precatalysts and ligands were mixed in 6mL of THF to form the catalyst. The aliquots (100 μL) of catalyst solutions were hold in 1.5 mL autosampler vials and placed on the tray of the autosampler. A mixture of 75 μL of PhI and 250 μL of $Bu_3SnCH=CH_2$ in 3 mL THF were taken as the reactants which also contain 24 μL of dodecane as the internal standard. Reactants were loaded in gas-tight syringe and driven by SP1 in a constant flow. The autosampler was cycling to inject all catalyst solutions. After loading all reaction zones into the capillary, SP2 was turned off to stop the flow and the heater was turned on. Then the reactions were carried out in the reactor for varying times at a certain temperature. When reaction was complete, SP2 was turned on and all reaction zones were pushed out of the capillary and analyzed as described above.

2.2.6 Statistical calculation of yield

A calibration curve was prepared from standard solutions of styrene and the internal standard (IS) dodecane. A series of stock solutions with various mole ratios of styrene and IS were prepared in THF to obtain standards for GC analysis. The calibration curve for product yield determination was obtained by plotting the mole ratios of styrene to IS as a function of peak area ratios of styrene to IS.

2.3 RESULTS AND DISCUSSION

2.3.1 Microreactor operation mechanism

Sample injection by syringe pump and autosampler

I used a syringe pump to load reagents continuously into a six-port dual-position injector. A standard HP 1050 autosampler loads catalysts serially into the injector. Two flow streams are mixed first at equal flow rates, which are optimal at 15 µL/min, to ensure equal proportion of reagent and catalyst. The combined solutions then fill the loop and are injected into the capillary reactor by SP2. The schematic view of the injection section of the microreactor is shown in Figure 12.

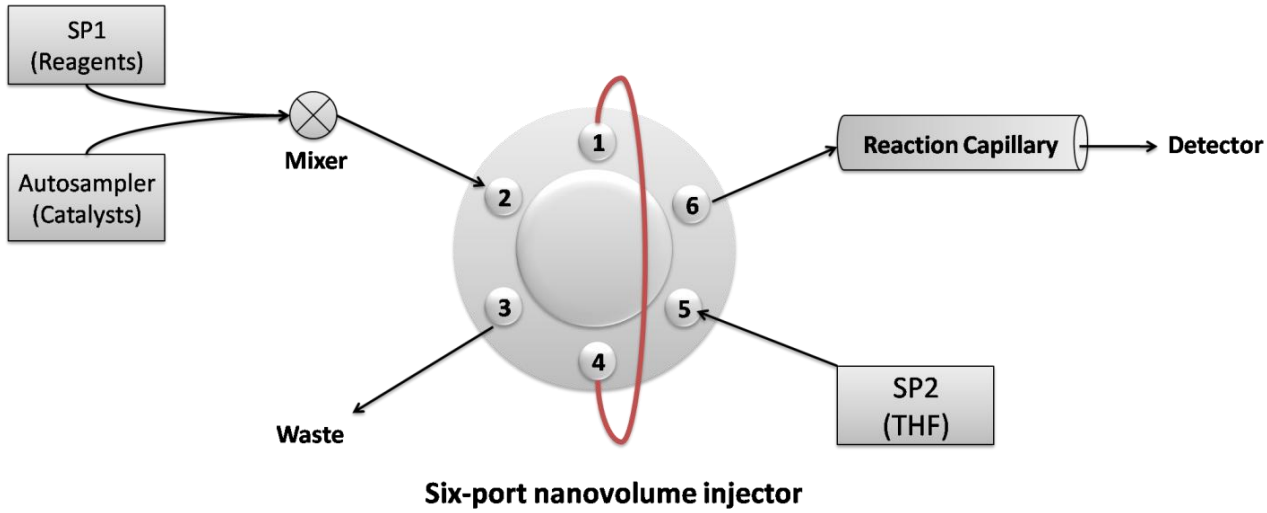

Figure 12. Schematic view of the sample loading section of the microreactor system.

The autosampler is claimed as capable of microliter sampling; however, in fact it is not so reliable for injecting volumes of samples less than tens of microliters. To have a reproducible microscale injection for each sample, I changed the typical functioning program of the

autosampler to let the internal syringe aspirate the sample from the vial and then eject the sample into the injection port that connects to the mixer by a short capillary. This procedure skips the function of autosampler pump and is very effective to create a significant wide plateau in the concentration-time profile of samples emanating from the autosampler when 25 μL of samples are withdrawn. This enables catalysts to be injected into the six-port injector with reproducible volumes and concentrations, which is very important for reaction reproducibility and screening reliability. To minimize the carryover of serial injections by the autosampler, a regular HPLC pump is connected to wash internal tubes and the needle of the autosampler between adjacent catalyst injections by setting the functions of the autosampler. Thus, the autosampler is the key controller of the injection section of this microreactor.

Parallel reactions in the capillary

All reaction samples are injected into the reaction capillary by SP2. The flow rate of SP2 controls the residence time of reaction zones in the capillary when continuous-flow mode is applied. However, for slow reactions with long reaction time like the Stille reaction which usually takes 5 h or more, a stop-flow approach is better for the throughput. Reaction zones are loaded in the capillary and then SP2 flow is stopped, so all zones stay and react in parallel for the required time. When reactions finish, SP2 is turned on and all zones are pushed serially out of the capillary.

An important concern for this parallel reaction method is bandspreading between adjacent zones caused by hydrodynamic dispersion. Unlike the typical slug-flow approach that employs immiscible biphase liquids, I used the same solvent THF to separate reaction zones whose solvent is also THF. This single phase approach avoids the usage of expensive fluorous solvents that needs additional efforts for recycling; however, the single phase method may result

in bandspreading of zones in the open capillary like chromatography peaks, leading to unwanted reaction zone overlapping. Therefore, small-diameter capillary tubing has to be used because axial dispersion of molecules can be markedly lessened when channel dimension is downsized to a certain extent. However, it is obvious that the smaller the channel dimensions, the higher the flow backpressures, especially for a long capillary. In our experiment, I used 75 μm i.d. tubing as the reaction capillary that is small enough and backpressure is still tolerable for syringe pump.

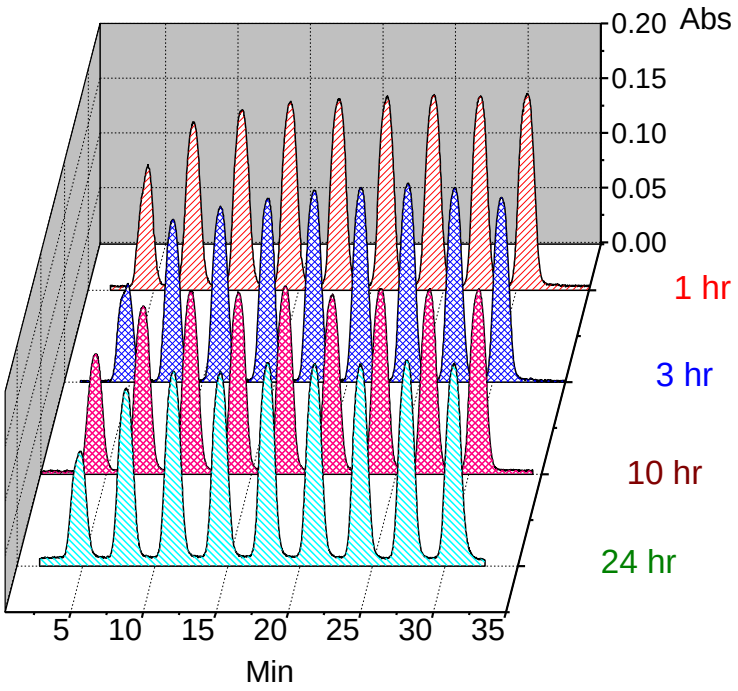

Figure 13. Absorbance response (wavelength 525 nm) of parallel zones of neutral red solution staying in the reactor capillary at varied residence times.

(Photograph is reproduced with permission from ACS.[1])

Due to the bandspreading, it is necessary to control the distance between adjacent reactions zones. The zone that is filled with solvent THF is defined as non-reactive zone whose

length is controlled by time. Two times play roles: one is the time required by the autosampler to withdraw the catalyst and eject it into the loop of six-port injector. It is the sample loading time controlled by sampling rate of the autosampler, which dictates the non-reactive zone length (time). The other is the time needed to empty the loop and inject sample into the reactor, which is the reaction zone time. SP2 rate and loop size control this time. SP2 also controls the velocity of zones flowing in the reactor. When a small loop 750 nL is used, SP2 flow rate and above two times are primarily responsible for the bandspreading and the total time needed to fill and empty all zones through the reactor capillary. In Figure 13, I tested zone bandspreading with neutral red solutions. Absorbances were detected by a UV-Vis optical fiber detector at 530 nm. The neural solution was made by THF, same to the carrier solvent THF of SP2. The zones are loaded into the reactor and stayed for different times. It shows that there is no significant difference of zone widths between 24 h and 1 h. Actually, absorbance signals of all four times seem identical, indicating bandspreading of zones mainly comes from flow dispersion while static diffusion leads to only little broadening when zones stay in the capillary without moving.

Automated analysis by online GC

The analysis section includes an optic fiber UV-Vis detector, a 10-port double-loop double-position injector, a M6 pump and a GC system without autosampler. The schematic view of the analyzer section is shown in Figure 14.

When reaction time is reached, SP2 is then turned on and all zones are pushed out of the reactor capillary in sequence. Zones first go through a cross-shape flow cell which is connected to a fiber optic UV-Vis detector. The absorbance response of zones captured by the detector is sent to a screening software written by our lab which is used to trigger the injector switch and start the GC program. The software window is shown in Figure 15. I can set a number of

parameters in this software, in which I empirically define the start of a zone as 0.8 (absorbance ascending) and the end as 0.2 (absorbance descending). When the absorbance signal of a zone reaches the end point 0.2, the software will alert the injector to switch positions so that the just-detected zone is captured and sent to GC inlet by a M-6 pump for chromatographic analysis.

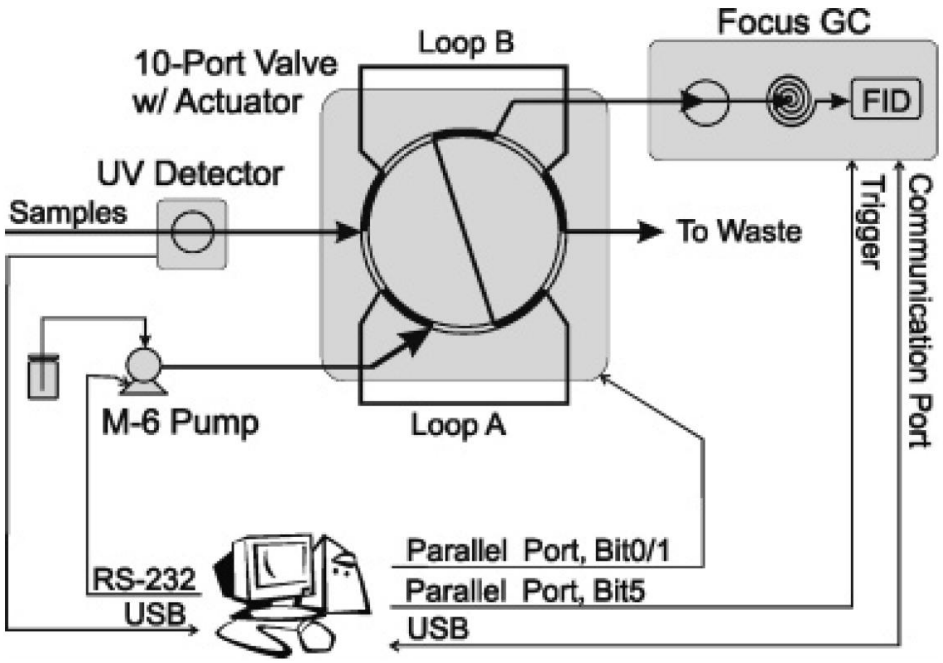

Figure 14. The schematic view of the analysis section of the microreactor system.

(Photograph is reproduced with permission from ACS.[1])

A very short capillary connects the flow cell (UV-Vis detector) to the 10-port injector. After zones leave the detection point of the cell, they will immediately enter the loop of the injector. The 10-port injector has two loops, and the configuration of flow path enables one loop connecting to the reactor outlet while the other connecting to the GC inlet. The alternating switch of two positions A and B makes it possible to conduct sample loading and GC analysis simultaneously and continuously. The schematic view of 10-port injector is shown in Figure 16.

The switch of the injector is automatically controlled by the screening software whose signals come from absorbance response of zones captured by the UV-Vis detector.

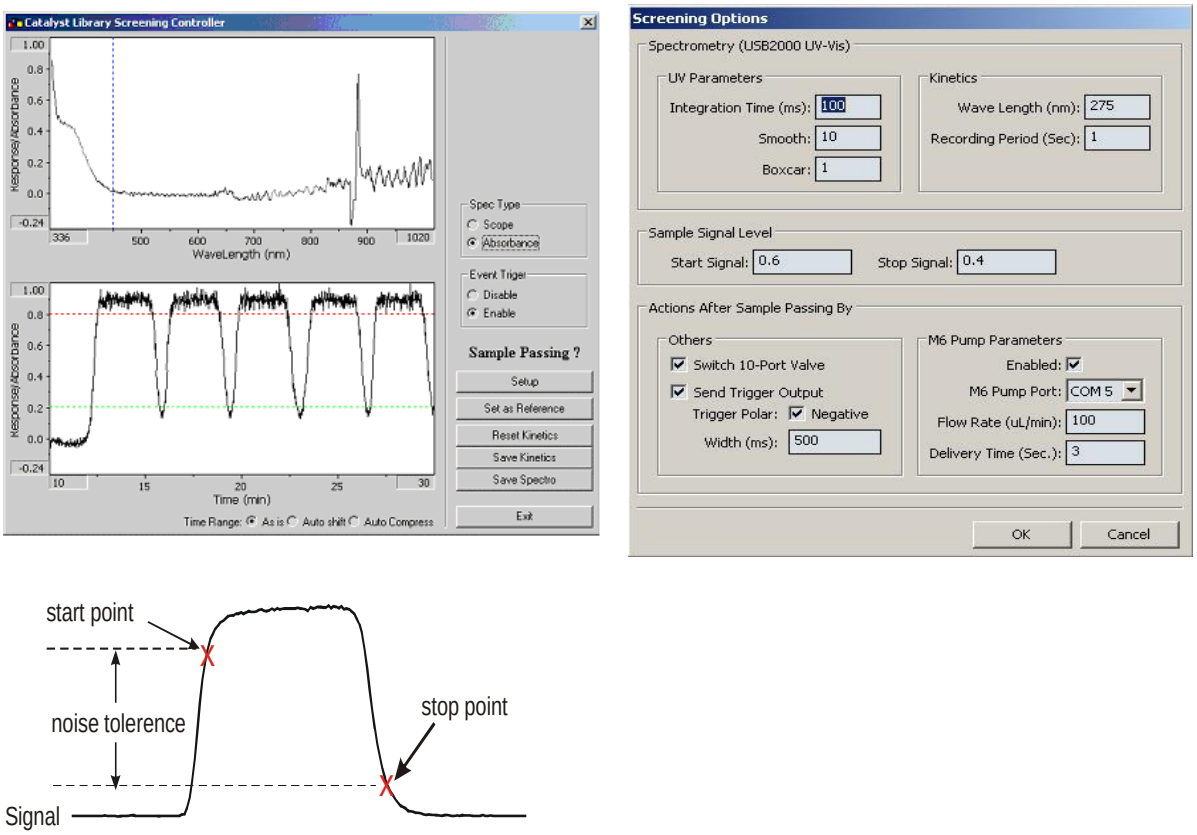

Figure 15. The screening software window and its controlling parameters.

A short capillary is used to connect the 10-port injector with the GC inlet. The capillary is inserted directly into the vaporization chamber of GC through the septum. The M6 pump, which is also controlled by the screening software, delivers a high-speed pulse of flow to push the contents of the loop into the GC inlet. GC, in the same time, starts the temperature program to analyze the reaction sample.

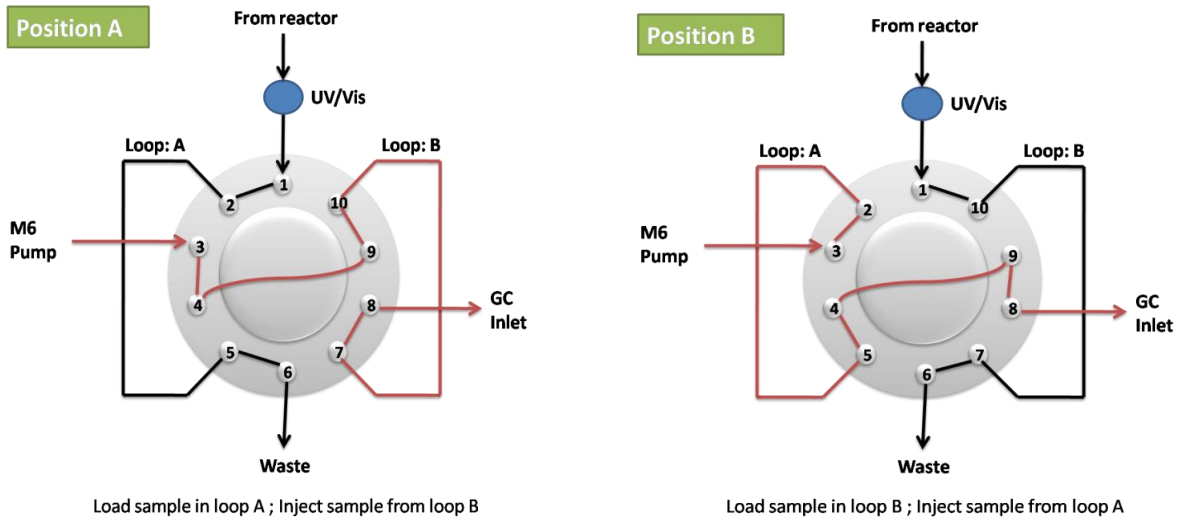

Figure 16. The schematic view of the 10-port double-loop injector working at two positions A and B for simultaneous loading and injection.

The whole analysis process is automated under the computer control with the aid of the self-programmed screening software. When UV-Vis detector sense a reaction zone loaded into the loop, 10-port injector valve, M6 pump and GC are all triggered in a synchronized manner, which ensures automated analysis without any human involvement.

2.3.2 The Stille reaction and GC separation

The Stille reaction is a well-studied carbon-carbon formation process which is usually catalyzed by palladium-ligand complex catalysts. The activity of catalysts largely depends on the combination of palladium precatalysts and the ligands. A diverse set of catalysts can be generated based on the combinatorial coupling of metals and ligands. Thus, this process is very suitable to validate the microreactor's efficiency and robustness. A model reaction of

iodobenzene and tributyl (vinyl) tin is shown below. Both substrate and product styrene are commerically available and appropriate for GC analysis.

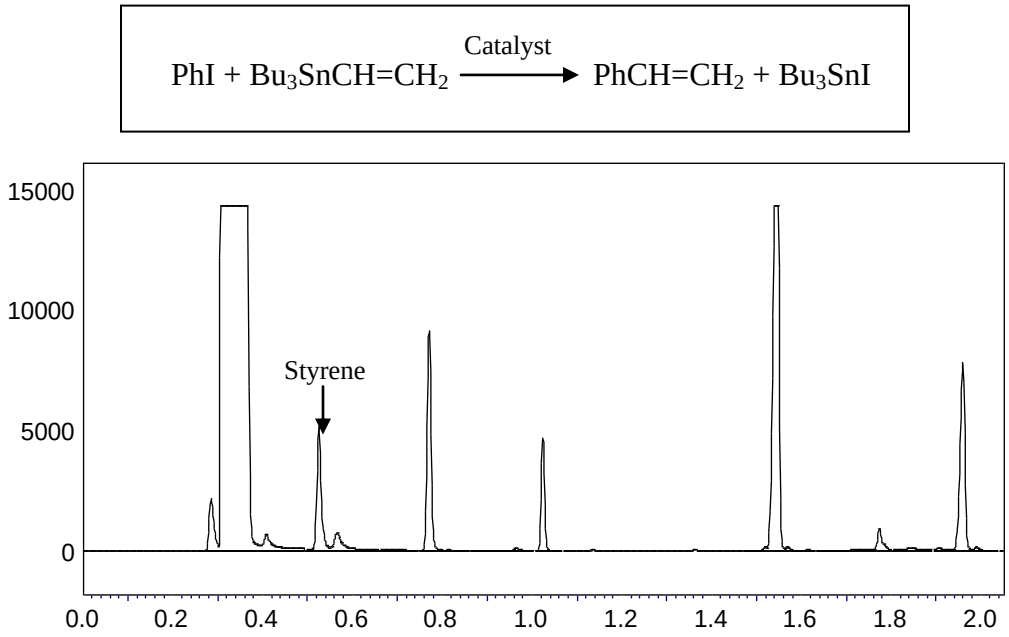

Figure 17. Chromatogram of products of the Stille reaction by online GC.

GC is used to analyze reaction outcomes and determine product yield. Besides the substrates, there are a few by-product peaks eluted later behind styrene (Figure 17). A calibration curve made from standard solutions of styrene and dodecane are used to quantify the yield. The curve for styrene/dodecane is farily linear (R^2=0.997) in the range from 0 to 100% yield.

2.3.3 Screening efficiency and microreactor performance

Parallel reactions are carried out in the microreactor and the maximum number of reactions in a 6.7-meter-long reaction capillary is 20 reactions under non-optimized conditions. More reactions can be done in a longer reactor capillary. The UV response of 20 zones coming out of the

capillary is shown in Figure 18. Since reaction time is 5 h, after loading all reaction zones, I stop the flow and let all zones stay in the capillary for 5 h at 50 ^{o}C. Referring to Figure 18, I see all zones are well separated with only a little overlapping.

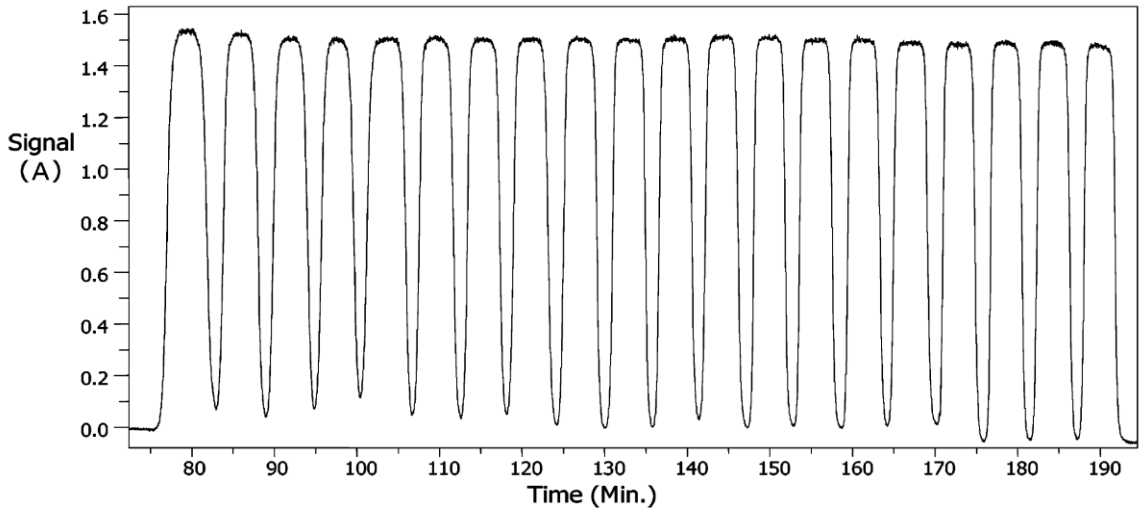

Figure 18. UV absorbance of 20 Stille reaction zones passing through the fiber optic UV detector after flowing out of the reactor outlet.

(Photograph is reproduced with permission from ACS.[1])

A small library of palladium precatalysts includes Pd_2dba_3, $Pd[(C_6H_5)_3P]_4$, $PdCl_2(C_6H_5CN)_2$, $PdCl_2[(C_6H_5)_3P]_2$, $Pd(OAC)_2$ and $PdCl_2(CH_3CN)_2$, and a library of ligands includes $AsPh_3$, PPh_3, $(2\text{-furyl})_3P$, $(4\text{-}FC_6H_4)_3P$ and $(4\text{-}ClC_6H_4)_3P$. The screening results are shown in Table 1. Precatalysts were first screened with a common good ligand $AsPh_3$ and the best one $PdCl_2(CH_3CN)_2$ was used to test a number of ligands under other identical conditions. The best ligand is still $AsPh_3$, which is in good accordance with the literature.[9] All catalysts were repeated in three successive reactions for statistical calculation and small standard deviations of yields indicate good reaction reproducibility in the microreactor.

Table 1. Yield of the Stille reaction with various palladium precatalysts and ligands.

Precatalysts	**Pd_2dba_3**	**$Pd[(C_6H_5)_3P]_4$**	**$PdCl_2(C_6H_5CN)_2$**	**$PdCl_2(CH_3CN)_2$**	**$PdCl_2[(C_6H_5)_3P]_2$**	**$Pd(OAC)_2$**
Yield (%)[a]	49.2 ±0.9	38.0 ±0.7	43.8 ±0.7	50.7 ±1.1	15.9 ±0.7	23.0 ±1.5
Ligands	**$AsPh_3$**	**PPh_3**	**$(2\text{-furyl})_3P$**	**$(4\text{-}FC_6H_4)_3P$**	**$(4\text{-}ClC_6H_4)_3P$**	
Yield (%)[b]	51.7 ±0.7	28.5 ±0.5	40.0 ±0.7	21.1 ±0.7	15.5 ±0.4	

[a] Reactants: 75 μL PhI + 250 μL $Bu_3SnCH=CH_2$ + 24 μL dodecane + 3 mL THF ; Catalysts: Pd compound (2 mole %)+ 8.2 mg $AsPh_3$ (4 mole %) + 3 mL THF, 50 °C for 5h in the microreactor. Results are shown as mean ± SEM, n=3.

[b] Reactants: 75 μL PhI + 250 μL $Bu_3SnCH=CH2$ + 24 μL dodecane + 3 mL THF ; Catalysts: $PdCl_2(CH_3CN)_2$ (2 mole %) + ligand (4 mole %)+ 3 mL THF, 50 °C for 5h in the microreactor. Results are shown as mean ± SEM, n=3.

The strength of this microreactor is not only for high-throughput catalyst screening, but can conduct process optimization by studying a large number of reaction parameters in a high efficient manner. After finding out the best precatalyst and ligand, I used the microreactor to optimize the ratio of precatalyst to ligand which plays a key role in catalyst reactivity. The results in Figure 19 show that the yield of styrene is only ~35% with 2 mole % $AsPh_3$ and 2 mole % $PdCl_2(CH_3CN)_2$; however, it increases to 65% as $AsPh_3$ increases to 6 mole % while the yield is reaching a plateau up to 12 mole %. I conclude that the catalyst composed of 2 mole % $PdCl_2(CH_3CN)_2$ and 6 mole % $AsPh_3$ is the most active. This stoichiometry was in accordance with batch synthesis,[9, 10] validating the screening efficacy of this microreactor system.

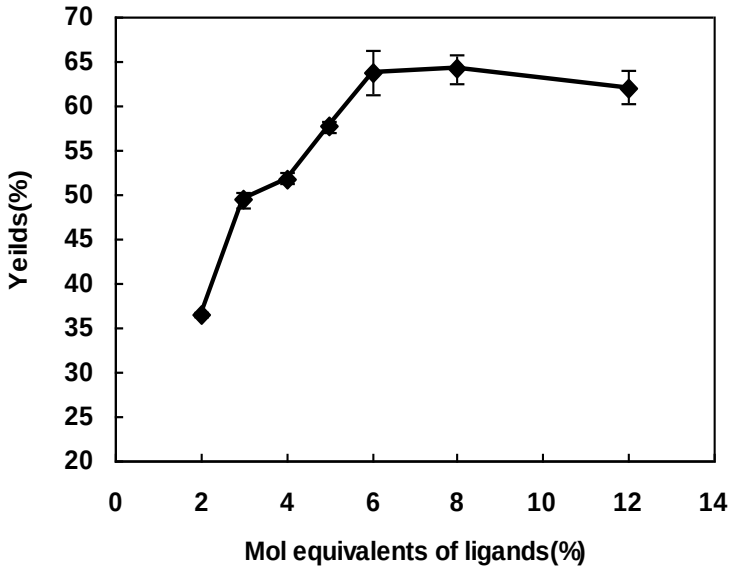

Figure 19. Yields of the Stille reaction with as a function of molar equivalents of $AsPh_3$ and $PdCl_2(CH_3CN)_2$.

(Photograph is reproduced with permission from ACS.[1])

2.4 CONCLUSION

In this section, the microreactor screening system based on capillaries and instruments were established and validated with the well-studied Stille reaction. Microliter volumes of reagents and catalysts can be combined and reacted in this capillary-based reactor for specific time and temperature. Online GC analyzed reaction products. The preliminary screening of six palladium precatalysts and five ligands were carried out in a high throughput approach and the investigation of mole ratios of precatalyst to ligand indicated $PdCl_2(CH_3CN)_2$ (2 mole %) and $AsPh_3$ (6 mole %) are the optimum catalyst which agrees with the traditional synthesis very well. It convinces the efficiency and efficacy of this microreactor system for high-throughput catalyst screening.

BIBLIOGRAPHY

1. Shi, G.; Hong, F.; Liang, Q.; Fang, H.; Nelson, S.; Weber, S. G., Capillary-based, serial-loading, parallel microreactor for catalyst screening. *Anal. Chem.* **2006,** 78, 1972-1979.

2. Burgess, K., Organometallic chemistry. *Chem. Ind.* **2001**, 189-190.

3. Littke, A. F.; Schwarz, L.; Fu, G. C., Pd/P(t-Bu)3: A mild and general catalyst for Stille reactions of aryl chlorides and aryl bromides. *J. Am. Chem. Soc.* **2002,** 124, 6343-6348.

4. Mitchell, T. N., Palladium-catalyzed reactions of organotin compounds. *Synthesis* **1992**, 803-15.

5. Su, W.; Urgaonkar, S.; McLaughlin, P. A.; Verkade, J. G., Highly active palladium catalysts supported by bulky proazaphosphatrane ligands for Stille cross-coupling: Coupling of aryl and vinyl chlorides, room temperature coupling of aryl bromides, coupling of aryl triflates, and synthesis of sterically hindered biaryls. *J. Am. Chem. Soc.* **2004,** 126, 16433-16439.

6. Su, W.; Urgaonkar, S.; Verkade, J. G., $Pd_2(dba)_3$/P(*i*-$BuNCH_2CH_2)_3N$-catalyzed Stille cross-coupling of aryl chlorides. *Org. Lett.* **2004,** 6, 1421-1424.

7. Beisler, A. T.; Sahlin, E.; Schaefer, K. E.; Weber, S. G., Analysis of the performance of a flow reactor for use with microcolumn HPLC. *Anal. Chem.* **2004,** 76, 639-645.

8. Sahlin, E.; ter Halle, A.; Schaefer, K.; Horn, J.; Then, M.; Weber, S. G., Miniaturized electrochemical flow cells. *Anal. Chem.* **2003,** 75, 1031-1036.

9. Farina, V.; Krishnan, B., Large rate accelerations in the Stille reaction with tri-2-furylphosphine and triphenylarsine as palladium ligands: mechanistic and synthetic implications. *J. Am. Chem. Soc.* **1991,** 113, 9585-95.

10. Scrivanti, A.; Matteoli, U.; Beghetto, V.; Antonaroli, S.; Crociani, B., Iminophosphine-palladium(0) complexes as catalysts for the Stille reaction. *Tetrahedron* **2002,** 58, 6881-6886.

3.0 PEPTIDE SCREENING FOR THE ALDOL REACTION

3.1 INTRODUCTION

In this section, I applied the microreactor system for studying the peptide-catalyzed direct asymmetric aldol reaction. The aldol reaction is one of the most powerful and best-studied carbon-carbon bond forming processes. Peptides and peptidomimetics represent novel organocatalysts for this reaction.[1-5] Compared to traditional metal based complex catalysts, e.g., for Stille reaction, peptides have many advantages: they are essentially non-toxic, possess high reactivity, relatively cheap and scaleable, and often demonstrate excellent regio- and enantioselectivity. They are also readily customized and work under benign reaction conditions. Peptides are believed to have better catalytic reactivity and selectivity than smaller organocatalysts such as L-proline because of their more complex structures and diverse functionalities.[6] However, most active catalysts discovered so far are proline-terminal peptides, representing only a small portion of the whole peptide family. I wonder if I could take advantage of the microreactor approach to explore a broad range of peptides facilitating the discovery of novel peptide catalysts for the aldol reaction.

I screened 21 commercially available amino acids in the microreactor initially for validation of the general approach. Subsequently, I screened 27 commercially available, short peptides in the microreactor. A major difficulty was the poor solubility of some amino acids and

peptides in common organic solvents. I solved this problem by allowing a condensation reaction to occur between peptides and benzaldehyde, one of the reaction substrates, followed by loading the resulting complex into the microreactor. The screening results demonstrated that γ-Glu- and β-Asp-containing peptides had better reactivity than other peptides. Catalytic activities determined in the microreactor were mostly in agreement with bench-top reactions under similar conditions. This work supports the idea that the structure of N-terminal amino acid has an important impact on the catalytic activity of the peptide. Enantioselectivities of reactive peptides were determined by analysis of bench-top reactions with chiral normal-phase HPLC. With this catalyst preparation approach, it is possible to screen peptide catalysts with various molecular weights and avoid solubility problems.

3.2 EXPERIMENTAL SECTION

3.2.1 Chemicals and Materials

HPLC grade acetonitrile, acetone, tetrahydrofuran (THF) and dodecane were purchased from Sigma (St.Louis, MO). ACS grade dimethyl sulfoxide (DMSO) and dimethylformamide (DMF) were purchased from J.T. Baker Chemical Co. (Phillipsburgh, NJ). Benzaldehyde, trans-4-phenyl-3-buten-2-one and L-(-)-proline were purchased from Acros (Morris Plains, NJ). Ethyl acetate, hexanes and isopropanol were purchased from EMD Chemicals Inc. (Gibbstown, NJ). L-alanine, L-valine, L-arginine, L-isoleucine, L-serine, L-leucine, L-lysine, L-histidine, L-phenylalanine, L-threonine, L-tyrosine, L-methionine, glycine, L-proline, *trans*-4-hydroxy-L-proline, L-glutamine, L-cystine, L-cysteine, L-glutamic acid, L-tryptophan, and L-asparagine were

purchased from Sigma (St.Louis, MO). Pro-Gly and Pro-Phe were purchased from Bachem (San Carlos, CA). Ala-Ala, $(Ala)_3$, $(Ala)_4$, β-Ala-Ala, Ala-Gly, β-Ala-Gly, Gly-Trp, Gly-Phe, Gly-Phe-NH_2, Asp-Ala, Asp-Gly, Asp-Val, α-Glu-Trp, α-Glu-Val, γ-Glu-Val, γ-Glu-Glu, γ-Glu-Gly, reduced L-glutathione (γ-Glu-Cys-Gly, GSH), oxidized L-glutathione (GSSG), *p*-Glu-His, *p*-Glu-Gly-Arg-Phe, β-Asp-Ala, β-Asp-Gly, β-Asp-Val, and albumin were purchased from Sigma (St.Louis, MO). Nitrogen, argon, hydrogen and compressed air were purchased from Valley National Gases Inc. (Washington, PA).

3.2.2 Instrumentation

Syringe pumps were purchased from Harvard Apparatus Inc. (Holliston, MA). The Waters M-45 pump was from Waters Corp. (Milford, MA). The HP 1050 autosampler was purchased from Agilent (Palo Alto, CA). VICI six-port injector (Model E60), VICI 10-port valve (model EPCA-CE) and a pump (M6) for injection into the GC were purchased from Valco Instruments Co, Inc. (Houston, TX). A USB 2000 optical fiber UV-visible absorbance detector was purchased from Ocean Optics, Inc. (Dunedin, FL). The heater for organic reactions was constructed locally. The temperature controller and standard round mica heater was from Minco Products Inc. (Minneapolis, MN). The fused-silica capillary with 75-μm i.d., 360-μm o.d. that was used as the reactor was purchased from Polymicro Technologies, L.L.C (Phoenix, AZ). The Focus GC was purchased from Thermo-Electron. It has a single column (RTX-5, 7 m × 0.32 mm (0.25-μm thick phase)) and detector (FID). The *X-LC* (UHPLC) was purchased from Jasco, Inc. The CHIRALPAK IA column (2.1 mm × 150 mm, 5 μm) was purchased from Daicel Chemical Industries, LTD).

3.2.3 Bench-top reactions

The general procedures for the conventional bench-top aldol reactions followed a literature precedence.[7] Amino acids or peptides (10 mole %) were suspended in 1 mL of a DMSO:acetone (4:1 v/v) mixture containing 0.2 mmol aromatic aldehyde (benzaldehyde/*p*-nitrobenzaldehyde). The mixture was stirred at room temperature for 24 h. The reaction yields were determined by GC analysis. To get pure products, reactions were quenched by adding 1 mL of sat. aq. NH_4Cl solution. The precipitated catalysts were removed with a syringe filter and the filtrate was extracted twice with 2 mL of ethyl acetate. The combined organic layers were washed with 1 mL of sat. aq. NaCl and dried (Na_2SO_4). Then, all volatile components were removed in vacuo by rotary evaporation and the residue was purified by chromatography on SiO_2. (hexanes:ethyl acetate, 1:3 (v/v), 40–63 μm particle size, 60 Å pore, Sorbent Technologies, Inc., Atlanta, GA).

^{1}H NMR spectra (see Appendix C) were recorded on a Brucker-300 MHz spectrometer. They were in accordance with the literature.[7] The enantiomeric excess of aldol product was determined by HPLC (Jasco XLC) with a Daicel CHIRALPAK IA column. Separation conditions: isocratic i-PrOH:hexanes, 5:95 (v/v), flow rate 0.22 mL/min, 25 ^oC, injection volume 0.5 μL, UV-Vis absorbance detector at 210 nm. The retention times t_R for the enantiomers are 8.45 min and 9.12 min.

4-Hydroxy-4-phenyl-butan-2-one: ^{1}H NMR (300 MHz, $CDCl_3$) δ 7.23-7.36 (m, 5H), 5.14 (dd, 1H), 3.26 (brs, 1H), 2.83 (2×dd, 2H), 2.18 (s, 3H).

4-Hydroxy-4-(4'-nitrophenyl)-butan-2-one: ^{1}H NMR (300 MHz, $CDCl_3$) δ 8.20 (d, J = 8.7 Hz, 2H), 7.53 (d, J= 8.7 Hz, 2H), 5.25 (m, 1H), 3.56 (d, J = 3.3 Hz, 1H), 2.83 (m, 2H), 2.20 (s, 3H).

3.2.4 GC analysis of aldol products

The initial oven temperature of 80 °C was held for 0.3 min. The temperature was increased from 80 °C to 200 °C at 100 °C/min. Two minutes were allowed for cooling. Typically, flow-splitting was used to inject 5% of the 750-nL reaction mixture into the loop. A programmed M6 pump filled with isopropanol pushed the contents in the loop into the GC inlet at a flow rate of 100 μL/min with a duration time of 3 seconds. GC was triggered to start analysis at the same time of sample injection by the M6 pump.

3.2.5 Screening experiments in the microreactor

Preparation of catalyst solutions:

Amino acids or peptides (10 mole %) were suspended in 1 mL of DMSO with 0.2 mmol of benzaldehyde and stirred at room temperature until the catalysts were totally soluble.

Screening of amino acids and peptides:

The aldol reaction was carried out in DMSO:acetone (1:1) at room temperature for 24 h. Solutions of amino acid or peptide catalysts in DMSO were placed into 1.5-mL glass autosampler vials. The catalyst vials were placed into the autosampler tray. The reagents (3 mL of acetone containing 30 μL of dodecane (internal standard)) were loaded in a syringe and driven by SP1. As the flow rates of SP1 and injection rate of autosampler were equal, the injected reaction zone contained half catalyst solution and half acetone. The flow of SP2 was stopped after all the zones were loaded into the reactor capillary. After reaction completion, SP2 was turned on and reaction zones were analyzed by online GC as described above.

3.2.6 Calibration curve and statistical calculation of yields

A calibration curve was prepared from standard solutions of product 4-hydroxy-4-phenyl-butan-2-one (locally synthesized), the major side product *trans*-4-phenyl-3-buten-2-one (commercially available) and the internal standard (IS) dodecane. A series of stock solutions with various mole ratios of pure product, side product and IS were prepared in acetone to obtain standards for GC analysis. The calibration curve for product yield determination was obtained by plotting the mole ratios of product to IS as a function of peak area ratios of product to IS.

3.2.7 Capillary electrophoresis for identification of reaction intermediates

The crude reaction mixture was injected into ISCO 3850 Electropherograph System by vacuum with a duration time of 10 seconds. The separation column is a fused-silica capillary tube (50 μm i.d., 70 cm length). The separation voltage is set at 20 kV (polarity '+') and the buffer solution is 50 mM phosphate aqueous solution at pH 1.80. The UV-Vis detector is set at 210 nm.

3.2.8 LC-ESI-MS for identification of reaction intermediates

The crude reaction mixture placed in vials was injected into HP 1100 (LC/ESI-MS) by an autosampler. The LC column is Xterra MS C18, 3.5 μm particle, 4.6 mm ×100 mm. The separation conditions are: 0.5 mL/min, gradient 10-90% AN/water (0.1% HCOOH) in 10 min, held for 5 min, oven 40 ^{o}C.

3.3 RESULTS AND DISCUSSION

3.3.1 The aldol reaction

In the literature, *p*-nitrobenzaldehyde and acetone are commonly used substrates for investigations of peptide catalysts. However, GC is not suitable for quantitative analysis of their aldol product due to its high boiling point. I prefer GC to HPLC because GC is more efficient and sensitive, requiring much simpler method development for the analysis of complex samples. GC is especially advantageous for separating low-molecular-weight organic compounds. Thus, I chose benzaldehyde as the substrate for studying the aldol reaction in the microreactor (Scheme 1). Reaction yields were determined by online GC. Figure 20 shows fast separation of a crude reaction mixture by achiral GC, containing product, dehydration side product, substrates and internal standard (IS) dodecane.

Scheme 1. The direct aldol reaction of benzaldehyde and acetone catalyzed by peptide.

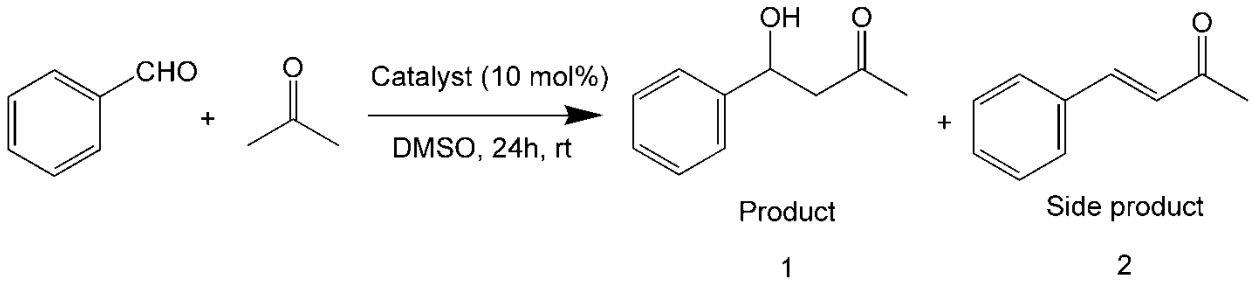

3.3.2 Solubility of peptides

Many amino acids and peptides are poorly soluble in pure organic solvents due to their high polarity. Water is generally not used in the direct asymmetric aldol reaction because excess water

can severely compromise the reaction rate and enantioselectivity.[8, 9] DMSO is one of the most commonly used aprotic solvent for the aldol reaction due to its high polarity; however, it is still a poor solvent to dissolve amino acids or peptides. Low solubility does not affect bench-top synthesis because the conventional method allows catalysts suspended in solution which can dissolve gradually upon reaction progress.[10] However, in order to prevent clogging in the microreactor, it is necessary to prepare a homogeneous catalyst solution before starting the reaction.

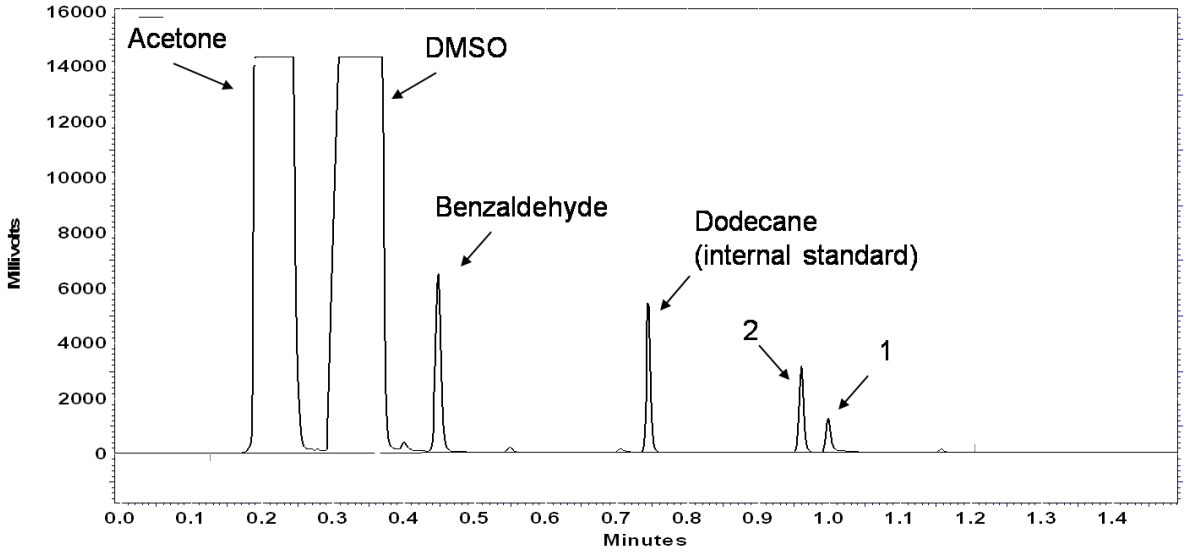

Figure 20. GC chromatogram of the aldol reaction products. Peak 1: product ; peak 2: major byproduct.

Reactant: benzaldehyde, 75 nmol; Catalyst: 10 mole % L-proline; Solvent: acetone:DMSO, 1:1 (v/v, 750 nL total). Column: RTX-5, 7 m×0.32 mm (0.25 μm stationary phase coating). Initial temperature, 80 °C; held for 0.3 min; then increased at 100 ℃/min to 200 ℃; held for 0 min.

A straightforward way to solve the solubility problem is to lower the catalyst concentration below the saturation level. However, for the aldol reaction, catalyst concentration has a significant effect on reaction rate and yield. In the literature, due to the side reactions

between catalyst and substrate, the aldol reaction is always performed with a relatively large catalyst loading (20-40 mole %) in order to get a high reaction yield.[3, 8, 11] Figure 21 shows that the yield in the bench-top aldol reaction has almost a linear dependence on the Pro-Gly concentration. I used *p*-nitrobenzaldehyde as the substrate rather than benzaldehyde in this study because the former has a higher reactivity at lower catalyst concentration. I can take advantage of this linear yield-concentration relationship for catalyst screening in the microreactor. When the catalyst concentration is lowered to a tolerable level for the microreactor, although reaction yield decreases, reaction still occurs. In this way, relative catalyst efficiency can be evaluated from the relative reaction yields. However, under typical conditions with catalyst loading less than 5 mole %, reaction yield is too low to be quantitated, and therefore it is still necessary to find an appropriate solubilization method that can increase catalyst solubility to a level where enough product can be formed for quantitative analysis by GC.

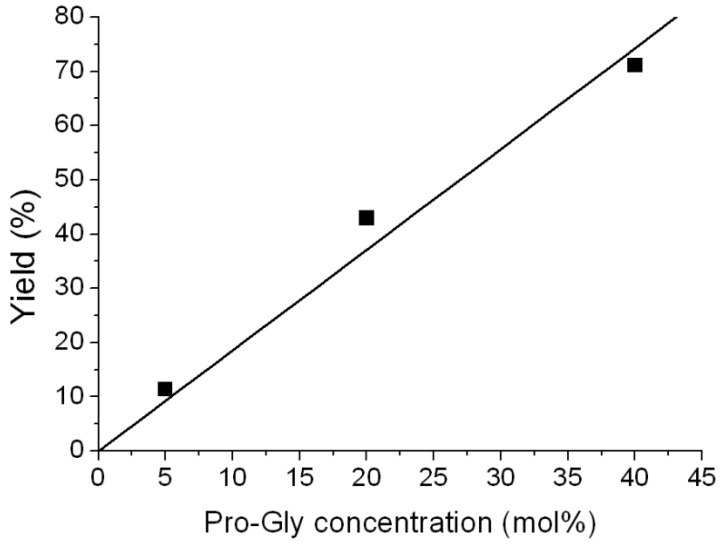

Figure 21. The effect of catalyst concentrations of Pro-Gly on reaction yields.

I tested a number of chemical methods to increase peptide solubility. For example, I tried to added organic additives (e.g., organic acids or bases), surfactants (e.g., Aerosol OT) or cosolvents (e.g., ionic liquids[12]) into the DMSO to prepare the catalyst solution. Unfortunately, all of these methods caused a significant drop in yield. Some reagents like surfactants can also lead to channel clogging by forming large micelles during the reaction.

I observed during bench-top reactions that amino acids and peptides eventually dissolve in the reaction mixture. This phenomenon has been reported by List[10] and a number of other researchers who studied the direct aldol reaction catalyzed by L-proline. Actually, Orsini[13] reported in the 1980s that amino acids and aliphatic/aromatic aldehydes can rapidly form imines and then transform into oxazolidinones in organic solvents in a process involving the imine-oxazolidinone equilibrium. Both cyclic (proline) and acyclic amino acids can react with aldehydes.

In 2004, List[14] found that not only aldehydes, but ketones can react reversibly to form imines and oxazolidinones with proline during the aldol reaction. The ketone-proline enamines, which are the key aldol reaction intermediates, are actually in equilibrium with ketone-proline oxazolidinones. The generally proposed catalytic mechanism by proline is shown in Figure 22. These oxazolidinones are believed to be soluble in organic solvents. In 2007, Seebach[15] stated that oxazolidinones are indeed not a by-product of the aldol reaction but rather play an important role in the catalytic cycle. The authors believed that the catalytic process might follow the 'oxazolidinone route', in which oxazolidinone intermediates are involved in all steps of the aldol reaction.

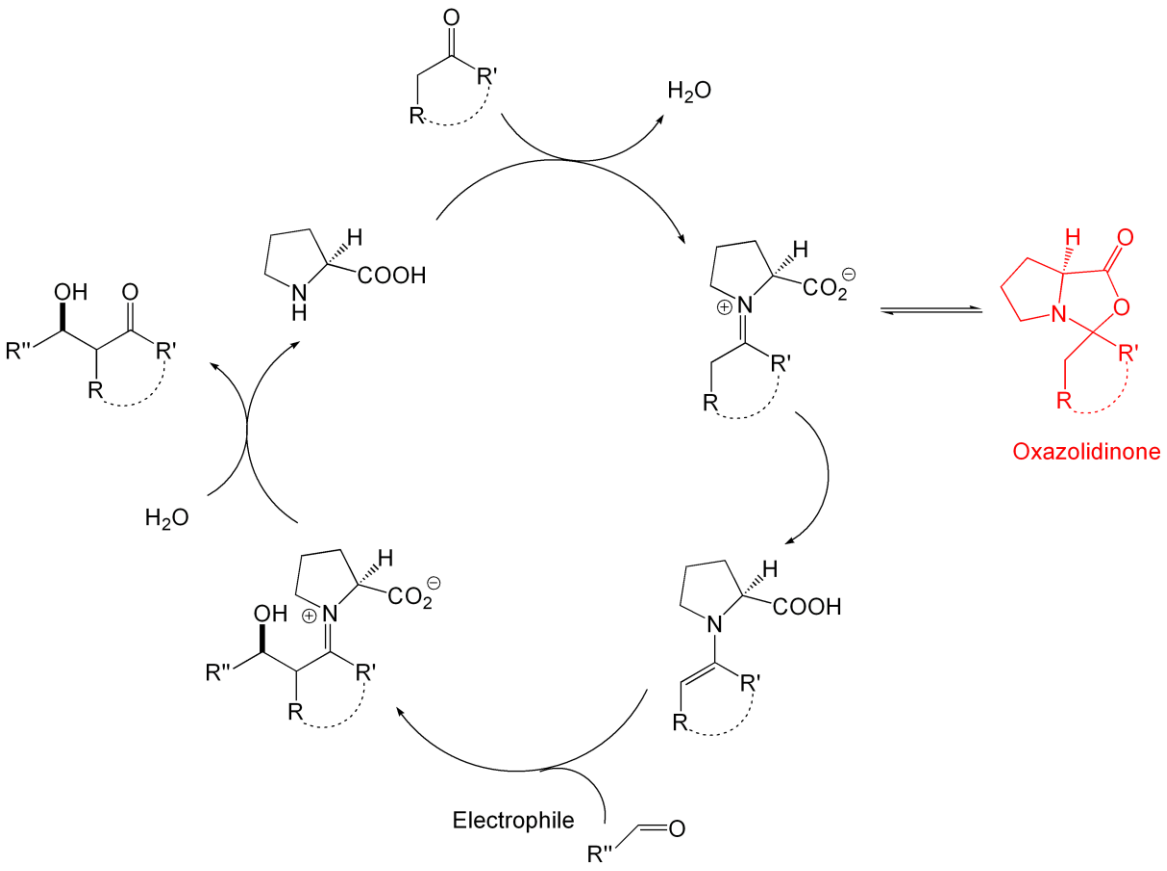

Figure 22. The catalytic cycle of L-proline-catalyzed direct aldol reaction.

Inspired by the solubility of oxazolidinones, I tried a novel approach to prepare homogeneous catalyst solutions by reacting amino acids or peptides with one of the substrates in DMSO before loading the mixture into the reactor in combination with the other substrate. I tested both benzaldehyde and acetone as reactants, and found that benzaldehyde improved the solubility to a greater extent than acetone. The α-carboxylic acid group in an amino acid is essential for the formation of an oxazolidinone; however, peptides do not have this functionality. Thus, I believe peptides and benzaldehyde mostly form imine intermediates which are soluble in DMSO, while amino acids may also form oxazolidinones through the imine-oxazolidinone equilibrium.[13] I found that when acetonitrile was added to a DMSO solution of the

benzaldehyde-catalyst complex, peptides or amino acids can precipitate out of the solution, as the precipitate is confirmed by NMR. This effect indicates that the solubilization is indeed a reversible process. Northrup and MacMillan[16] have successfully performed the direct enantioselective aldehyde-aldehyde dimerization reaction by proline catalysis, supporting the reversibility of the formation of imines and oxazolidinones from aldehydes and catalysts.

The aldol reaction proceeds when acetone is mixed with the benzaldehyde-catalyst complex solution. I hypothesize that when a large amount of acetone is present, the formation of acetone-catalyst enamines and/or oxazolidinones will drive the dissociation of benzaldehyde-catalyst imines and/or oxazolidinones simply by a concentration-dependent equilibrium shift. The formation of aldol products can also lead to the generation of acetone-catalyst enamines. Possible routes for the solubilization of catalysts and the subsequent aldol reaction are shown in Scheme 2.[13, 14, 17]

Scheme 2. Possible pathways for catalyst preparation and the aldol reaction in the microreactor.

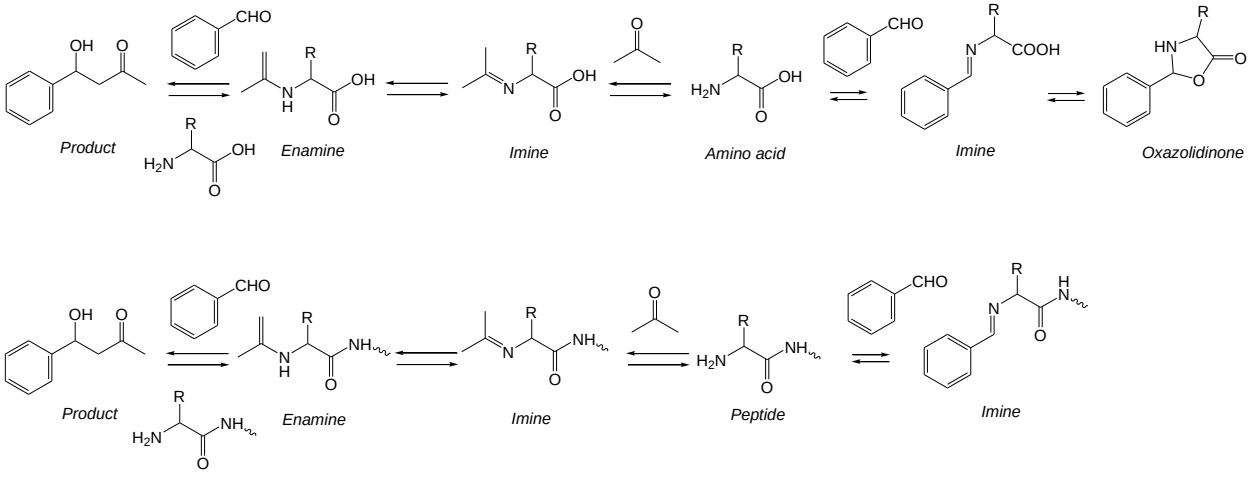

3.3.3 Identification of key reaction intermediates

In order to validate above proposed solubilization and reaction approach, I need to confirm the presence of some key reaction intermediates like benzaldehyde-catalyst imines or acetone-catalyst imines. Since these intermediates are mostly charged species, I decided to use capillary electrophoresis (CE) to study the reaction mixture in order to find the presence of some charged intermediates. I prepared four samples in regular vials: the first sample contains only pure peptide Pro-Phe in DMSO; the second contains the mixture of Pro-Phe and benzaldehyde after overnight stirring; the third contains the mixture of Pro-Phe and acetone after overnight stirring; and the last one contains both substrates and the catalyst carrying out a complete aldol reaction. Samples were injected into CE column directly with aqueous buffers. The goal of this study is to confirm that peptide can form charged intermediates with benzaldehyde and acetone respectively. A problem is that neutral molecules like substrates and solvents may interfere with the separation of charged species, resulting in a complex CE spectrum. An easy way to address this problem is to delay the elution of neutral compounds by using very acidic buffer to hinder the electroosmotic flow in the fused-silica capillary channel, allowing charged molecules moving much faster than neutral compounds under only electrophoretic motivation.

CE spectra of four reaction samples are shown in Figure 23, in which all peaks represent positively charged species because neutral compounds like acetone requires more than 90 min to elute out of the channel. In Figure 23, the sample containing pure Pro-Phe show only one large peak that is positively charged peptide itself. The samples containing Pro-Phe/benzaldehyde and Pro-Phe/acetone have shown one significant peak respectively that elutes at different times, indicating they are intermediates with different molecular weights and likely to be Pro-Phe/ benzaldehyde and Pro-Phe/acetone adduct complexes. The intermediate of benzaldehyde/Pro-

Phe elutes slower than that of acetone/Pro-Phe, which agrees with the electrophoretic principle that larger molecules move slower than smaller molecules under same electrophoretic conditions. The aldol reaction mixture is much more complex, including a number of peaks shown in the CE spectrum that correspond to the presence of multiple charged species.

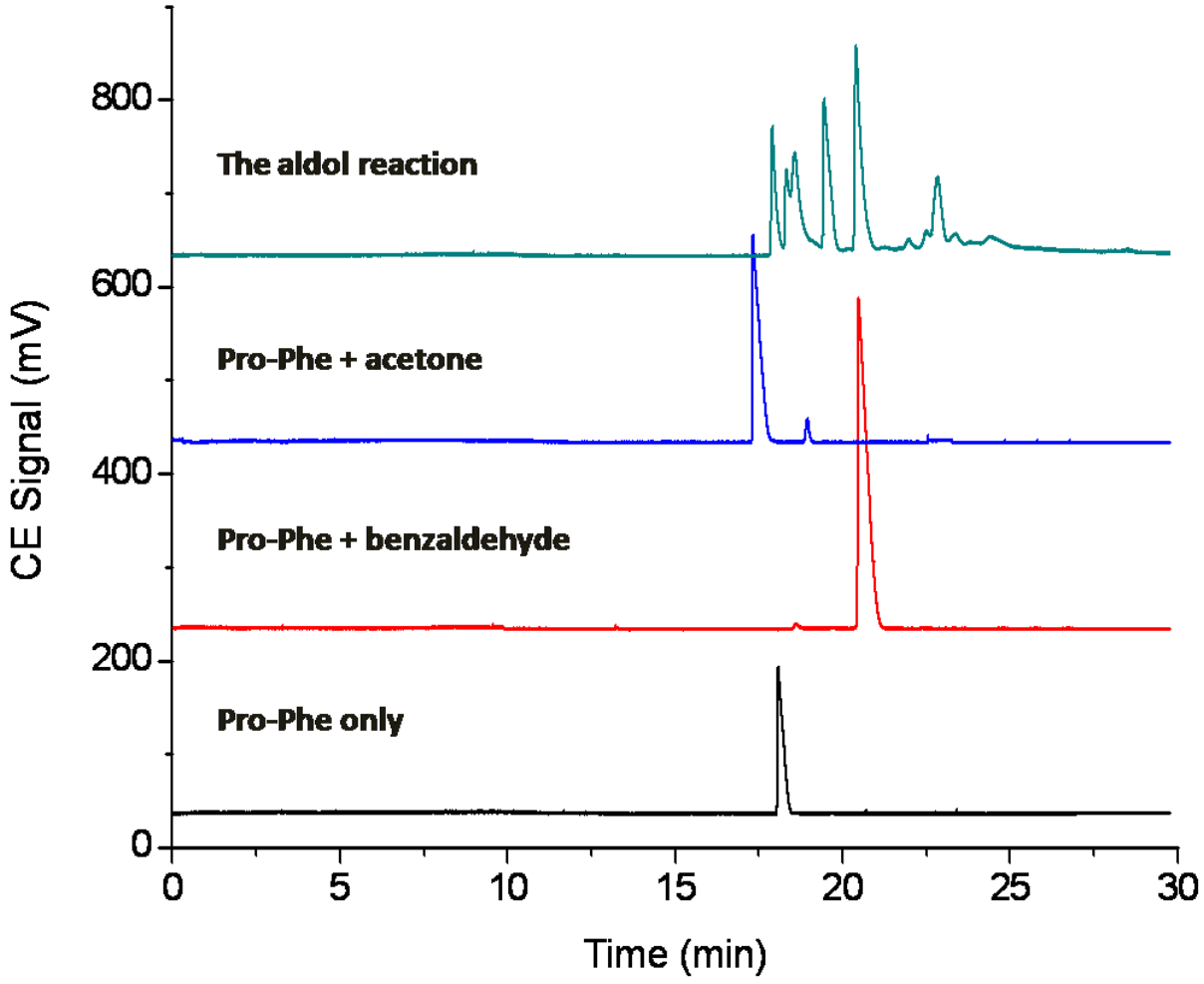

Figure 23. CE spectrums of positively charged species formed in four different samples.

CE Column: fused-silica capillary (50 μm i.d., 70 cm length); Separation voltage: 20 kV (polarity '+'); Buffer solution: 50 mM aqueous phosphate solution at pH 1.80; UV-Vis detector 210 nm.

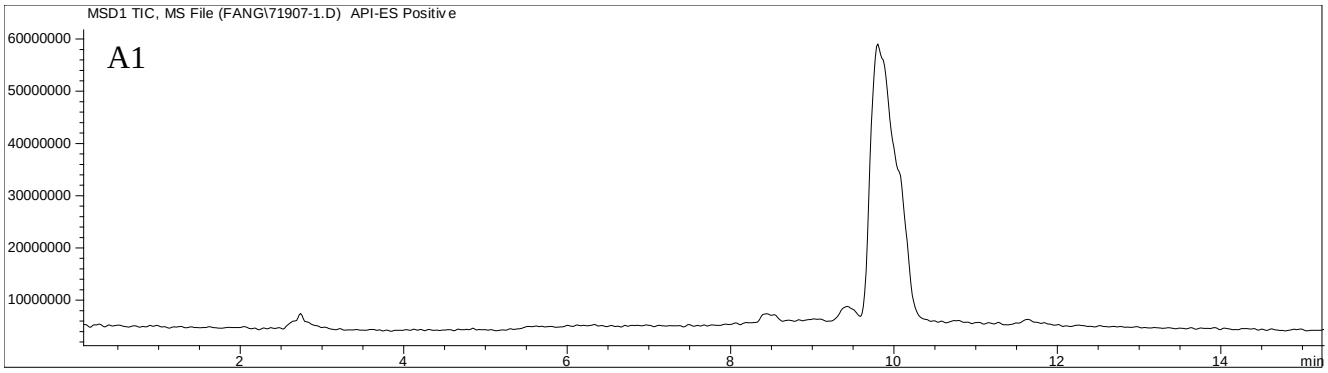
MSD1 TIC, MS File (FANG\71907-1.D) API-ES Positive
A1
60000000
50000000
40000000
30000000
20000000
10000000
2
4
6
8
10
12
14
min

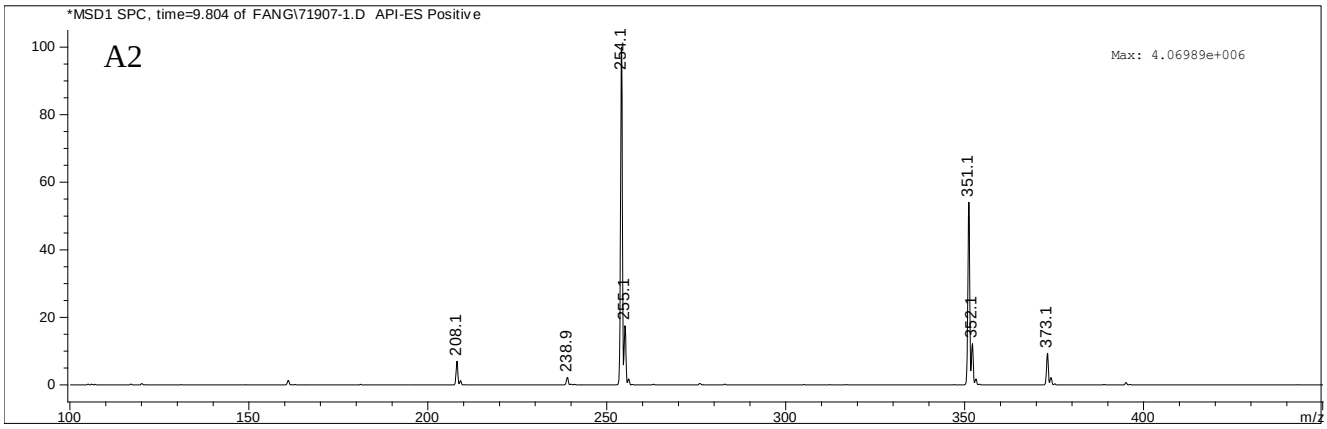
*MSD1 SPC, time=9.804 of FANG\71907-1.D API-ES Positive
A2
Max: 4.06989e+006
254.1
351.1
208.1
238.9
255.1
352.1
373.1
100
80
60
40
20
0
100
150
200
250
300
350
400
m/z

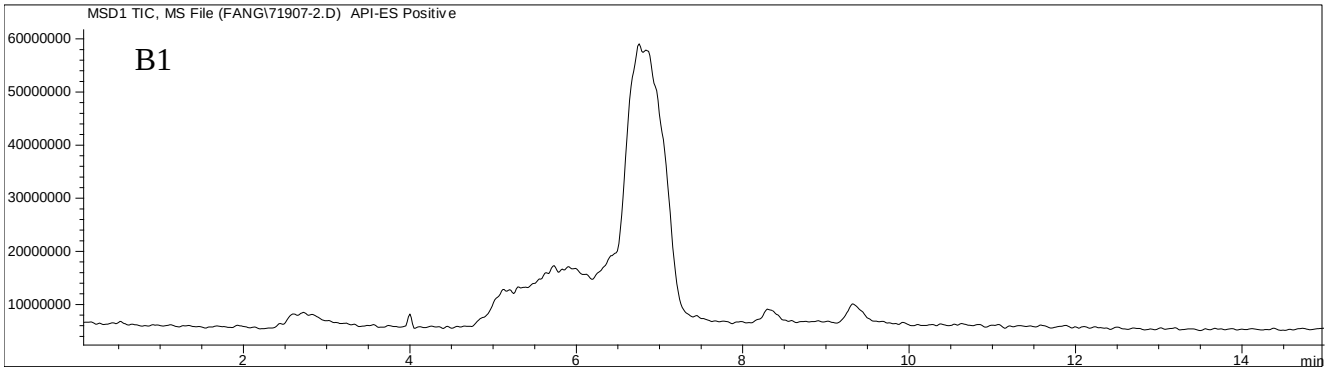
MSD1 TIC, MS File (FANG\71907-2.D) API-ES Positive
B1
60000000
50000000
40000000
30000000
20000000
10000000
2
4
6
8
10
12
14
min

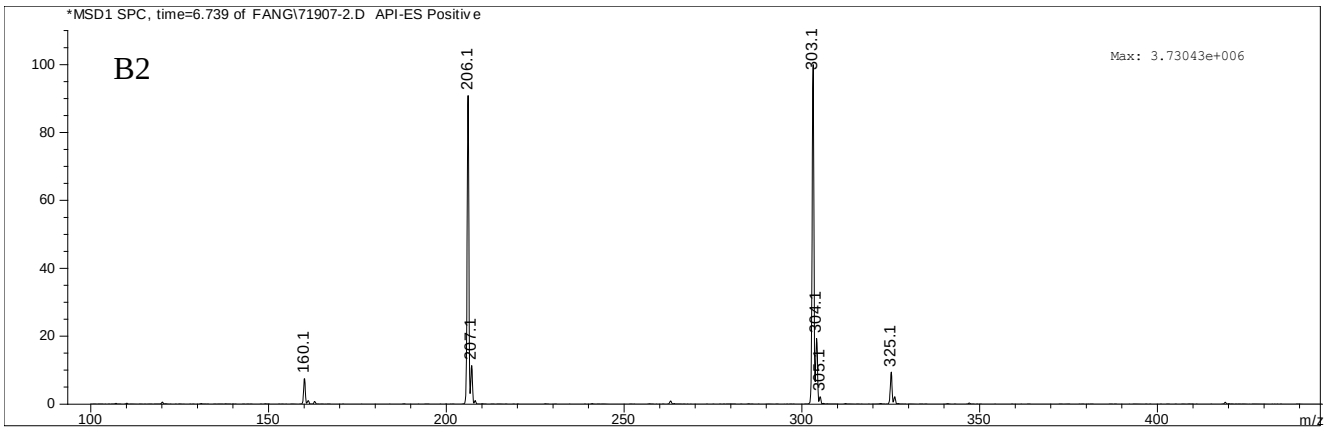
*MSD1 SPC, time=6.739 of FANG\71907-2.D API-ES Positive
B2
Max: 3.73043e+006
206.1
303.1
160.1
207.1
304.1
305.1
325.1
100
80
60
40
20
0
100
150
200
250
300
350
400
m/z

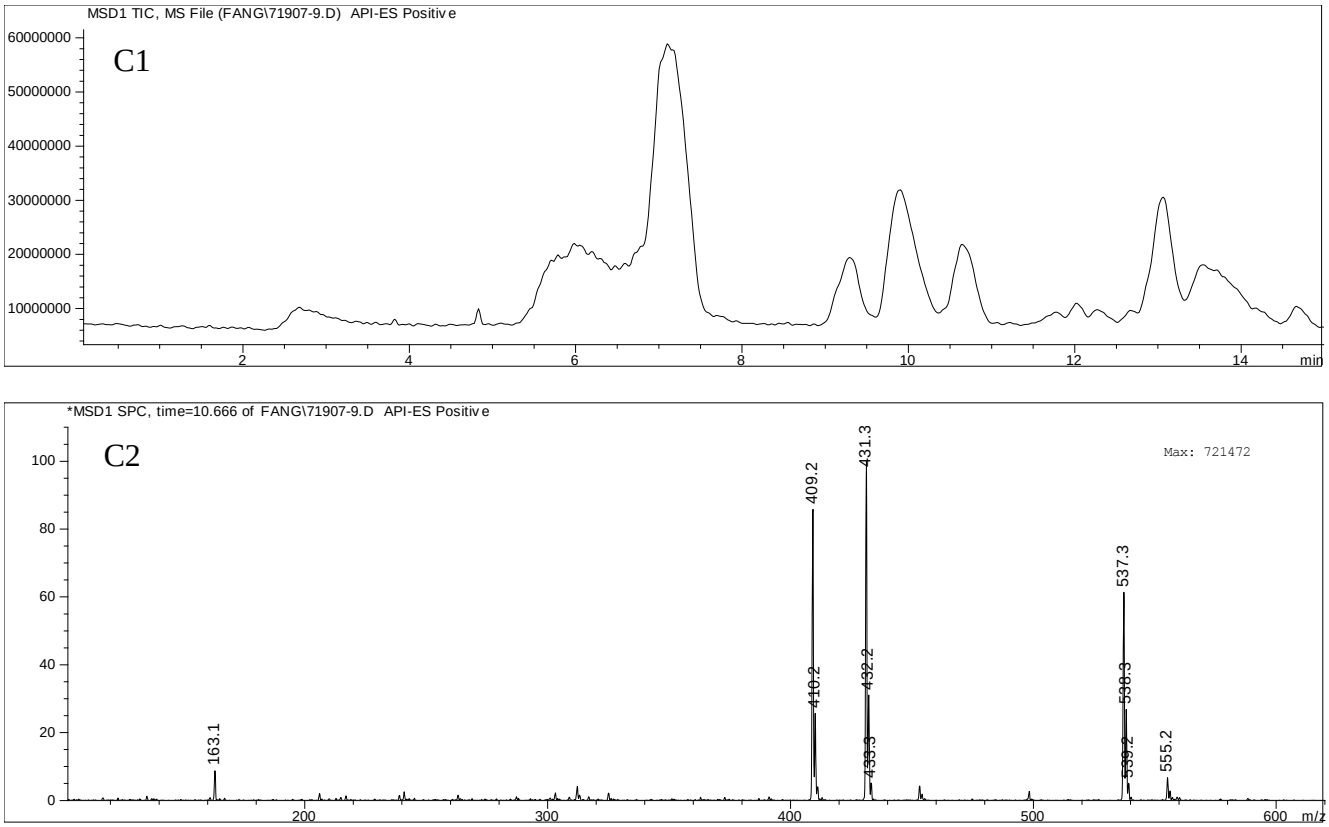

Figure 24. LC-MS studies of aldol reaction intermediates.

A1. Total ion chromatogram of benzaldehyde/Pro-Phe mixture; A2. MS spectrum of chromatographic peak in A1 at t_R=9.8 min; B1. Total ion chromatogram of acetone/Pro-Phe mixture; B2. MS spectrum of chromatographic peak in B1 at t_R=6.8 min; C1. Total ion chromatogram of benzaldehyde/acetone/Pro-Phe mixture; C2. MS spectrum of chromatographic peak in C1 at t_R=10.6 min.

CE is good for separating charged species; however, with only UV-Vis detector, it is hard to identify the structures of those intermediates. LC-MS is an excellent tool for structure clarification. I prepared three reaction samples, benzaldehyde/Pro-Phe, acetone/Pro-Phe and benzaldehyde/acetone/Pro-Phe (complete aldol reaction), and injected them directly into LC-MS with electron spray ionization (ESI). The LC-MS results are shown in Figure 24.

The homogeneous mixture of benzaldehyde and Pro-Phe exhibits only one significant peak as shown in the chromatogram of Figure 24-A1 after overnight stirring, which is in accordance with those CE studies. This peak is likely to be the intermediate that leads to the dissolution of peptides. Mass spectrum in Figure 24-A2 identifies two ions, *m/z* 351 and *m/z* 373, corresponding to molecular ions of this intermediate and its sodium-plus ion. The structure of this benzaldehyde/Pro-Phe adduct is shown in Figure 25.

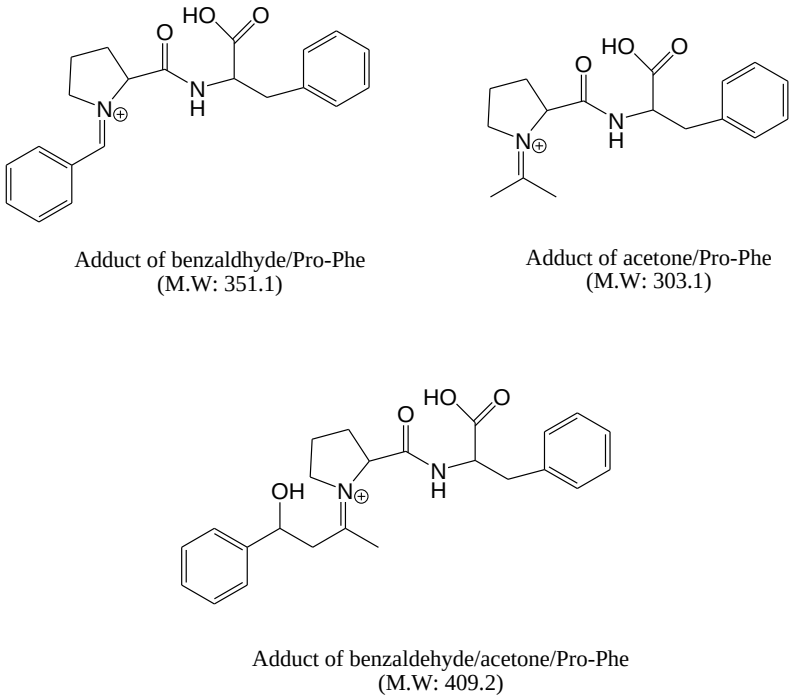

Adduct of benzaldhyde/Pro-Phe
(M.W: 351.1)

Adduct of acetone/Pro-Phe
(M.W: 303.1)

Adduct of benzaldehyde/acetone/Pro-Phe
(M.W: 409.2)

Figure 25. The possible structures of reaction intermediates idnetified by LC-MS.

Acetone/Pro-Phe shows similar results. In chromatogram Figure 24-B1, there is only one large peak and it corresponds to the molecular ions, *m/z* 303 and *m/z* 325, in the mass spectrum of Figure 24-B2. The aldol reaction mixture, containing both substrates and Pro-Phe, exhibits a number of peaks in the chromatogram of Figure 24-C1, one of which elutes at t_R=10.6 min corresponding to characteristic molecular ions, *m/z* 409 and *m/z* 431, matching the molecular

weight of the adduct of benzaldehyde, acetone and Pro-Phe (Figure 25). Actually, in the chromatogram of Figure 24-C1, I can also see the peaks of both intermediates of benzaldehyde/Pro-Phe (t_R=9.8 min) and acetone/Pro-Phe (t_R=6.8 min), proving the reaction mixture contains all those intermediates.

The studies of key reaction intermediates by CE and LC-MS demonstrate that in our catalyst preparation approach, benzaldehyde form soluble adduct with Pro-Phe, which can then transform into acetone/Pro-Phe adduct with the addition of large amounts of acetone through equilibrium. The reaction process basically follows the proposed catalytic mechanisms.

3.3.4 Experimental validation of the catalyst solubilization method

In addition to mechanistic studies by CE and LC-MS, I also performed experiments of screening model catalysts to validate this approach. I chose 21 commercially available amino acids and screened them in the microreactor with the above catalyst preparation method. The autosampler loaded each catalyst three times in succession. The microreactor (with 6.7-m-long capillary) can run 21 twenty-four-hour reactions in a single run that include 7 catalysts in triplicate repetition. Figure 26 shows the passage of 21 reaction zones through the UV-Vis fiber optic detector followed by online GC analysis. Zones are well separated with little overlapping. Bench-top reactions were also carried out under similar conditions. Each catalyst was examined in one bench-top reaction for comparison.

Yields of both product **1** and side product **2** are shown in Table 2. A comparison of reaction yields of amino acids in the microreactor and in bench-top reactions shows that most amino acids lead to somewhat lower yields in the microreactor. When the yields were normalized by dividing them by the maximum yield in the microreactor and bench-top reactions,

the relative yields in the microreactor were mostly in agreement with those of bench-top reactions as shown in Figure 27.

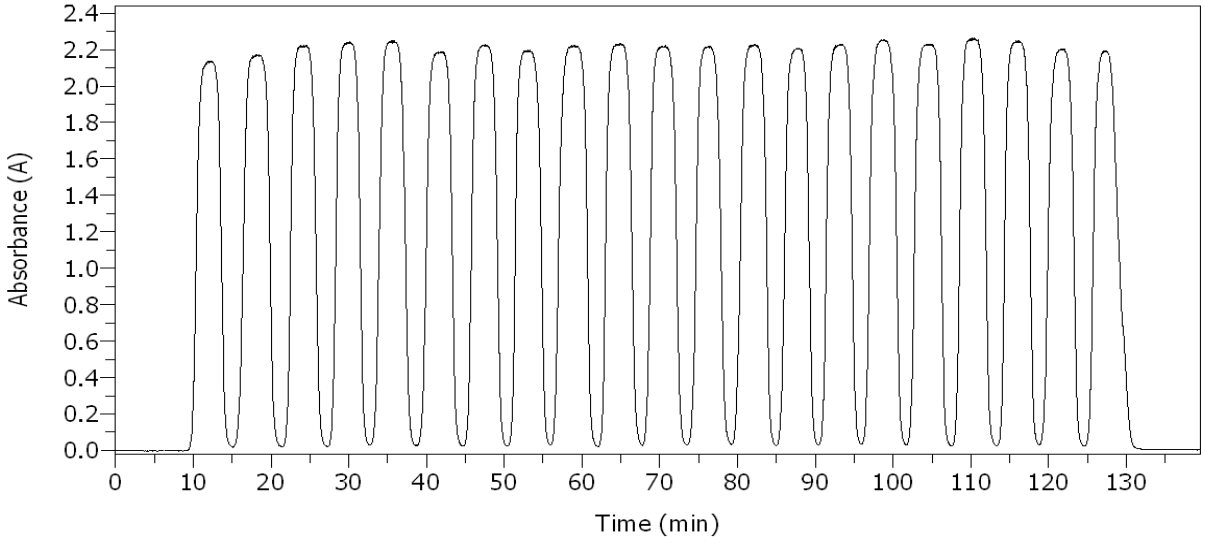

Figure 26. Absorbance response of 21 reaction zones passing through the UV-Vis detector. Detection wavelength: 260 nm; Solvent of SP2: THF; Flow rate: 250 nL/min; Zone volume: 750 nL. Each catalyst is present in three successive zones.

Among all amino acids, L-proline and *trans*-4-hydroxy- L-proline have the largest yield loss in the microreactor although they still show higher yields than other amino acids. I hypothesize that enamines or oxazolidinones formed by benzaldehyde and secondary amine of proline are more stable than those formed by benzaldehyde and primary amines. If the addition of acetone cannot shift the benzaldehyde-catalyst equilibrium, less catalyst will be released to participate in the aldol reaction, and will result in a lower reaction yield because it greatly depends on catalyst concentration. In fact, it has been found that the formation of benzaldehyde-proline oxazolidinones is more favorable than the formation of acetone-proline enamines.[14] As a result, the ketone is usually used in large excess to suppress the formation of oxazolidinones.

Table 2. Yields of the aldol reaction of acetone and benzaldehyde catalyzed by amino acids.

Entry	Catalyst	Yield (%) of **1** (product)[a]		Yield (%) of **2** (side product)	
		Microreactor[b]	Batch reaction[c]	Microreactor	Batch reaction
1	L-alanine	2.5 ±0.3[d]	4.4[e]	5.6 ±0.6	2.2
2	L-valine	1.3 ±0.2	1.5	1.7 ±0.3	1.3
3	L-arginine	1.2 ±0.2	0.3	8.8 ±0.8	0.6
4	L-isoleucine	4.2 ±0.5	2.9	8.0 ±0.4	10.9
5	L-serine	6.6 ±0.1	6.3	4.5 ±0.2	13.5
6	L-leucine	2.2 ±0.1	6.3	4.4 ±0.2	9.1
7	L-lysine	1.3 ±0.1	1.3	7.6 ±0.2	19.3
8	L-histidine	3.6 ±0.2	2.3	11.9 ±0.7	13.8
9	L-phenylalanine	3.0 ±0.1	4.5	4.1 ±0.8	10.1
10	L-threonine	3.1 ±0.1	10.5	1.7 ±0.1	11.8
11	L-tyrosine	3.5 ±0.1	5.0	2.9 ±0.1	7.2
12	L-methionine	4.7 ±0.2	6.2	3.9 ±0.1	12.2
13	glycine	10.8 ±0.7	8.8	18.9 ±1.5	27.1
14	L-proline	8.4 ±1.6	33.8	0.3 ±0.0	19.7
15	*trans*-4-hydroxy-L-proline	19.3 ±0.9	48.3	0.7 ±0.1	13.2
16	L-glutamine	2.3 ±0.1	4.7	1.8 ±0.1	3.7
17	L-cystine	0.4 ±0.1	0	0.3 ±0.1	0
18	L-cysteine	0.1 ±0.0	0.1	0.2 ±0.0	0.6
19	L-glutamic acid	1.7 ±0.1	6.7	1.7 ±0.1	5.7
20	L-tryptophan	1.4 ±0.1	6.0	1.7 ±0.0	8.6
21	L-asparagine	0.8 ±0.0	1.1	8.3 ±0.6	19.1

[a] Yields of product and side product are determined by GC.

[b] 10 mole % amino acids, 75 nmol benzaldehyde, acetone:DMSO, 1/1 (v/v, 750 nL total). Reactions conducted at room temperature for 24 h in the microreactor.

[c] 10 mole % amino acids, 0.2 mmol benzaldehyde, acetone:DMSO, 1/4 (v/v, 1 mL total). Reactions conducted at room temperature for 24 h in the vials.

[d] Average yield for three runs (mean ± SEM, n=3).

[e] Yield from a single run.

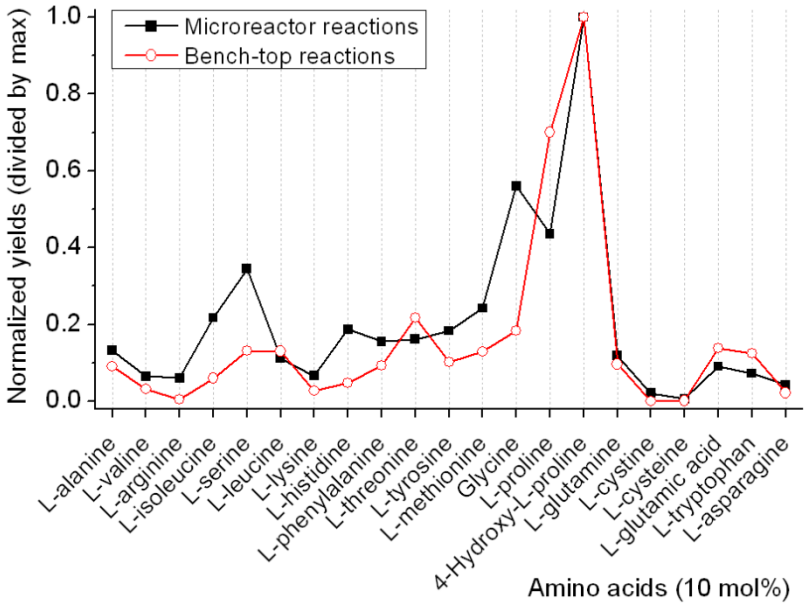

Figure 27. Normalized yields of the aldol reactions catalyzed by amino acids. Normalization is done by dividing yields by the maximum.

The objective of catalyst screening is to identify the relative activities of the catalysts. I am less concerned about yield because the objective is not to produce product. Thus, although the microreactor approach may result in a somewhat lower yield, it can still be used for rapid preliminary screening of large catalyst libraries based on relative reaction yields. Some catalysts with better activities can be further studied in batch reactions under fully-optimized conditions.

3.3.5 Screening of peptides in the microreactor

I screened 27 commercially available peptides in the microreactor. L-glutathione (GSH) in reduced form is γ-Glu-Cys-Gly and its oxidized form (GSSG) is the disulfide. Screening of peptides follows the procedures of screening amino acids. Catalyst solutions were prepared by

the same method. Each catalyst was studied in three successive reactions. I also carried out bench-top reactions for those 27 peptides for comparison. Yields of both product **1** and side product **2** are shown in Table 3. The normalized yields are shown in Figure 28.

Table 3. Yields of the aldol reactions of acetone with benzaldehyde catalyzed by peptides.

Entry	Catalyst	Yield (%) (**1,** product)[a]		Yield (%) (**2**, side product)	
		Microreactor[b]	Batch reaction[c]	Microreactor	Batch reaction
1	Ala-Ala	0.6 ±0.0[d]	1.1[e]	0.6 ±0.0	0.6
2	Ala-Ala-Ala	0.9 ±0.1	0.7	1.1 ±0.0	0.3
3	Ala-Ala-Ala-Ala	0.9 ±0.0	0.9	0.7 ±0.0	0.9
4	β-Ala-Ala	0.3 ±0.0	0.1	2.7 ±0.1	1.0
5	β-Ala-Gly	0	0.1	1.7 ±0.1	1.1
6	Ala-Gly	0.7 ±0.0	0.9	0.7 ±0.1	0.4
7	Gly-Trp	0.2 ±0.0	0.3	0.7 ±0.0	0.3
8	Gly-Phe	1.3 ±0.1	0.9	2.0 ±0.1	0.4
9	Gly-Phe-NH_2	0.3 ±0.0	1.5	0.6 ±0.0	0.1
10	Albumin	0.2 ±0.0	0	0.4 ±0.1	0.1
11	Pro-Gly	0	2.6	0.3 ±0.0	1.5
12	Pro-Phe	0.2 ±0.0	6.1	0.4 ±0.0	2.1
13	Asp-Ala	0.4 ±0.0	0.7	0.6 ±0.1	0.5
14	Asp-Val	0.8 ±0.2	0.4	1.1 ±0.1	0.4
15	Asp-Gly	1.1 ±0.2	0.4	1.4 ±0.3	0.4
16	α-Glu-Val	0.2 ±0.0	0.8	0.4 ±0.0	1.0
17	α-Glu-Trp	0.2 ±0.0	0.4	0.4 ±0.0	0.3
18	γ-Glu-Val	4.7 ±0.2	3.5	3.8 ±0.1	4.6
19	γ-Glu-Glu	6.9 ±0.4	3.0	10.2 ±0.7	4.2
20	γ-Glu-Gly	9.9 ±0.4	3.0	14.1 ±0.8	4.1
21	β-Asp-Gly	5.8 ±0.2	1.8	8.7 ±0.7	2.5
22	β-Asp-Val	5.2 ±0.3	-	7.3 ±0.5	-
23	β-Asp-Ala	7.2 ±0.4	-	19.6 ±1.3	-
24	Glutathione (oxidized)	7.2 ±0.2	-	33.7 ±1.5	-
25	Glutathione (reduced)	3.1 ±0.1	-	17.2 ±0.3	-
26	*p*-Glu-Gly-Arg-Phe	0.1 ±0.0	-	0.4 ±0.0	-
27	*p*-Glu-His	0.7 ±0.4	-	3.2 ±0.9	-

[a] Yields of product and side product are determined by GC.

[b] 10 mole % peptides, 75 nmol benzaldehyde, acetone:DMSO, 1/1 (v/v, 750 nL total). Reactions conducted at room temperature for 24 h in the microreactor.

[c] 10 mole % peptides, 0.2 mmol benzaldehyde, acetone:DMSO, 1/4 (v/v, 1 mL total). Reactions conducted at room temperature for 24 h in the vials.

[d] Average yield for three runs (mean ± SEM, n=3).

[e] Yield from a single run.

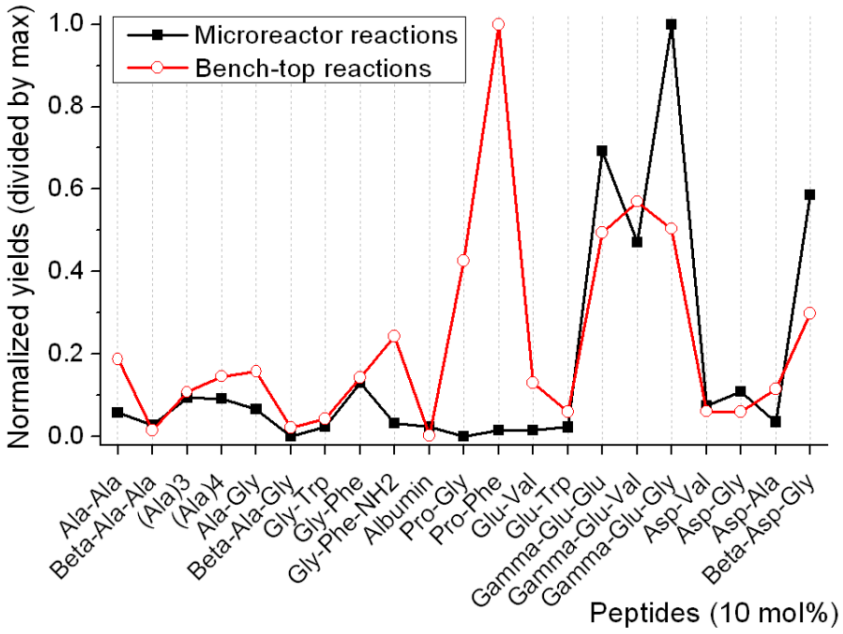

Figure 28. Normalized yields of peptides in the microreactor and bench-top reactions. The normalization is done by dividing yields by the maximum in the microreactor and bench-top reactions.

In Figure 28, it shows that two groups of peptides show relatively higher reactivities than other peptides, namely γ–Glu- and β–Asp-containing peptides. Bench-top reactions agree mostly with the microreactor except for Pro-Gly and Pro-Phe which exhibit nearly no reactivity in the microreactor. Their yield loss should be due to the similar reasons discussed above for L-proline.

L-proline is a well-studied catalyst for the aldol reaction and its proposed catalytic mechanism is based on the plausible tricyclic transition state **I** (Figure 29) stabilized by intermolecular hydrogen bonding between the enamine intermediate and the carbonyl group on the aldehyde.[10] This transition state also accounts for the stereochemistry of the aldol products. The proton on the carboxylic acid group plays a key role in the formation of this hydrogen-bonded framework. It is believed that other acyclic amino acids can also form a similar chair-like bicyclic transition state **II**.[5] *trans*-4-hydroxy- L-proline shows a better yield than L-proline in our study which agrees with results reported in the literature.[10] I hypothesize that its higher reactivity may be due to the hydroxyl group's participation in the hydrogen-bonding network of the enamine, contributing to the higher stability of transition state **III**. The enantioselectivity of *trans*-4-hydroxy- L-proline is also reported to be higher than L-proline,[10] which is also indicative of the contribution of the hydroxyl group to the transition state **III**.

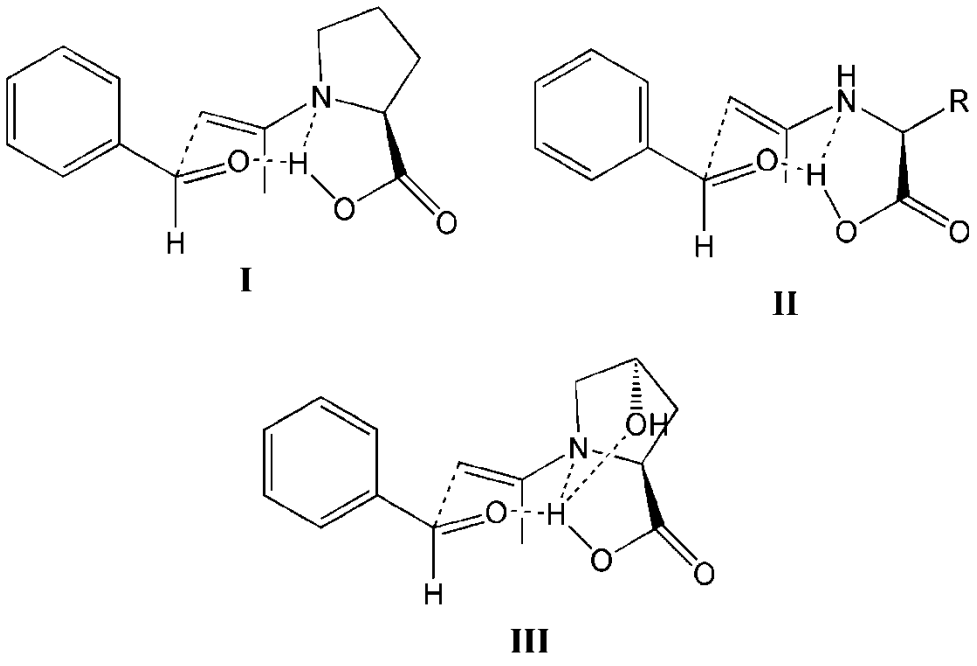

Figure 29. Plausible transition states of amino acid catalyzed aldol reaction.

Short peptides are believed to operate by a catalytic process similar to amino acids. However, in peptides, the N-terminal amine and C-terminal carboxylic acid group are on remote amino acid residues, the reactivity of peptides basically depends on the spatial proximity of the amine to a carboxylic acid. Some active peptides published in the literature,[6] e.g., L-pro-L-pro-L-asp-NH_2 and L-pro-D-ala-D-asp-NH_2, have turn-like 3D conformations in which the secondary amine function of proline is in close proximity to the carboxylic acid of aspartic acid. Short N-terminal-proline peptides, e.g., dipeptides, are proposed to have a transition state **IV**[4] and other short acyclic-amino-acid peptides have a plausible transition state **V** (Figure 30).[5] Since peptides have more complex and restricted conformations, they are usually superior to amino acids in stereoselectivity because the peptide backbone can assist in the stabilization of the transition state. The N-terminal amino acid in short peptides is believed to control most of the reaction enantioselectivity.[5] However, the chirality of the C-terminal amino acid for some turn-like peptides mentioned above has an important effect on the asymmetric catalysis as well.[6]

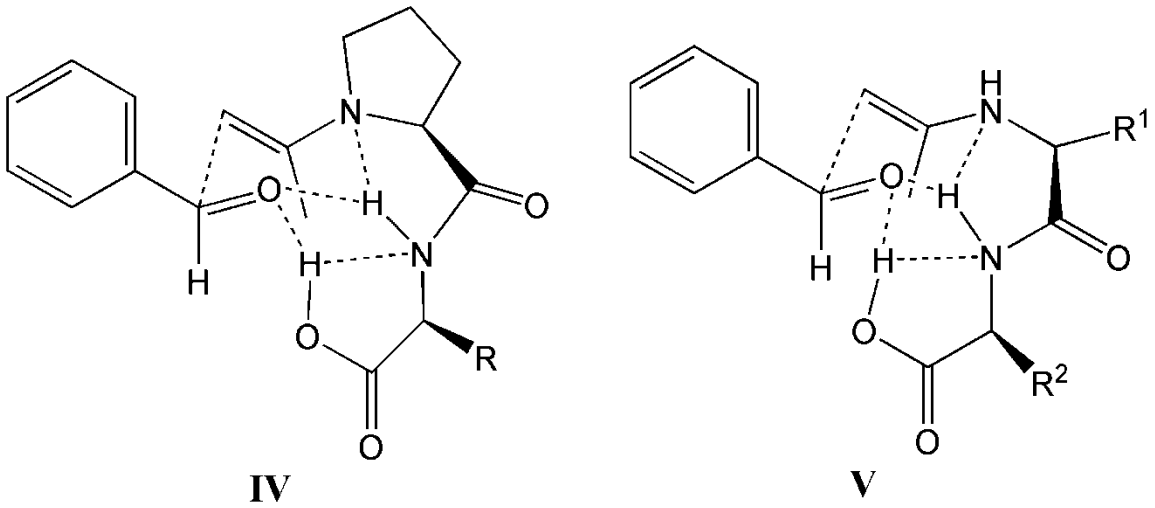

Figure 30. Plausible transition states of dipeptide catalyzed aldol reaction.

In addition to proline peptides, other peptide catalysts with N-terminal acyclic amino acids have also been investigated.[18, 19] Those peptides show good reactivity and stereoselectivity towards different substrates. Here, I found that two groups of short peptides, γ–Glu and β–Asp, have relatively higher reactivity than other peptides, which has not yet been reported. The structures of γ–Glu or β–Asp peptides have a unique common characteristic (Figure 31). The primary amine of the N-terminal amino acid is in proximity to a carboxylic acid just like in an amino acid. As for proline-terminal peptides, I believe that the reactivity and stereoselectivity of those two groups of peptides mostly depends on the N-terminal amino acids, γ–Glu and β–Asp. In these cases, catalysis is likely to proceed through transition state **II**. As the yields of the γ–Glu and β–Asp peptides are not identical, I infer that there is an influence of peptide backbone structure.

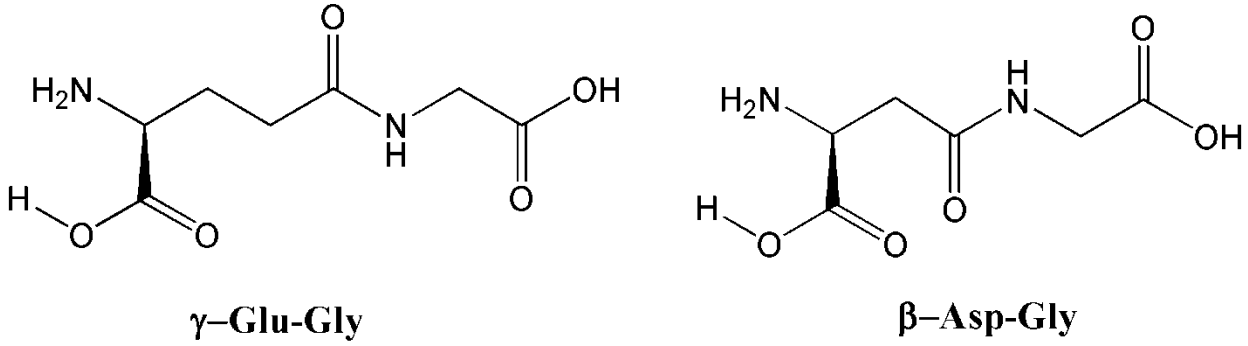

Figure 31. Structures of γ–Glu-Gly and β–Asp-Gly.

In Table 3, GSH provides approximately half the yield of GSSG in both the microreactor and bench-top reactions. GSSG has two γ–Glu moieties; this apparent doubling of catalyst

loading may be responsible for the approximate proportional increase in yield. This effect is a testimony to the reliability of this catalyst screening approach.

3.3.6 Enantioselectivity of peptide-catalyzed aldol reaction

Peptides are chiral catalysts and reaction stereoselectivity is an important criterion to determine catalyst activities. Since I used achiral GC for online analysis, I initially performed chiral separation by chiral GC with Chiraldex GTA column. The chromatogram of a crude reaction mixture is shown in Figure 32, in which a pair of enantiomers is separated within a short time period. However, a potential problem is that this chiral column "Chiraldex GTA (10 m×0.32 mm)" with a stationary phase of trifluoroacetylated ((2,6-di-*O*-pentyl-3-trifluoacetyl) γ-cyclodextrin) is very vulnerable to water moisture, especially at high temperature when GC runs. Even a minute amount of water can hydrolyze the column and compromise its selectivity. DMSO is a notoriously hygroscopic solvent, and therefore the robustness of this column is not very good when reaction mixture is directly analyzed by GC without pretreatment.

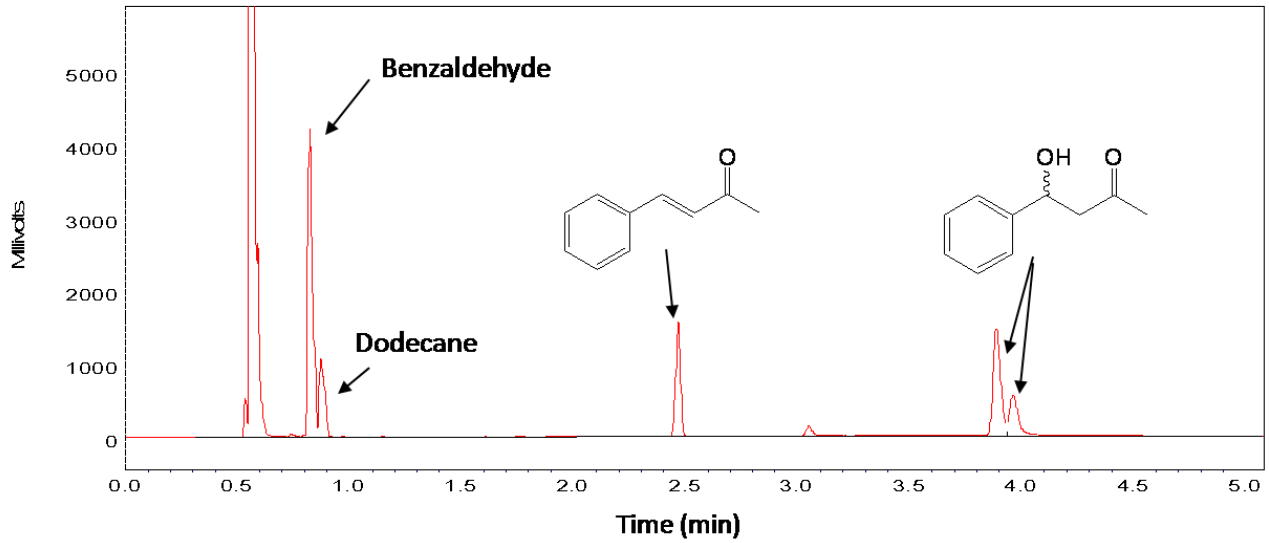

Figure 32. Chromatogram of aldol products analyzed by chiral GC.

GC column: Chiraldex GTA, 10 m × 0.32 mm; Separation conditions: Oven temperature from 70 °C to 150 °C at 16 °C/min, He flow 6.5 mL/min, inlet temperature 250 °C, flow spilt ratio 50.

Due to this potential problem of chiral GC column, I switched to chiral HPLC for analysis of aldol products. I offline studied reaction enantioselectivities of several relatively reactive amino acids and peptides that are discovered in the screening by chiral normal-phase HPLC. The column is Chiralpak IA (2.1mm ×150 mm, 5 μm silica gel) with a stationary phase of Amylose tris (3,5-dimethylphenylcarbamate). The LC chromatogram is shown in Figure 33.

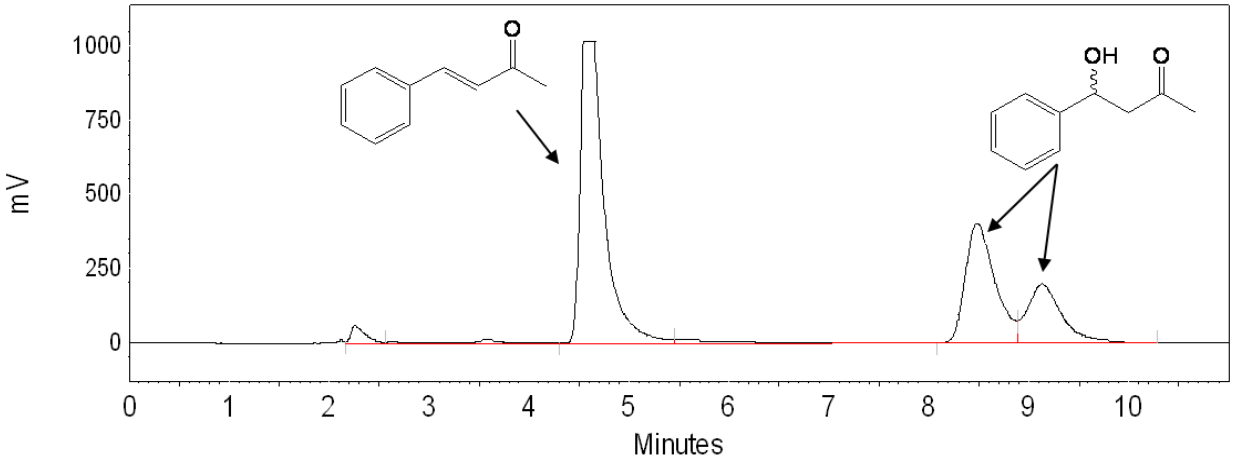

Figure 33. Chromatogram of aldol products separated by chiral HPLC.

HPLC column: Chiralpak IA (2.1mm ×150 mm); Separation conditions: 0.22 mL/min, isocratic hexane/isopropanol 95/5 (v/v), oven 25 °C, UV detector 210 nm.

Table 4 shows that L-proline, *trans*-4-hydroxy-proline and proline-terminal peptides have somewhat better enantioselectivities than γ–Glu and β–Asp peptides based on benzaldehyde and acetone substrates. Other peptides like Gly-Phe lead to poor stereoselectivity. This analysis clearly supports the concept that N-terminal amino acid is responsible for peptide stereoselectivity. As expected, *trans*-4-hydroxy- L-proline has a higher enantioselectivity than L-proline due to its additional hydroxyl group which can stabilize the transition state. The newly

discovered γ–Glu or β–Asp peptide catalysts have moderate reactivity and stereoselectivity towards the aldol reaction between benzaldehyde and acetone.

Table 4. Enantioselectivities of the aldol reaction catalyzed by amino acids and peptides.

Entry	Catalyst	ee (%)[a]
1	L-proline	58.1
2	*trans*-4-hydroxy-L-proline	71.2
3	Gly-Phe	10.5
4	Pro-Gly	58.8
5	Pro-Phe	73.0
6	γ-Glu-Glu	35.2
7	γ-Glu-Gly	41.4
8	Glutathione	38.5
9	β-Asp-Gly	26.2
10	β-Asp-Val	28.4

3.3.7 Throughput of the microreactor

I define the reactor throughput as the number of reactions done in a unit time. For the aldol reaction, I used a short 6.7-m-long capillary to load 21 reactions (containing 7 catalysts) in parallel and allow them to react for 24 h followed by online analysis. The times required for this operation are as follows: Catalyst weighing and solution preparation take about 18 h; loading catalysts into the reaction capillary takes about 2 h; GC analysis of all reaction zones takes about 2 h. Thus, the non-optimized throughput based on 6.7-m-long capillary is about 0.5 (24-h-reaction) reactions/h as shown in Eq. (1).

Technically, I am able to load more reaction zones in a longer reaction capillary to increase reactor throughput. In addition to the throughput, catalyst screening is mostly carried out in an automated way by the microreactor system, and the major human effort is the

preparation of catalyst solutions which usually takes about 1 h for weighing and dissolving of 7 catalysts. The effort for operating the microreactor is trivial. Consequently, the entire screening process is more efficient than traditional batch approach.

$$Throughput = \frac{Total\ number\ of\ reactions}{Total\ time\ (h)}$$

$$= \frac{21}{18\ h_{(catalyst\ \ prep)} + 24\ h_{(reaction\ \ time)} + 4\ h_{(loading\ and\ anlysis)}} \qquad (1)$$

$$\approx 0.5\ reactions/h$$

3.3.8 Green chemistry character of the microreactor

Catalyst screening in the microreactor requires much less reagent and solvent than a typical bench-top reaction. To load each reaction zone (750 nL) into the reactor capillary, the autosampler withdraws 25 μL of catalyst solution (DMSO) while SP1 delivered approximately 90 μL of reagent solution (acetone) at a flow rate of 15 μL/min. The flow rate of carrier solvent (THF) that delivers all zones through the capillary is set at 15 μL/h by SP2. The total running time is about 4 h for zone loading and GC analysis. Therefore, in this experiment, to screen 21 catalysts, the total solvent consumption is calculated below approximately 2.5 mL, or about 120 μL per catalyst. By further optimization of the operation, especially lowering the flow rate of SP1, the microreactor is capable of screening with even less solvent.

3.4 CONCLUSION

Peptides are important organocatalysts for the asymmetric aldol reaction. In this section, a model aldol reaction between benzaldehyde and acetone was chosen and a variety set of short peptides were screened in the capillary-based microreactor with good throughput. The volume of an individual reaction was 750 nL and reaction yield was determined by online GC. Considering the reaction is very slow, a stop-flow approach was employed to carry out the aldol reaction. To increase the peptide solubility in DMSO, I developed a benzaldehyde-peptide adduct approach to prepare homogeneous catalyst solutions before loading into the reactor. Two classes of peptides, γ-Glu- and β-Asp-containing peptides, were found to possess higher catalytic reactivities towards the aldol reaction. Chiral HPLC studies showed that these two types of catalysts have moderate stereoselectivity but are inferior to some known proline-containing peptides. The activities of those peptides are highly dependent on the γ-Glu and β-Asp residues, which demonstrate the notion that N-terminal amino acid is primarily responsible for peptide catalytic activities.

BIBLIOGRAPHY

1. Machajewski, T. D.; Wong, C.-H.; Lerner, R. A., The catalytic asymmetric aldol reaction. *Angew. Chem., Int. Ed.* **2000,** 39, 1352-1374.

2. Miller, S. J., In search of peptide-based catalysts for asymmetric organic synthesis. *Acc. Chem. Res.* **2004,** 37, 601-610.

3. Kobayashi, J.; Mori, Y.; Okamoto, K.; Akiyama, R.; Ueno, M.; Kitamori, T.; Kobayashi, S., A microfluidic device for conducting gas-liquid-solid hydrogenation reactions. *Science* **2004,** 304, 1305-1308.

4. Chen, F.; Huang, S.; Zhang, H.; Liu, F.; Peng, Y., Proline-based dipeptides with two amide units as organocatalyst for the asymmetric aldol reaction of cyclohexanone with aldehydes. *Tetrahedron* **2008,** 64, 9585-9591.

5. Cordova, A.; Zou, W.; Dziedzic, P.; Ibrahem, I.; Reyes, E.; Xu, Y., Direct asymmetric intermolecular aldol reactions catalyzed by amino acids and small peptides. *Chem. Eur. J.* **2006,** 12, 5383-5397.

6. Krattiger, P.; Kovasy, R.; Revell Jefferson, D.; Ivan, S.; Wennemers, H., Increased structural complexity leads to higher activity: peptides as efficient and versatile catalysts for asymmetric aldol reactions. *Org. Lett.* **2005,** 7, 1101-3.

7. Tang, Z.; Jiang, F.; Yu, L.-T.; Cui, X.; Gong, L.-Z.; Qiao, A.; Jiang, Y.-Z.; Wu, Y.-D., Novel small organic molecules for a highly enantioselective direct aldol reaction. *J. Am. Chem. Soc.* **2003,** 125, 5262-5263.

8. Sakthivel, K.; Notz, W.; Bui, T.; Barbas, C. F., III, Amino acid catalyzed direct asymmetric aldol reactions: a bioorganic approach to catalytic asymmetric carbon-carbon bond-forming reactions. *J. Am. Chem. Soc.* **2001,** 123, 5260-5267.

9. Akagawa, K.; Sakamoto, S.; Kudo, K., Direct asymmetric aldol reaction in aqueous media using polymer-supported peptide. *Tetrahedron Lett.* **2005,** 46, 8185-8187.

10. Fonseca, M. H.; List, B., Combinatorial chemistry and high-throughput screening for the discovery of organocatalysts. *Curr. Opin. Chem. Biol.* **2004,** 8, 319-326.

11. Kofoed, J.; Nielsen, J.; Reymond, J.-L., Discovery of new peptide-based catalysts for the direct asymmetric aldol reaction. *Bioorg. Med. Chem. Lett.* **2003,** 13, 2445-7.

12. Loh, T.-P.; Feng, L.-C.; Yang, H.-Y.; Yang, J.-Y., L-proline in an ionic liquid as an efficient and reusable catalyst for direct asymmetric aldol reactions. *Tetrahedron Lett.* **2002,** 43, 8741-8743.

13. Orsini, F.; Pelizzoni, F.; Forte, M.; Sisti, M.; Bombieri, G.; Benetollo, F., Behavior of amino acids and aliphatic aldehydes in dipolar aprotic solvents: formation and oxazolidinones. *J. Heterocycl. Chem.* **1989,** 26, 837-41.

14. Fonseca, M. H.; List, B., Combinatorial chemistry and high-throughput screening for the discovery of organocatalysts. *Curr. Opin. Chem. Biol.* **2004,** 8, 319-326.

15. Seebach, D.; Beck, A. K.; Badine, D. M.; Limbach, M.; Eschenmoser, A.; Treasurywala, A. M.; Hobi, R.; Prikoszovich, W.; Linder, B., Are oxazolidinones really unproductive, parasitic species in proline catalysis? - thoughts and experiments pointing to an alternative view. *Helv. Chim. Acta* **2007,** 90, 425-471.

16. Northrup, A. B.; MacMillan, D. W. C., The first direct and enantioselective cross-aldol reaction of aldehydes. *J. Am. Chem. Soc.* **2002,** 124, 6798-6799.

17. Clemente, F. R.; Houk, K. N., Density functional calculations: Computational evidence for the enamine mechanism of intramolecular aldol reactions catalyzed by proline. *Angew. Chem., Int. Ed.* **2004,** 43, 5766-5768.

18. Dziedzic, P.; Zou, W.; Hafren, J.; Cordova, A., The small peptide-catalyzed direct asymmetric aldol reaction in water. *Org. Biomol. Chem.* **2006,** 4, 38-40.

19. Tsogoeva, S. B.; Wei, S., *(S)*-Histidine-based dipeptides as organic catalysts for direct asymmetric aldol reactions. *Tetrahedron: Asymmetry* **2005,** 16, 1947-1951.

4.0 SCREENING OF ACID CATALYSTS FOR AN INTERNAL ACYLIMMINIUM ION CYCLIATION REACTION

4.1 INTRODUCTION

Acids are important catalysts for many organic transformations. In collaboration with Prof. Paul Floreancig's group, I want to apply our microreactor system to discover new acid catalysts for a novel internal cyclization reaction involved with acyliminium ion intermediate. This new synthetic protocol is useful for diversity-oriented organic synthesis, which can prepare structurally diverse amide libraries through either a one-pot synthesis or a two-step synthesis (Scheme 3).[1] By this protocol, a variety of bicyclic amide compounds can be synthesized from cynaohydrin ethers and the resulting products would be useful molecular scaffolds for constructing drug-like compounds.

Scheme 3. One-pot or two-step synthesis of bicyclic amide compounds via acid catalysis.

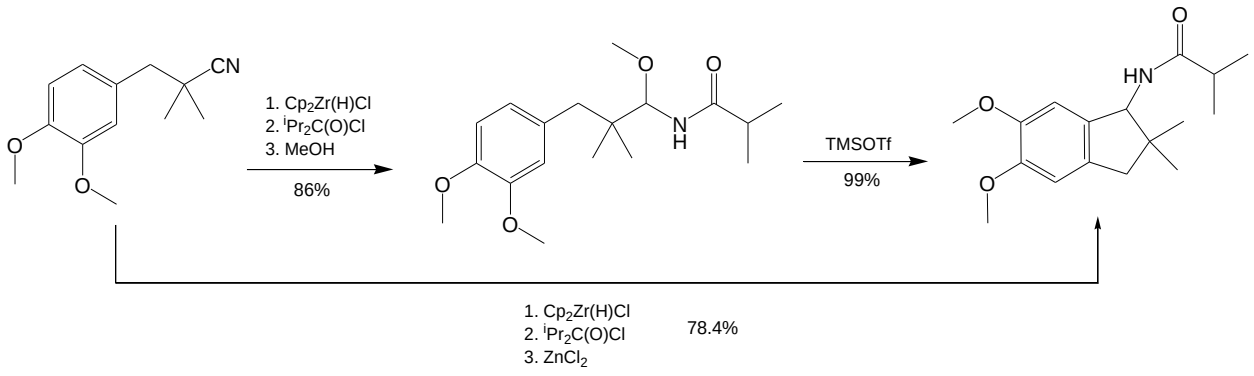

In the two-step synthetic protocol, a stable acyl aminal intermediate is isolated and purified first, then transformed into the bicyclic amide product by treatment of Lewis acids. I want to specifically study the second-step transformation from isolated acyl aminal to bicyclic amide because it can not only increase product yield and enhance the diastereocontrol, but is applicable for more substrates because one-pot synthesis is often compromised by decomposition of acylimine intermediate. The catalysis by acids is crucial for this cyclization process.

In the previous sections, I described the efficacy of coupling online GC to the microreactor for investigation of the Stille reaction and aldol reaction.[2] GC is a fast and highly reproducible instrument; however, it is only appropriate for separating volatile and thermally stable compounds, whereas HPLC is suitable for analysis of most organic compounds. For the above cyclization reaction, reaction substrate acyl aminal is thermally unstable and can quickly decompose in GC column at high temperature. Thus, I decide to couple HPLC instead of GC to the microreactor for online analysis of reaction products. However, conventional HPLC is not so efficient for separating complex reaction mixture, which may compromise the screening throughput a lot.

A new chromatography technique, Ultra-high Pressure LC (UHPLC), seems to be a good solution for our microreactor system. It allows very fast separation with adequate peak capacity. By using shorter columns packed with sub-2-μm particles, UHPLC is able to perform high efficiency separation of complex organic reaction mixtures.[3-9] In this section, I integrated a commercial Jasco *X-LC* system (UHPLC) to a Teflon-capillary-based microreactor[2] to build a new screening system. Compared to fused-silica tubing, Teflon capillary is very inert to acids, hardly protonated. This new microreactor is capable of conducting a large number of parallel reactions with online quantitative analysis by UHPLC.

I validated a continuous-flow approach for catalyst screening through the investigation of zone dispersion in the reaction capillary under varied flow rates. The analysis of 54 reaction samples in sequence confirmed UHPLC's high efficiency and reproducibility. The experimental throughput was about nine one-hour reactions/h.

I investigated several reaction parameters that are important for reaction conversion, including reaction time, temperature and catalyst concentration. Under similar conditions, I chose a diverse set of acids and screened them in a single run by a continuous flow approach. Results showed that product yield strongly depends on acid genre and its acidity. Byproduct analysis by GC-MS and LC-MS also showed different acids will lead to different side reaction pathways. Lewis acids were generally better than Brønsted acids in terms of reaction yield and selectivity. Among all acids, lanthanide catalysts were found to be the best, although they are much less acidic compared to other strong acids. Considering the exceptional capability and generality of lanthanide catalysts towards organic synthesis, I believe they will be highly potential catalysts for this bicyclic-amide-forming reaction.

4.2 EXPERIMENTAL SECTION

4.2.1 Chemicals and materials

HPLC grade acetonitrile (AN) was purchased from Sigma-Aldrich (St. Louis, MO). 4-ethylanisole and *p*-toluenesulfonic acid monohydrate were purchased from Fisher Scientific (Fairlawn, NJ). Acetic acid (glacial), hydrochloric acid (38%) and perchloric acid (72%) were purchased from J. T. Baker Chemical Co. (Phillipsburgh, NJ). Trifluoroacetic acid, chloroacetic

acid, dichloroacetic acid and trichloroacetic acid were purchased from Sigma-Aldrich (St. Louis, MO). Phosphoric acid (85%), sulfuric acid (98%) and nitric acid (70%) were purchased from EMD Chemicals (Gibbstown, NJ). Tin (V) chloride, antimony (V) chloride, boron trifluoride diethyl etherate, boron trifluoride tetrahydrofuran complex, europium (III) trifluoromethane sulfonate, ytterbium (III) trifluoromethane sulfonate, holmium (III) trifluoromethane sulfonate, erbium (III) trifluoromethane sulfonate, terbium (III) trifluoromethane sulfonate were purchased from Sigma-Aldrich (St. Louis, MO). Purified water was obtained from a Millipore A10 water purification system (Billerica, MA).

4.2.2 Instrumentation

The UHPLC system with dual wavelength UV-Vis detector was from Jasco, Inc (X-LC system, Easton, MD). The Acquity UHPLC BEH C18 1.7 μm 1.0 × 50 mm column was purchased from Waters Corp. (Milford, MA). The VICI six-port HPLC injector (Model E60), VICI UHPLC 15000-psi 10-port nanobore valve (model C72NX) and VICI UHPLC 15000-psi 6-port nanobore valve (model C72NX) were purchased from Valco Instruments Co, Inc. (Houston, TX). The UV light source (model D 1000CE) was purchased from Analytical Instrument Systems, Inc. (Flemington, NJ). A USB 2000 optical fiber UV-visible absorbance detector was purchased from Ocean Optics, Inc. (Dunedin, FL). Harvard Pump 11 Plus syringe pumps were purchased from Harvard Apparatus Inc. (Holliston, MA). The HP 1050 autosampler was purchased from Agilent (Palo Alto, CA). The Waters 515 HPLC pump was purchased from Waters Corp. (Milford, MA). The Teflon FEP tubing (100 μm i.d., 1/16" o.d.) that was used as the microreactor was purchased from Upchurch Scientific (Oak Harbor, WA).

4.2.3 Microreactor construction

Catalyst and reagent loading of this new microreactor is same to the previous reactor design. The different sections are the reaction and analysis parts (Figure 34). Instead of using fused-silica capillary, the reaction channel is made by a piece of 100 μm i.d., 1/16" o.d., 6.1 m long Teflon capillary tube. A water/oil bath with a thermometer is used for heating or cooling the reaction capillary to the required temperature. Syringe pump **2** constantly delivers carrier solvent acetonitrile (AN) to push all reaction zones in and out of the capillary. In a continuous flow mode, reaction time is controlled by the flow rate of AN and the length of reaction capillary.

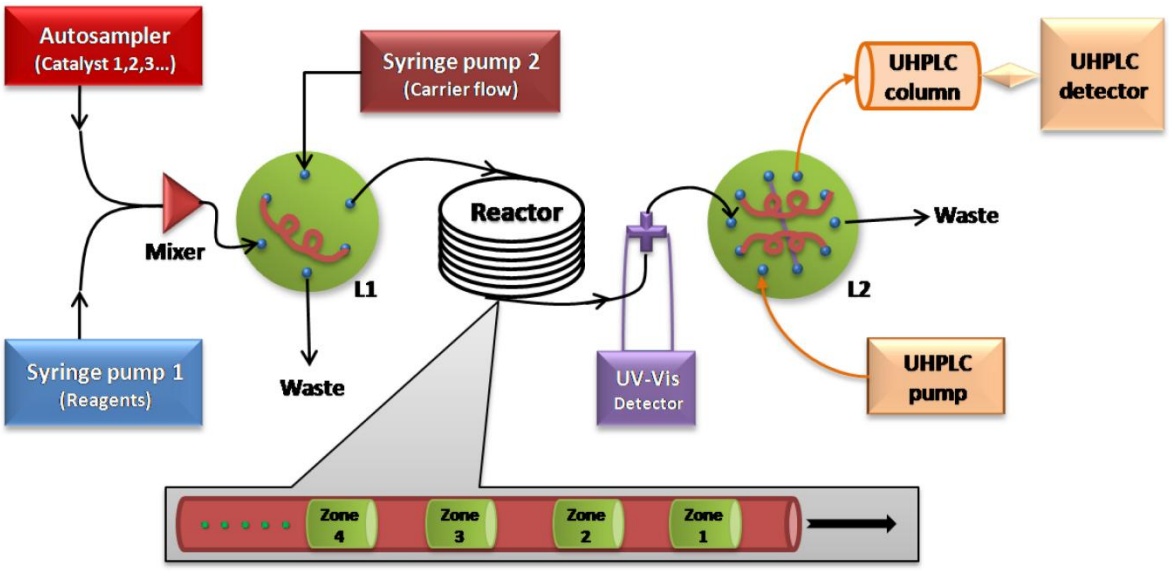

Figure 34. Schematic view of the microreactor system interfaced to UHPLC.

When reaction zones flow out of the capillary, they first go through a flow cell monitored by a UV-Vis fiber optic detector before entering a 10-port 2-position double-loop (1.0 μL) valve (L2). L2 is a 15,000-psi high pressure valve connected to UHPLC pumps and its column. The

detailed configuration is shown in Figure 35. It enables the loading of one loop from the reaction capillary while the contents of the other loop are chromatographed by UHPLC. A single UHPLC chromatographic run is set to analyze all reaction zones over a long period of time and serial injection of samples is done automatically by the switch of L2 which is triggered by the screening software that captures absorbance signals from the fiber optic detector.

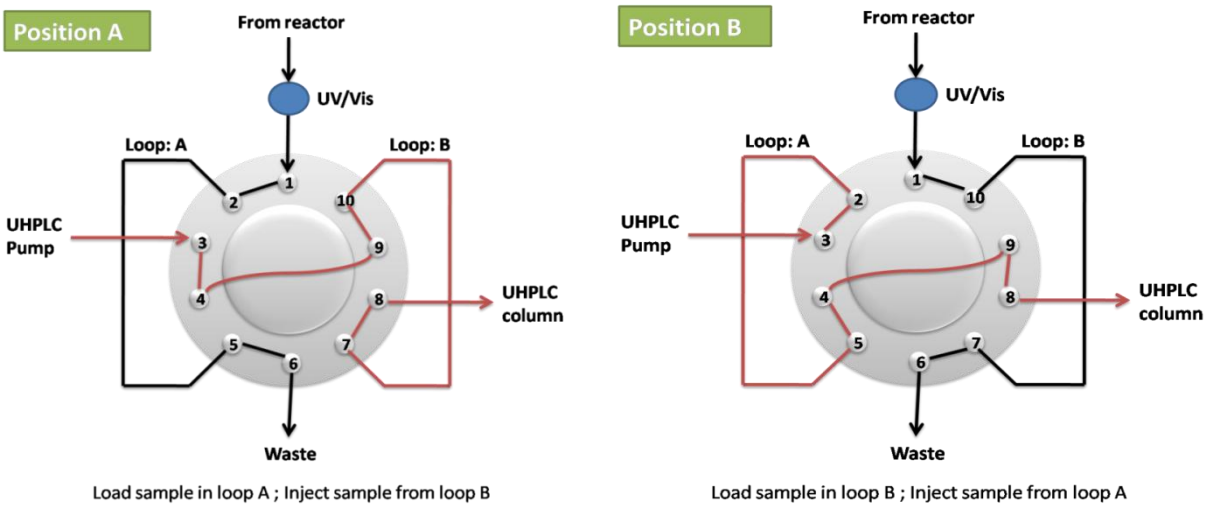

Figure 35. Schematic view of 10-port injector for continuous sample loading and analysis.

4.2.4 Synthesis of the substrate acyl aminals

The substrate of the cyclization reaction was synthesized and isolated by Dr. Qing Xiao in Prof. Floreancig's group. The synthesis procedures are described as follows.

N-(3-(3,4-dimethoxyphenyl)-1-methoxy-2,2-dimethylpropyl) isobutyramide:[10] A solution of 3-(3,4-dimethoxyphenyl)-2,2-dimethylpropanenitrile (0.4892 g, 2.23 mmol) in THF (23 mL) was treated with $Cp_2Zr(H)Cl$ (0.72 g, 2.79 mmol) at room temperature. The reaction mixture was stirred at room temperature for 60 min, then isobutyrylchloride (0.29 mL, 2.79 mmol) was

added. The mixture was stirred for another 30 min at room temperature. Then MeOH (2.7mL, 66.9 mmol) was added, and the mixture was stirred for another 10 min. The reaction was quenched with saturated $NaHCO_3$. The mixture was extracted with ethyl acetate. The extracts were washed with H_2O and brine then dried over $MgSO_4$. The solvent was evaporated under vacuum and the residue was purified by column chromatography to give the product as light yellow oil (0.621g, 86.0%).

^{1}H MNR (300 MHz, $CDCl_3$): δ 6.82-6.79 (m, 1H), 6.73-6.71 (m, 2H), 5.47 (d, 1H, *J* = 9.9 Hz), 4.83 (d, 1H, *J* = 10.2 Hz), 3.87 (s, 3H), 3.86 (s, 3H), 3.32 (s, 3H), 2.64 (d, 1H, *J* = 13.3 Hz), 2.52 (d, 1H, *J* = 13.3 Hz), 2.30 (sept, 1H, *J* = 6.9 Hz), 1.10 (d, 3H, *J* = 6.9 Hz), 1.09 (d, 3H, *J* = 6.9 Hz), 0.92 (s, 3H), 0.91 (s, 3H);

^{13}C NMR (300 MHz, $CDCl_3$): δ 177.5, 148.6, 147.8, 131.1, 123.0, 114.3, 111.1, 86.2, 56.09, 56.08, 56.04, 43.7, 39.6, 36.2, 24.3, 22.2, 19.8, 19.7;

IR (neat): 3306.7, 2965.7, 2934.1, 2832.4, 1657.0, 1589.3, 1515.3, 1465.4, 1271.4, 1236.3, 1089.6, 1029.2, 765.5 cm^{-1};

High Resolution MS (Electron Ionization): calculated for $C_{18}H_{29}NO_4$ 323.2097, found *m/z* 323.2094.

4.2.5 UHPLC analysis

The chromatographic separation was done in an isocratic mode. The column was Acquity UHPLC BEH C18 1.7 μm 1.0 × 50 mm column. The mobile phase was composed of AN:Water (24:76, v/v) at a flow rate of 0.35 mL/min. The column oven was set at 70 ^oC and injection volume (double loops of L2) was 1.0 μL. A single chromatographic run was set to analyze all reaction zones.

4.2.6 Continuous flow reactions in the capillary

Investigation of reaction parameters

Acid solutions (x mole % in AN) were placed in 1.5-mL glass autosampler vials. Catalyst vials were set on the tray of the autosampler. The reagents containing 0.01 M substrate and 0.01 M 4-ethylanisole (internal standard, IS) in AN were loaded in a 2.5 mL gas-tight syringe (Hamilton Company, Reno, Nevada) and constantly driven by syringe pump **1**. Syringe pump **2** delivered the carrier solvent AN at a certain flow rate to push all reaction zones through the capillary. The flow rate is set to correspond to the required reaction time. For example, for 1-h-reaction, the flow rate was set at 0.9 μL/min; for 2-h-reaction, the flow rate was set at 0.45 μL/min. The capillary was heated or cooled in an oil bath to the required temperature. Reaction zones were serially analyzed by online UHPLC when they flow out of the reaction capillary.

Screening of catalysts

Solutions of a diverse set of Brønsted and Lewis acids (20 mole % in AN) were loaded by the autosampler following the above procedure. The reagents (0.01 M substrate and 0.01 M 4-ethylanisole in AN) were loaded by syringe pump **1**. Syringe pump **2** delivered the carrier solvent (AN) at a certain flow rate to push all reaction zones through the capillary followed by online analysis by UHPLC.

4.2.7 Calibration curve for yield and conversion determination

A calibration curve was prepared from standard solutions of product, substrate and internal standard (IS) 4-ethylanisole (commercially available). A series of stock solutions with various

mole ratios of pure product, substrate and IS were made in AN to obtain standards. I chromatographed those stock solutions by UHPLC. The calibration curve for product determination was made by plotting the mole ratios of product to IS as a function of peak area ratios of product to IS. The calibration curve for substrate conversion was made by plotting the mole ratios of substrate to IS as a function of peak area ratios of substrate to IS.

4.2.8 Byproduct analysis by GC-EI-MS and LC-ESI-MS

Crude reaction mixtures are injected directly into GC-MS and LC-MS for analysis without pretreatment. GC-MS system: Shimadzu GC-17A and QP5050A. GC column: XTI-5, 30 m, thickness 0.25 μm, diameter 0.25 mm. GC separation conditions: 100 ^{o}C → 250 ^{o}C at 25 ^{o}C/min, held 10 min, inlet temperature 250 ^{o}C, carrier flow 3 mL/min He, split ratio 50. LC-MS system: Shimadzu UFLC SIL-20AC and ABI API2000 QqQ (LC/MS/MS) with turbo electron spray. LC column: Dionex Acclaim C18, 3 μm, 120 Å pore, 2.1mm ×150 mm. LC separation conditions: 0.2 mL/min, gradient 5-95% ACN/water (0.1% CH_3COOH) in 20 min, oven 40 ^{o}C, UV detector 220 nm.

4.3 RESULTS AND DISCUSSSION

4.3.1 Continuous flow reactions in the capillary

The cyclization reaction starting from acyl aminals is a relatively fast reaction (Scheme 4) that is usually complete within an hour. Therefore, I carried out this reaction using a continuous-flow approach by delivering all zones through the capillary by a constant flow stream of AN.

Scheme 4. Acid catalyzed cyclization reaction forming bicyclic amide libraries.

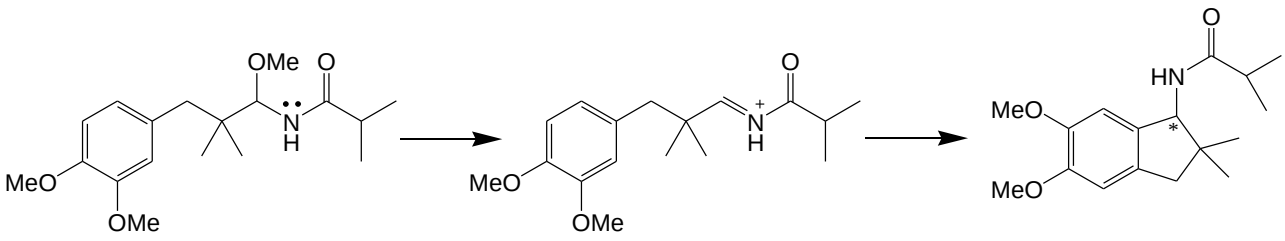

In the capillary, flow dispersion due to hydrodynamics can cause spreading of zones in the capillary which have been discussed in previous sections. The zone shapes are schematically shown in Figure 36. When zones are just injected into the reaction capillary, they are in rectangular shape without dispersion; while when they flow in the capillary, they usually show some extent of dispersion like chromatographic peaks. The dispersion extent depends on a number of factors such as flow rate, temperature, channel diameter, diffusion coefficients and viscosity.[11] Because the wings of dispersed zones have lower concentrations of reagents and catalysts due to dilution, reaction yield might show large variations in these regions of zones. Thus, I programmed the screening software to inject only the center region of reaction zones into the UHPLC for best reaction reproducibility.

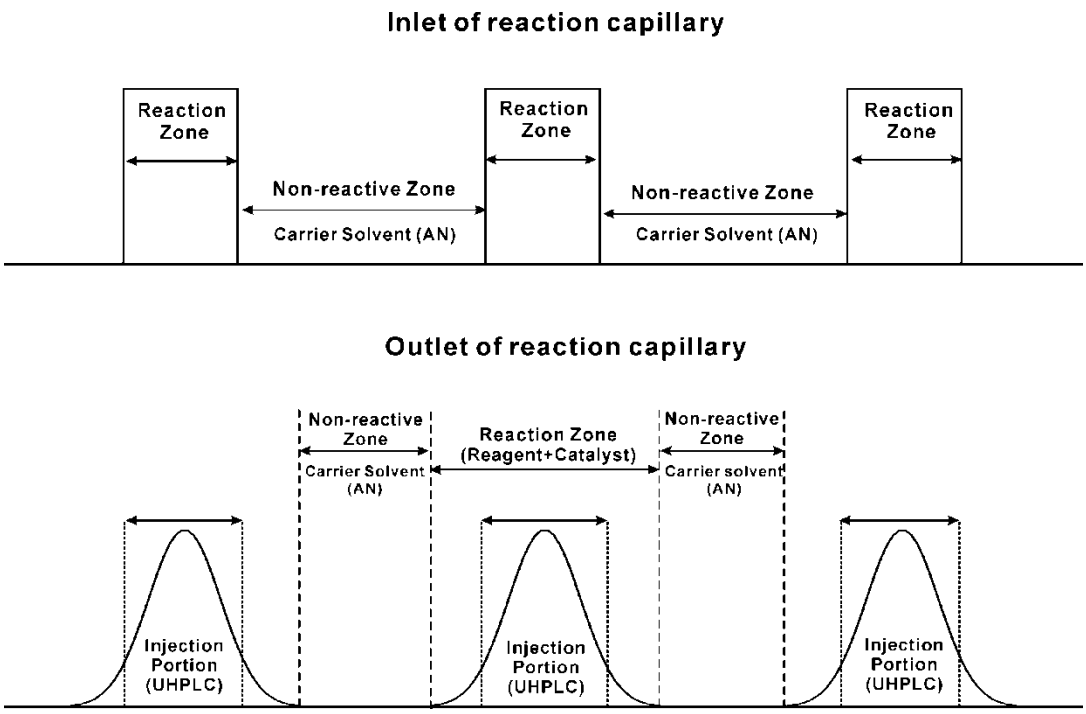

Figure 36. Schematic view of flow dispersion of reaction zones.

Zones are first in rectangular shape after immediate injection, and then disperse when flowing through the channel. The peak maximum has highest product concentration, while the peak wings have lower product concentration.

In the continuous-flow mode, the residence time of zones is mainly controlled by the flow rate that also determines the extent of dispersion. Basically, the higher the flow rates, the shorter the residence time and then the narrower the zones. I studied the effect of flow rates on dispersion by loading and pushing reaction zones continuously through the capillary under varied flow rates. Figure 37 shows the shapes of three reaction zones at varied flow rates. I see at high flow rate, zones are very narrow but still in good symmetry without much tailing. The width and height of zones are very reproducible, indicating good reproducibility of the microreactor system which is important for catalyst screening. By simply controlling the distance between adjacent

zones, I can effectively minimize zone overlapping. In Figure 37, zones can be well separated even when residence time is more than 3 h.

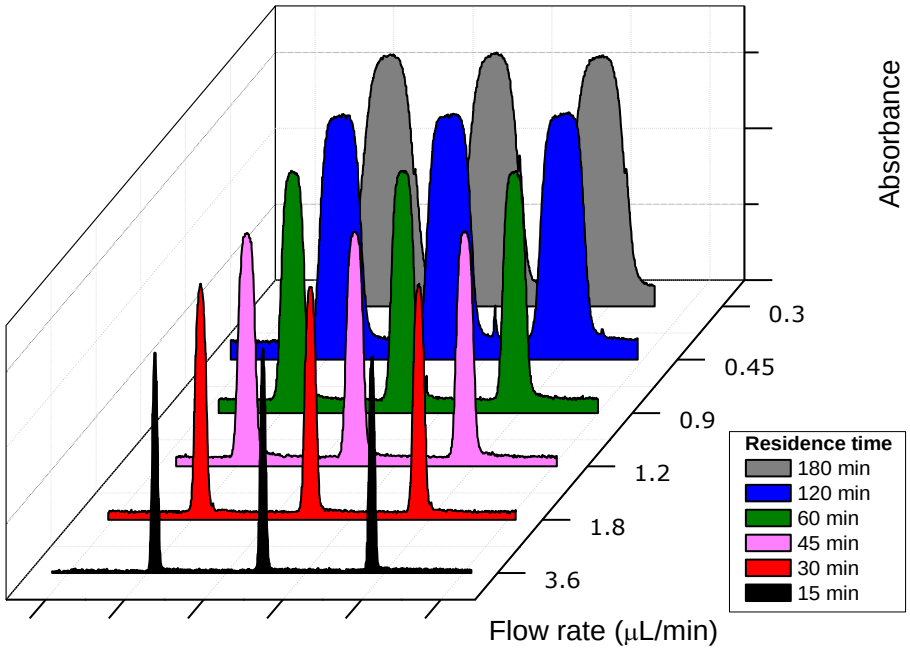

Figure 37. UV response of zones going through the reactor capillary at different flow rates. The Teflon capillary is 6.1 m, 100 μm i.d.; Solvent is acetonitrile; UV detection wavelength is 225 nm. Residence times of zones correspond to their flowing time in the reaction capillary.

A major concern for any screening approach is reaction reproducibility. Many operational factors play a role, such as flow rate, zone volume, mixing ratio of catalyst and reagent and temperature. The flow rate determines the reaction time, zone shape, dispersion and overlapping. I used a Harvard syringe pump to deliver precision flow for accurate control. Figure 38 shows an example of absorbance response of 54 reaction zones serially passing through the reactor capillary with a residence time of 1 h. I repeated three reactions for studying one catalyst and therefore, it is clearly shown that the absorbances of three successive zones are mostly identical, indicating reproducible product concentrations in repetitive zones. The space between adjacent

zones is highly reproducible. As shown in Figure 39, a linear regression curve is plotted based on the time points when the zones hit the UV-Vis detector as a function of zone numbers. The first zone has a residence time of 60 min which equals to the reaction time. Since individual zones should take the same time to load and flow through the reaction capillary, then they should come out of the capillary in equally-spaced time periods. The perfect linearity (R^2=0.99999) of times of all 54 zones shown in Figure 39 confirms the excellent system stability over a long period of time. Therefore, screening a large number of zones in a continuous flow is technically possible under precise instrumental control as long as the syringes can feed enough reagents and solvents to the reaction capillary.

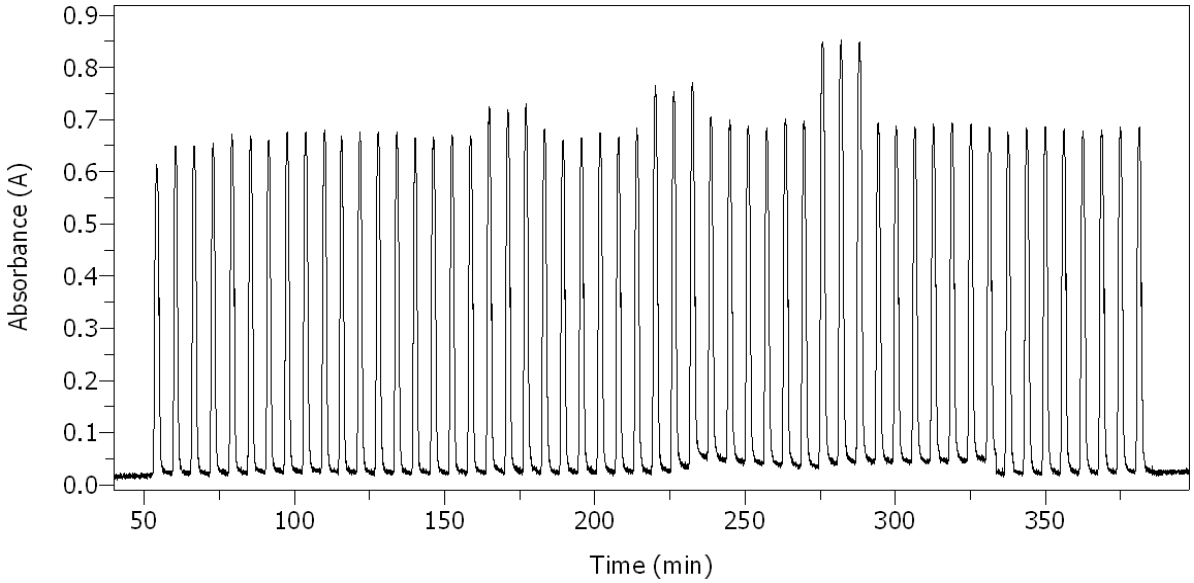

Figure 38. Absorbance response of 54 reaction zones flowing out of the reactor and passing through the UV-Vis optical detector at a flow rate of 0.9 µL/min.

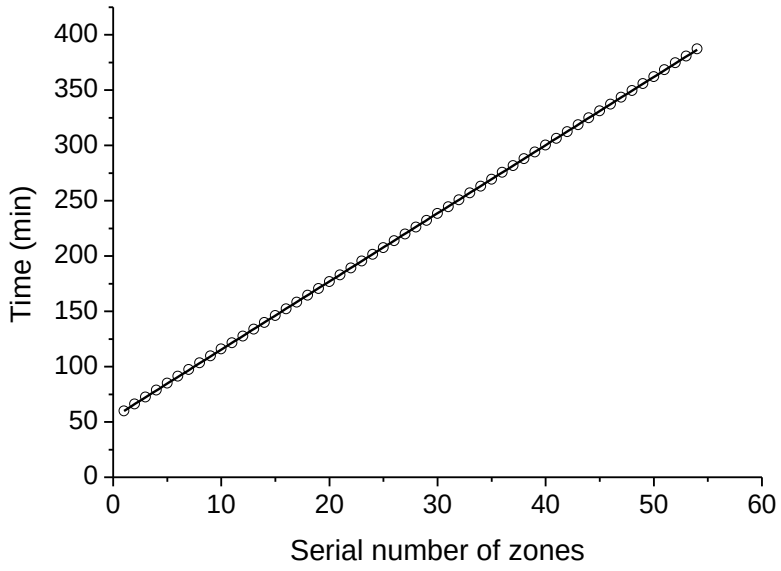

Figure 39. The linear regression of time points when 54 zones hit the UV-Vis detector in a continuous flow (R^2=0.99999).

As mentioned before, the product concentrations vary in a single reaction zone. In principle, if all zones have the same composition, they should have the same shape and width. However, in reality, reaction substrates and products will have different concentrations in different zones depending on reaction conversion. The detection wavelength of UV-Vis optic fiber detector is empirically set at 225 nm and at this wavelength, molar absorptivities of product and substrate are close because they have similar major chromophore groups. Most catalysts, protic acids or transition-metal Lewis acids, have low absorbance at this wavelength. Thus, generally, the peak height and peak width of all zones should have little difference because the total concentration of product and substrate is constant for all zones. In Figure 40, the peak width at half height of 54 zones is plotted as a function of zone numbers. It shows that zone width has a little variation represented as a time length of 84.2±3.9 sec. The relative standard deviation is

4.6%. This small variation of half widths indicates the product concentration variations in zones do have a little effect on peak shapes. Moreover, the presence of some unknown byproducts that may have different molecular absorptivities can also contribute to the variation of peak height and peak width.

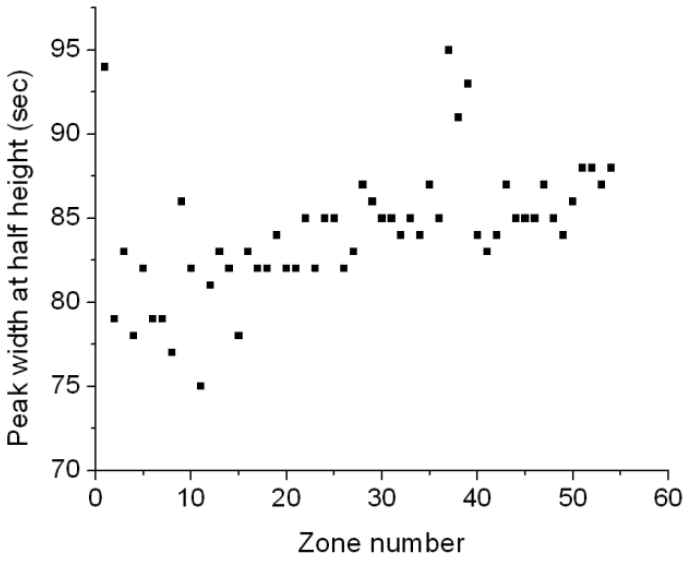

Figure 40. Peak widths at half height of 54 reaction zones. The average half width is 84.2 ±3.9 seconds.

4.3.2 Online UHPLC analysis

The high throughput screening capacity of the microreactor is largely dependent on the online analysis efficiency. UHPLC is interfaced to the outlet of reaction capillary via a 10-port double-loop valve. The separation column was chosen based on its generality, separation efficiency, pH and temperature tolerance. Waters Acquity UHPLC BEH column fits our requirement very well. This column contains 1.7 μm C18 silica particles and it has very high efficiency and broad

applicability for organic compounds. The maximum temperature is 90 ^{o}C and its pH range is from 1 to 12. It is very suitable for analyzing reaction mixtures containing strong acids.

A typical chromatogram including peaks from 54 reaction zones in a single screening run is shown in Figure 41-a, in which peaks from all zones are densely packed. Figure 41-b shows a tiny portion of the whole chromatogram containing peaks from one reaction zone which has a number of by-products, product, internal standard (IS) and substrate. By separating reaction samples at high temperature, high flow rate and high pressure (>10000 psi), the excellent peak capacity can be gained. Besides, the separation shows very good reproducibility in terms of peak height, width, retention time and resolution, after more than 6 h operation (Figure 41-c).

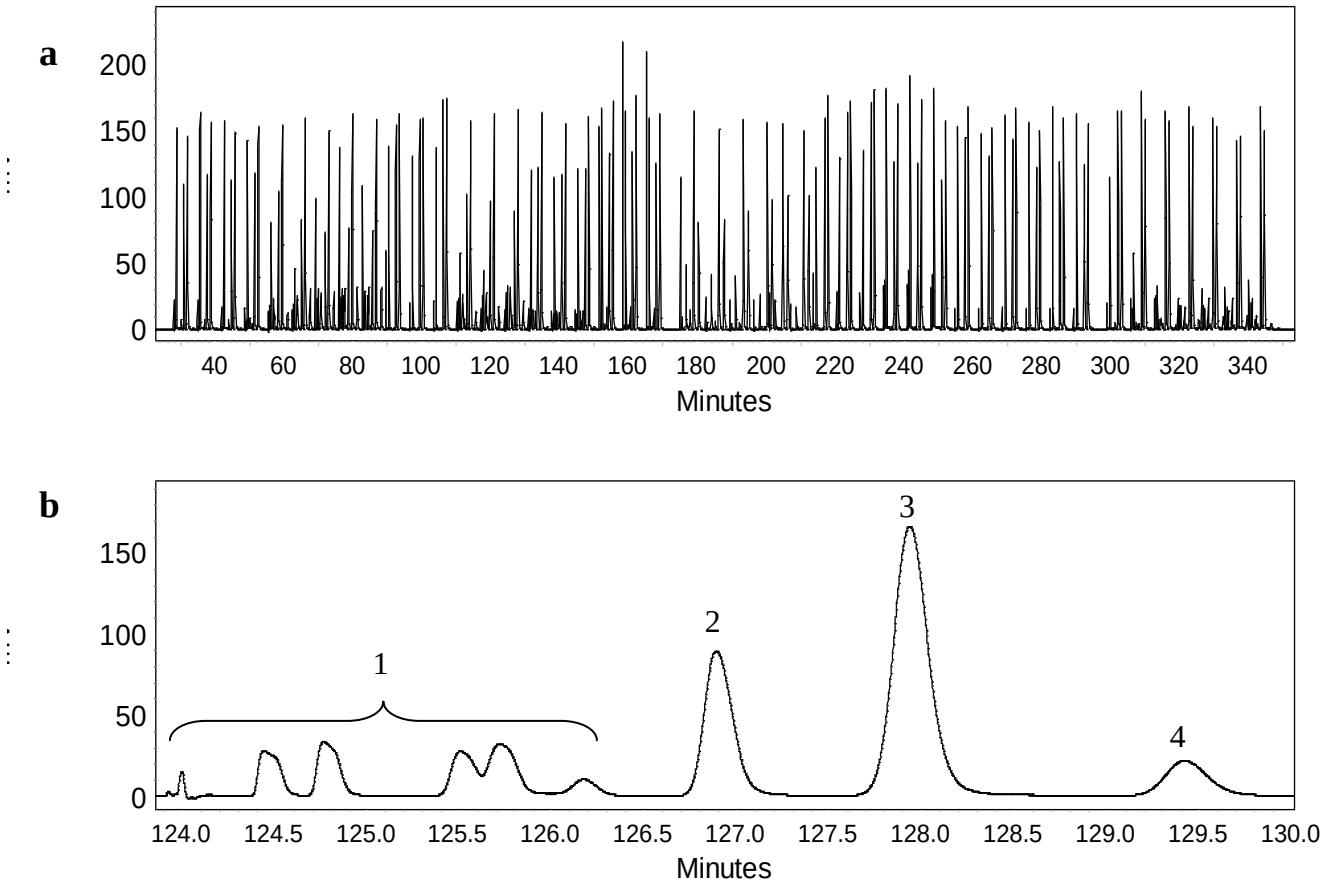

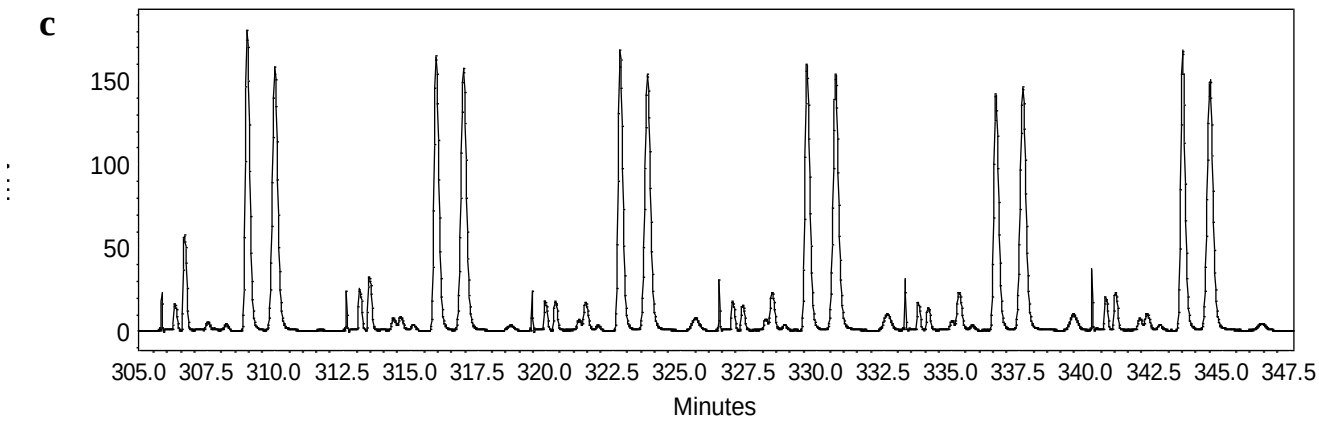

Figure 41. Online UHPLC analysis of continuous-flow reaction zones.

a. total chromatogram of 54 reaction zones; b. peaks from one reaction zone containing several by-product (1), product (2), internal standard (4-ethylanisole) (3), and substrate (4); c. partial chromatogram of last six zones containing 2 catalysts (each catalyst is contained in three zones).

In an automated system, there is no opportunity to intervene and make corrections, thus system stability and reproducibility are critical. I have quantitatively studied two parameters: the adjusted retention time, $t_R^{'}$, of the product, and the peak area of the IS. In Figure 42, I normalize $t_R^{'}$ and peak area by dividing them by the mean of the 54 zones. The normalized retention times show very good consistency with a relative standard deviation of 0.8% (n=54). Thus, there is no concern about drift in retention times. On the other hand, the peak area of the IS shows some random variations with a relative standard deviation of 9.7% (n=54). The purpose to incorporate IS is to correct several related errors, one of which is the injection variability. In Figure 40, we have seen that small variations of half peak widths of reaction zones. The trigger for sensing the presence of a zone is based on optical absorbance. Thus, zones with different maximum absorbances or slightly different shapes (widths) may trigger the injection at different times (with respect to the centroid of each individual reaction zone), which can cause different portions of

zones that contain different amounts of reagents injected into UHPLC due to dilution. I believe this factor plays a key role of injection volume variation. Another is evaporation of solvent leading to concentration changes. I would expect a continually increasing IS peak area resulting from solvent evaporation, but this I do not see. The whole reactor system is completely sealed to prevent solvent leaking, so solvent evaporation is very unlikely to happen. In any cases, it is clear that the IS is necessary to achieve accurate results.

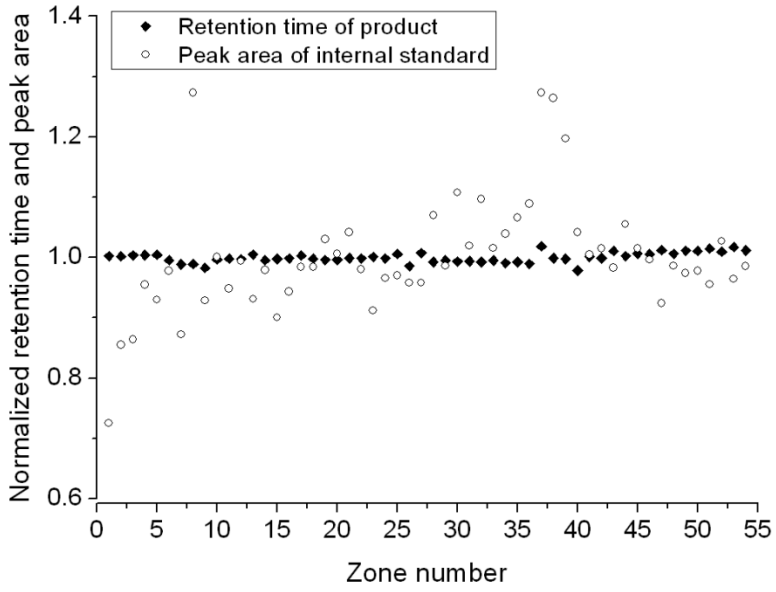

Figure 42. The normalized retention times (product) and peak areas (IS, 4-ethyl anisole) in all 54 reaction zones.

4.3.3 Reaction parameters investigation

In order to have a good understanding of the reaction process, I studied several parameters by the microreactor before screening catalysts, which include reaction time, temperature and catalyst concentration. I chose some moderately active acids like diphenyl phosphate and trichloroacetic acid as model catalysts to investigate above reaction parameters.

Temperature

Temperature has an important effect on catalyst activity. Four different temperatures, 0 ^{o}C, 20 ^{o}C, 40 ^{o}C and 60 ^{o}C, were studied. At each temperature, three successive reactions were carried out for statistical calculation of yield and conversion. The yield is determined by comparing peak area of the product with that of the IS while the conversion is calculated by comparing the peak area of substrate with that of the IS. Higher temperature above 60 ^{o}C was not investigated because solvents will probably form bubbles in the reactor channel.

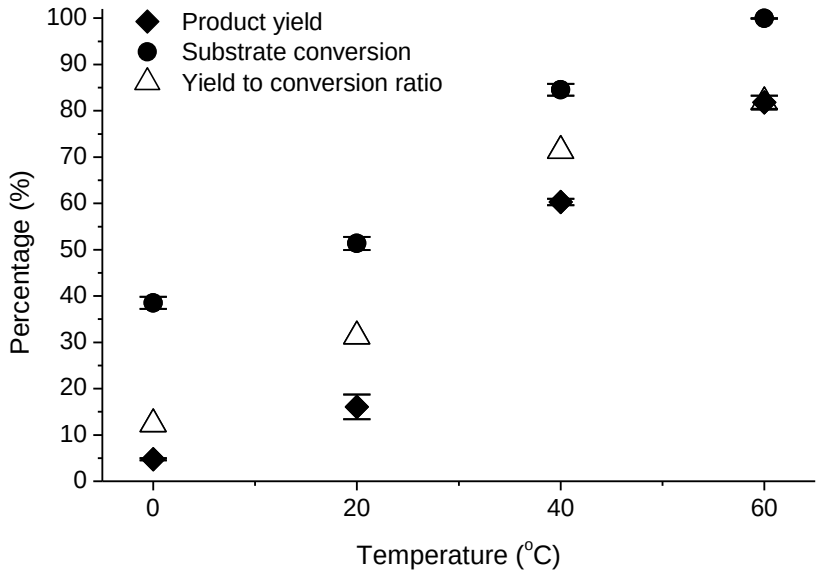

Figure 43. The effect of temperature on yield, conversion and selectivity.

Catalysts: 1.0 molar equivalent (eq) of diphenyl phosphate in AN; Conditions: continuous flow reaction in the microreactor for 1 h. Yield & Conversion = mean ± SEM (n=3).

In Figure 43, we see that higher temperature is more favorable for the conversion and the ratio of yield to conversion has an almost linear increase with the rising temperature. The maximum ratio at 60 ^{o}C is about 80% whose data point is overlapping with the yield data. Higher

temperature leads to faster reaction rate, then better reaction selectivity, which indicates the presence of kinetically competing side reactions to the major cyclization process. I chose the benign temperature 40 ^{o}C for further experiments. In terms of the small standard errors of yield/conversion, reactions in the microreactor are very reproducible.

Catalyst concentration

Catalyst concentration is an important factor affecting reaction kinetics and product yield. I study the catalyst concentrations of two acids, diphenyl phosphate (Figure 44) and trichloroacetic acid (Figure 45). Results show that for both acids, yield and conversion are strongly dependent on the catalyst concentrations. The ratio of yield to conversion also increases almost linearly with increasing catalyst concentrations. However, at very high concentrations of catalysts, the yield and conversion seem to reach an equilibrium which is clearly shown in Figure 45.

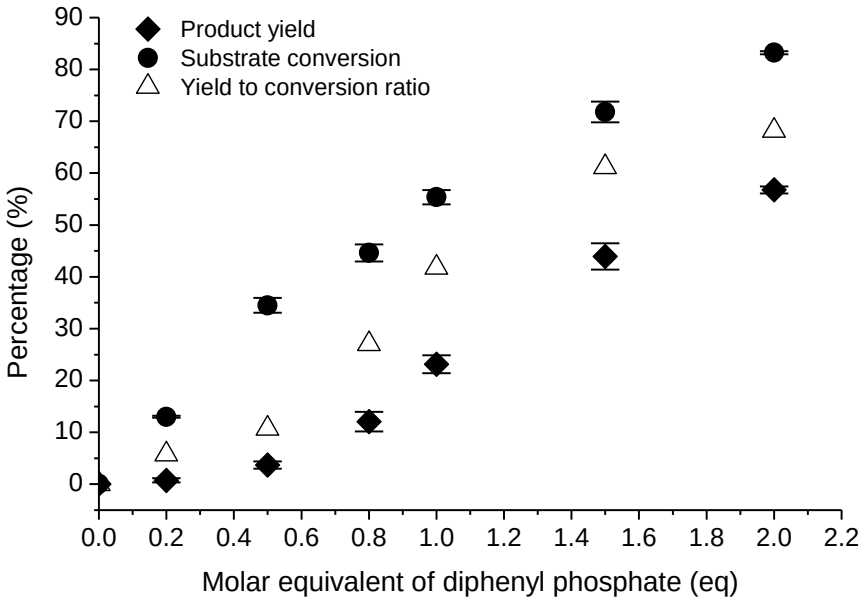

Figure 44. Reaction yield, conversion and selectivity as a function of catalyst concentrations (Diphenyl phosphate).

Reagents: 0.01 M substrate and 0.01 M 4-ethylanisole (IS, 1 eq) in AN; Catalysts: x mole % diphenyl phosphate in AN; Conditions: 1 h continuous flow reaction in the microreactor. Yield & Conversion = mean ± SEM (n=3).

Based on those results and above temperature studies, I believe that reaction kinetics play a significant role in this process. Under the catalysis of acids, a number of side reactions may compete with the major cyclization process that can become more favorable at faster reaction rates induced by higher temperature and larger catalyst concentrations.

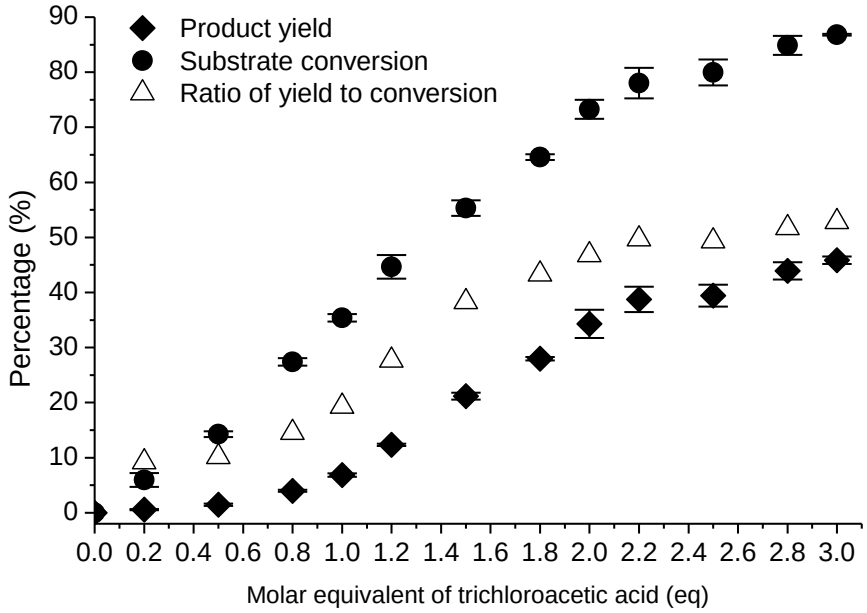

Figure 45. Reaction yield, conversion and selectivity as a function of catalyst concentrations (trichloroacetic acid).

Reagents: 0.01 M substrate and 0.01 M 4-ethylanisole (IS, 1 eq) in AN; Catalysts: x mole % trichloroacetic acid in AN; Conditions: 1 h continuous flow reaction in the microreactor. Yield & Conversion = mean ± SEM (n=3).

Reaction time

The effect of reaction time on the yield and conversion is shown in Figure 46. The cyclization process reaches the equilibrium in about 3 h to give the maximum conversion about 90% under the catalysis of weak acid diphenyl phosphate. This equilibrium can be seen in Figure 45 at very high catalyst concentrations as well. A possible reason for this equilibrium is due to the accumulation of methanol in the reaction solution which may react with the acyliminium ion intermediate to reverse the process.

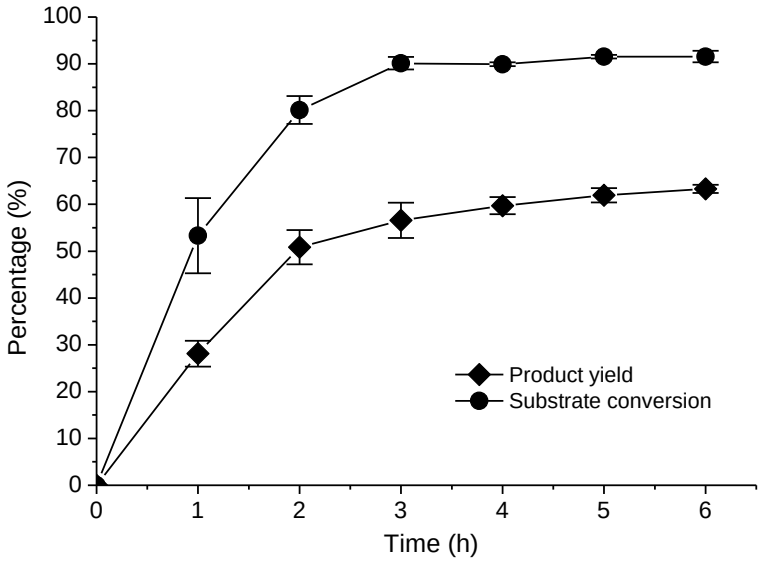

Figure 46. Reaction yield and conversion as a function of time.

Reagents: 0.01 M substrate and 0.01 M 4-ethylanisole (IS, 1 eq) in AN; Catalysts: 1 eq diphenyl phosphate in AN; Yield & Conversion = mean ± SEM (standard error) (n=3).

4.3.4 High-throughput screening of acid catalysts

The aforementioned studies indicate reaction rate plays a key role on reaction yield and conversion. To improve the yield, weak acids like trichloroacetic acid or diphenyl phosphate

have to be used with high concentration in order to accelerate the catalytic process. However, for strong acids or extremely strong acids like perchloric acid, lower concentration will be enough to gain good conversion. Using too much amount of strong acids may lead to more unexpected side reactions, and also damage the stainless tubing and column of UHPLC system. Therefore, for catalyst screening, I reduced all acid concentrations to the catalytic amounts. As mentioned in previous chapters, I can evaluate the catalyst efficiencies based the relative reaction yields.

Table 5. Screening of acids in the microreactor at two different temperatures.

Entry	Catalyst	Temperature, 0 °C [a]			Temperature, 40 °C [b]		
		Yield (%) [c]	Conversion (%)	Ratio of yield/ conversion (%) [d]	Yield (%)	Conversion (%)	Ratio of yield/ conversion (%)
1	H_2SO_4 (98%)	9.4 ± 1.2	79.5 ± 0.6	11.8	61.4 ± 0.3	98.8 ± 0.1	62.1
2	H_3PO_4 (85%)	2.2 ± 2.4	53.6 ± 4.0	4.1	40.9 ± 0.2	72.1 ± 0.1	56.7
3	HNO_3 (70%)	0	44.8 ± 2.1	0	38.7 ± 1.2	71.5 ± 0.5	54.1
4	$HClO_4$ (70%)	63.3 ± 0.8	98.3 ± 0.2	64.3	80.1 ± 3.0	99.6 ± 0.6	80.4
5	HCl (38%)	2.6 ± 2.4	55.4 ± 4.1	4.8	47.1 ± 3.9	84.8 ± 3.1	55.6
6	CH_3SO_3H	4.4 ± 0.8	69.9 ± 3.3	6.3	61.4 ± 0.3	97.9 ± 0.1	62.6
7	$TosOH.H_2O$	11.8 ± 0.3	78.8 ± 1.1	14.9	61.5 ± 0.1	100	61.5
8	CF_3COOH	0	22.8 ± 6.0	0	5.1 ± 2.4	24.7 ± 5.4	20.7
9	CCl_3COOH	0	17.3 ± 0.5	0	1.3 ± 0.3	8.2 ± 2.9	16.3
10	$SnCl_4$	48.6 ± 1.5	96.9 ± 0.2	50.1	78.5 ± 0.3	100	78.5
11	$SbCl_5$	51.1 ± 0.3	98.8 ± 0.2	51.6	58.8 ± 0.6	100	58.8
12	$BF_3.O(C_2H_5)_2$	52.3 ± 0.4	99.0 ± 0.1	52.8	70.0 ± 0.2	100	70.0
13	BF_3.THF	56.7 ± 0.2	99.0 ± 0.1	57.2	65.9 ± 0.3	100	65.9
14	$Eu(OTf)_3$	32.8 ± 6.4	91.1 ± 4.5	36.1	88.2 ± 5.4	97.2 ± 0.9	88.2
15	$Tb(OTf)_3$	25.8 ± 2.8	83.9 ± 1.3	30.8	85.5 ± 3.1	91.8 ± 1.2	93.2
16	$Er(OTf)_3$	23.6 ± 1.4	82.3 ± 0.8	28.7	93.2 ± 0.3	95.7 ± 0.1	97.4

[a] Reagents: 0.01 M substrate and 0.01 M 4-ethylanisole (IS, 1 eq) in AN; Catalysts: 20 mole % acids in AN; Conditions: 0 °C, 1 h continuous flow reaction.

[b] Reagents: 0.01 M substrate and 0.01 M 4-ethylanisole (IS, 1 eq) in AN; Catalysts: 20 mole % acids in AN; Conditions: 40 ^{o}C, 0.5 h continuous flow reaction.

[c] Yields of product and conversions of substrate are determined by UHPLC. Yield & conversion = mean ± SEM (n=3)

[d] Percentage ratio of yield to conversion.

I chose a diverse set of acids including 9 Brønsted acids and 7 Lewis acids. Screens were done at two different temperatures, 0 ^{o}C and 40 ^{o}C in two separate runs. In each run, 48 reactions were carried out containing 16 catalysts. The screening results are shown in Table 5, in which it clearly shows that high temperature 40 ^{o}C is better than lower temperature 0 ^{o}C in terms of reaction conversion, yield and selectivity. It agrees with the previous temperature studies in Figure 43 that side reactions are more serious at lower temperature. Among those protic acids, perchloric acid shows good yield and high conversion even at low temperature. I believe its high activity is just due to its very strong acidity, allowing the cyclization process fast enough to compete over other side reactions. It is noteworthy that a lot of reactions catalyzed by low concentrations of strong acids can achieve 100% conversion without exhibiting the equilibrium trend, which is a proof that strong acids may lead to some unknown side reactions which can deplete the substrate completely.

Lewis acids are generally better than Brønsted acids in terms of conversion and selectivity. Both strong and weak Lewis acids show good yield and conversion at high temperature; while at low temperature, strong Lewis acids (entry 10 to entry 13) show only a little yield loss. Lanthanide series of Lewis acids (entry 14 to entry 16) show higher yield and selectivity at 40 ^{o}C than any other acids. When looking at the chromatogram, few by-products peaks are present in the reaction samples catalyzed by lanthanides. Even at low temperature, they

still have moderate conversion and yield that are better than some strong Brønsted acids. This is a surprising discovery because I initially thought catalyst activities mainly depend on their acidities. I believe the exceptional reactivities of lanthanide catalysts rely on their strong oxygen-binding capacity, making it easier to eliminate methoxy group and form the acyliminium ion intermediate.[12] Few side reactions happen as a result of their weak acidities. They seem to be very promising catalysts for the cyclization reaction. Other organic processes that employ the similar route may also take advantage of lanthanide series of catalysts.

4.3.5 Throughput of the microreactor

In the continuous flow approach, reactor throughput is largely dependent on the sample loading time and reaction time. The analysis time by UHPLC is short enough, so it can be neglected because sample loading, reaction and analysis are carried out simultaneously. The current non-optimized throughput of the microreactor is about 9 one-hour reactions per hour for studying 54 reactions with a typical sample loading time of 5.5 min. Flow rate depends on reaction time. Slower reaction needs lower flow rate to increase residence time.

$$Reactor\ Throughput = \frac{\#\ of\ reactions}{time} = \frac{N}{t_i + t_r + t_a}$$

t_i: sum of loading times of all reaction zones; t_r: single zone flowing-out time (reaction time) ; t_a: single zone analysis time.

$$Current\ throughput = \frac{54}{[5.5\ (\mathrm{min}) \times 54]_{loading} + [60\ (min)]_{reaction} + [5.5\ (min)]_{analysis}}$$

$$\approx 9\ reactions/h$$

In the above calculation, the loading time for a single reaction zone is about 5.5 min and analysis time is also 5.5 min. The flowing time is equal to the reaction time. If N is very large, reaction and analysis time can be both neglected in the calculation. So reactor throughput only depends on the loading time of individual zones, and the above reactor throughput will become 11 reactions/h with the loading time of 5.5 min. It is clear that shorter loading time can significantly increase reactor's throughput with large N, which can be realized by optimization of sample loading parameters and procedures. When N is not so large, reaction time plays a role in the reactor throughput. Slower reaction leads to somewhat lower throughput which can be counterbalanced by screening larger numbers of zones in a single microreactor run.

4.3.6 Side reaction analysis

From above studies, I know that the cyclization reaction is in the competition with some unknown side reaction processes. I want to identify those side reactions, which could help better understanding the reaction mechanisms. In Figure 47, UHPLC chromatograms of three reaction zones catalyzed by strong perchloric acid (Figure 47-A) and weak dichloroacetic acid (Figure 47-B) exhibit two different by-product peaks, which I defines as Unknown 1 and Unknown 2. Perchloric acid and other strong acids mainly lead to the formation of a large Unknown 1 peak whose area is comparable to the product. This by-product eludes very early, indicating it has a much higher polarity than the product and substrate. Weak acids like dichloroacetic acid, on the contrary, result in very little Unknown 1 but a significant amount of Unknown 2 which is in close proximity to the isolated aldehyde byproduct as shown in chromatogram Figure 47-B. Few products are formed when weak acids are applied, which means the cyclization process is largely

inhibited. These two by-products resulting from two different acids are indicative of the presence of two different side reaction pathways that are directly related to the acid catalysts.

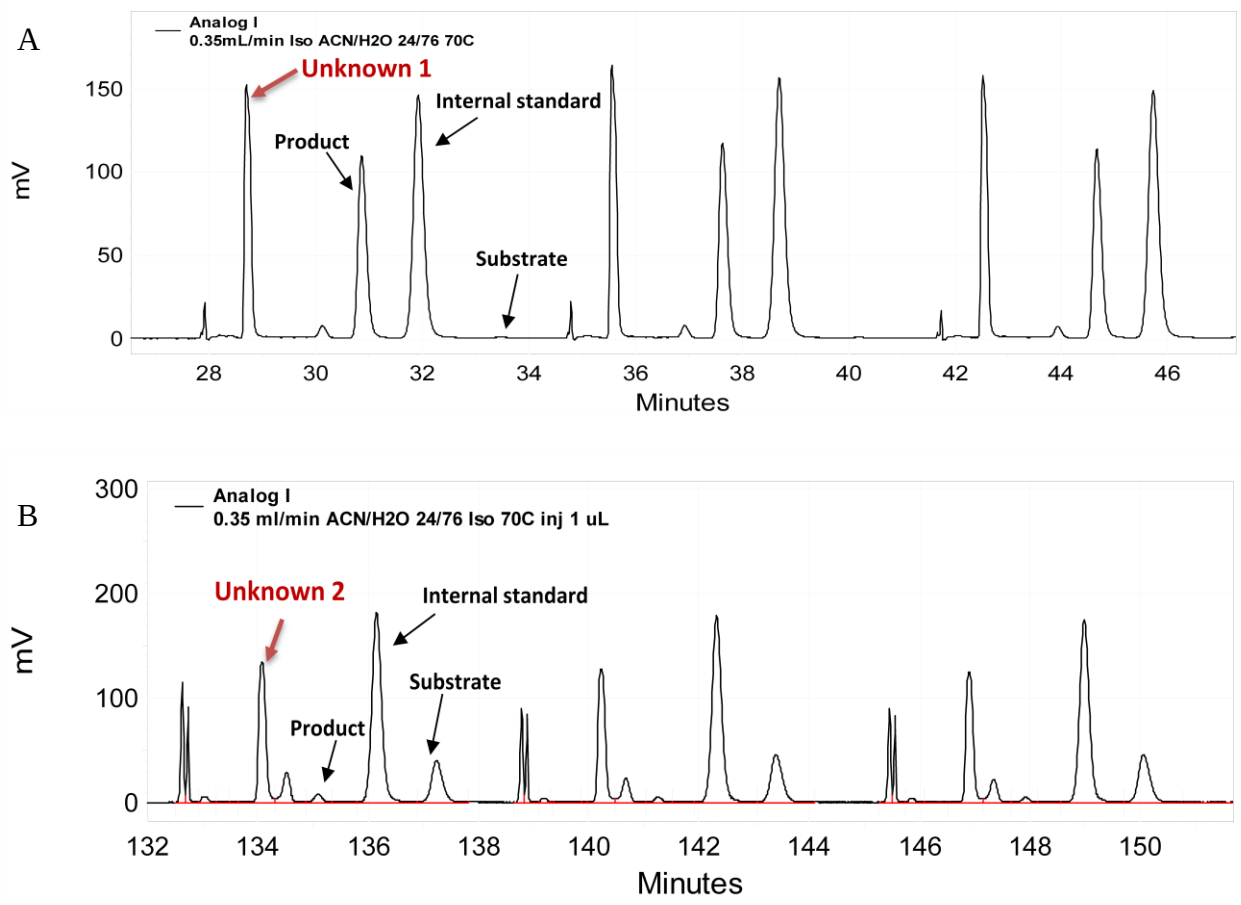

Figure 47. Chromatogram of cyclization reactions catalyzed by strong acid $HClO_4$ (A) and weak acid $CHCl_2COOH$ (B).

GC-MS and LC-MS are common tools to characterize synthetic intermediates when they are hard to be isolated by column chromatography. I prepared the reaction samples with acid catalysts in the regular vials and injected those samples directly into GC-MS and LC-MS without purification. In Figure 48-A, Unknown 1 and the product are well separated by GC. In Figure 48-B, the mass spectrum of Unknown 1 peak shows the possible molecular ion of 263 *m/z*. When comparing it to the product mass spectrum (Figure 48-C), we see that except their molecular ions

(product, 291 *m/z*), most of their fragmentation ions are identical. This consensus implies that Unknown 1 should have similar basic structures to the product with only minor difference.

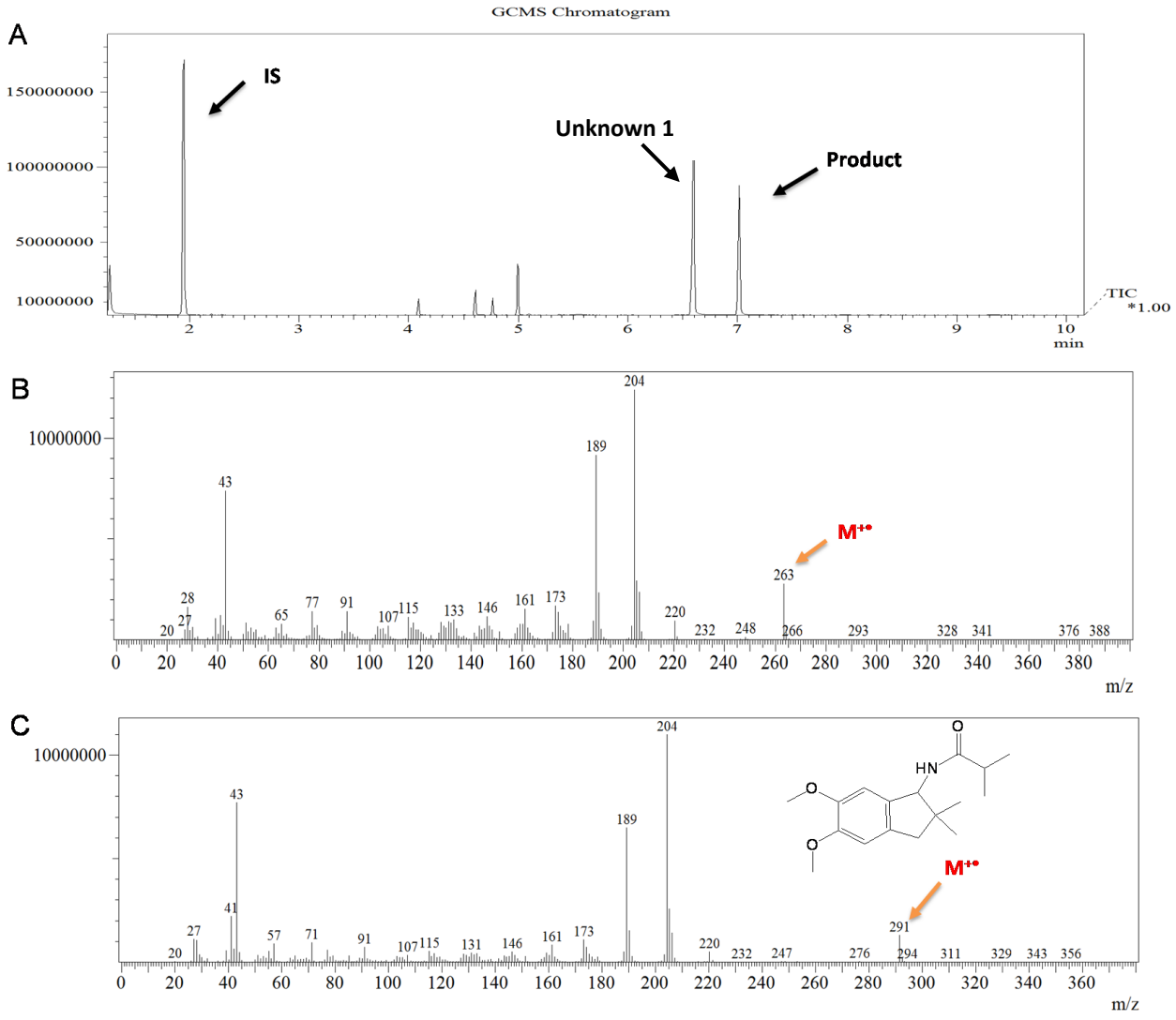

Figure 48. GC-MS studies of batch reaction catalyzed by perchloric acid.

GC chromatogram of reaction solution (A), mass spectrum of Unknown 1 (B) and mass spectrum of product (C).

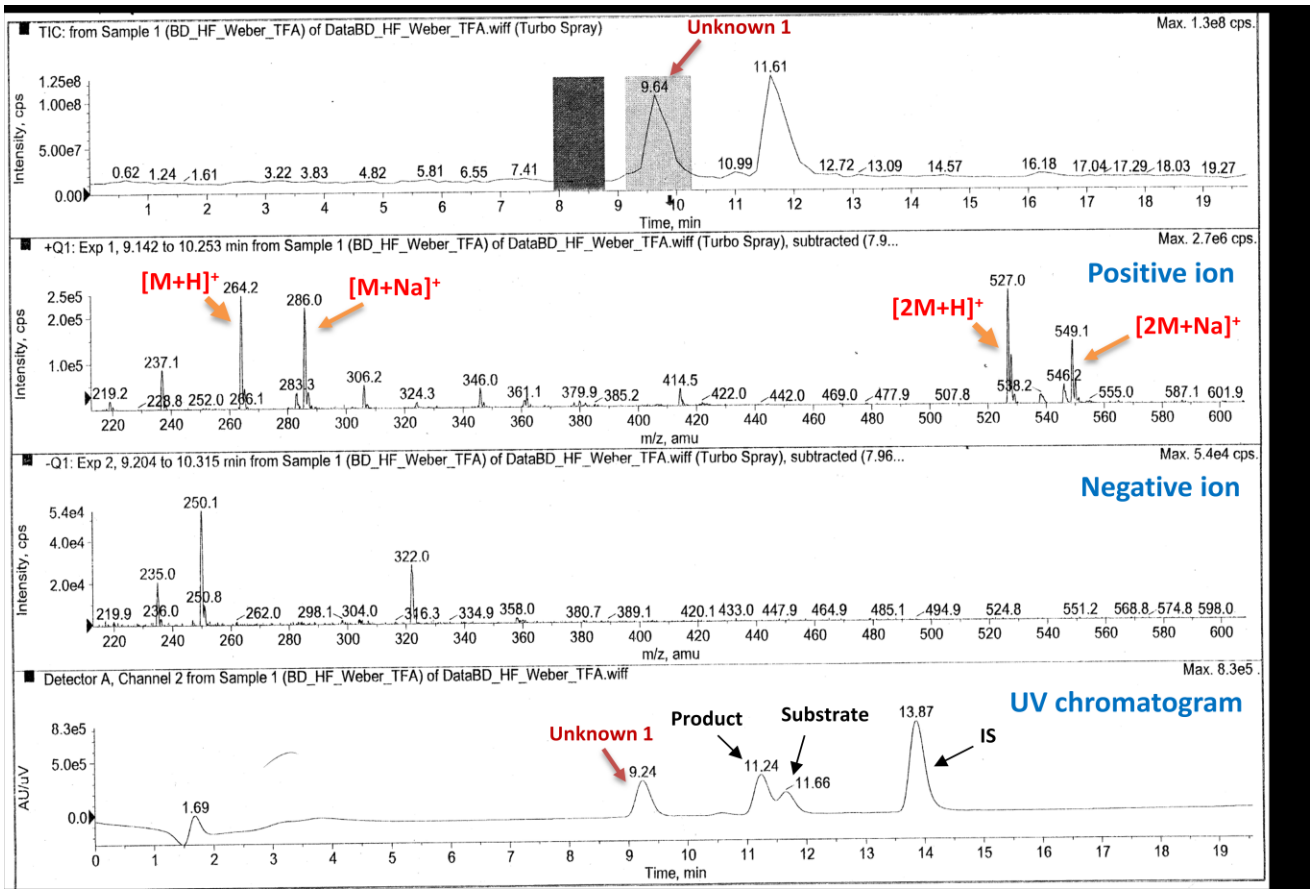

Figure 49. LC-MS studies of reaction sample catalyzed by trifluoroacetic acid.

The results of LC-MS analysis of reaction outcomes are shown in Figure 49. Positive ion spectrum shows the protonated molecular ion of Unknown 1 is 264 *m/z* and sodium plus ion is 286 *m/z*. The molecular weight of Unknown 1 should be just 263, similar to the GC-MS study. With the knowledge of its molecular weight and similar structure to the product, I deduct that Unknown 1 is a bicyclic acetamide that is quite similar to the product isobutylamide. The possible structure of Unknown 1 is shown in Scheme 5 and this side reaction probably follows the well-known Ritter process[13, 14] in which strong acids can decompose the product into benzylic cation intermediate that react with the solvent acetonitrile and transform into the acetamide with the addition of water. This side process happens only under the presence of

strong acids and may consume some products. However, in principle, it does not influence the cyclization reaction, so substrate conversion by strong acids is usually very good.

Scheme 5. Possible mechanism of Unknown 1 formation via the Ritter process.

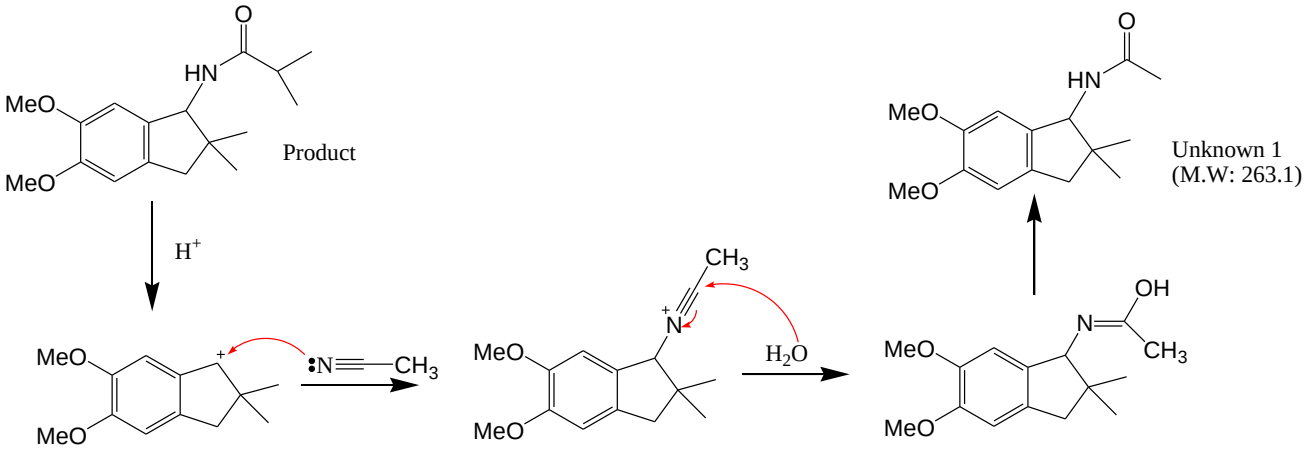

Unknown 2 is predominantly formed as weak acids are applied. Weak acids often lead to very low product yield and moderate substrate conversion. I first tried to use GC-MS to get the molecular weight and structure information of this byproduct; however, as shown in Figure 50, the substrate is not stable at high temperature and can decompose in GC column to form a large bump overlapping with a number of peaks in the GC chromatogram. The only identifiable peak is the isolated aldehyde byproduct whose mass spectrum and exact structure is shown in Figure 50. This known aldehyde byproduct largely comes from the thermal decomposition of the substrate. Thus, Unknown 2 is hardly identified by GC-MS when a large amount of substrate is present in the reaction solution. This is not a problem for the identification of Unknown 1 because when strong acids are applied, substrate can be totally depleted during the reaction and GC chromatogram is very clean without much interference from the substrate (Figure 48-A).

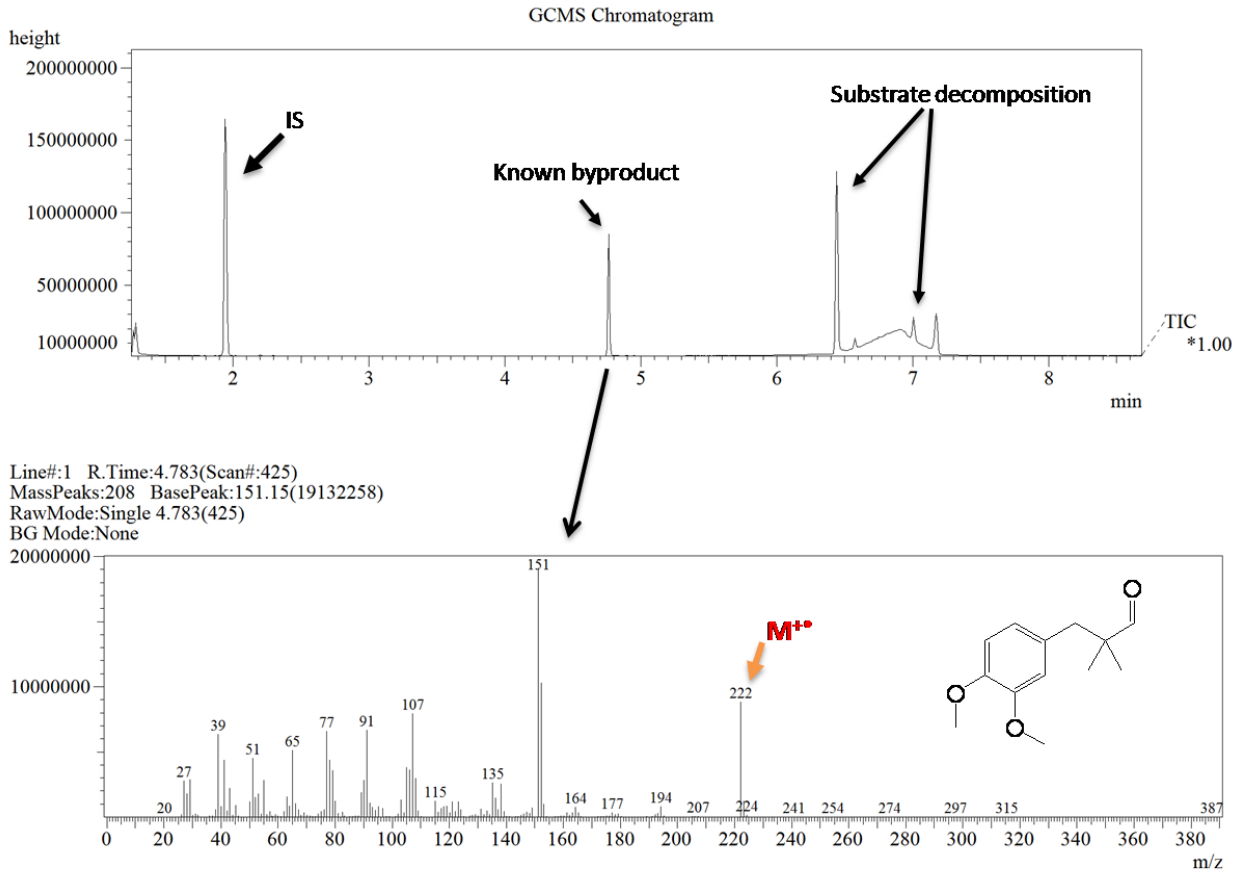

Figure 50. GC-MS studies of reaction sample catalyzed by trichloroacetic acid.

LC-MS is good to analyze reaction samples containing weak acid catalysts. In Figure 51, positive ion spectrum shows two fragment ion peaks corresponding to the molecular ion of Unknown 2 as 309 *m/z*. This byproduct is prone to lose a hydroxyl group during ionization, resulting in a major fragmentation ion of 292 *m/z*. From the negative ion spectrum, I can deduct the same molecular weight. Therefore, I hypothesize that Unknown 2 is unstable and prone to dehydrolyze. The possible mechanism to form Unknown 2 is shown in Scheme 6, in which water reacts with the acyliminium ion intermediate and lead to the formation of Unknown 2. This byproduct can also decompose into the known aldehyde byproduct. This side reaction is likely to consume a lot of acyliminium ion intermediates that can compromise the cyclization process

severely. When low concentrations of weak acids are used, the cyclization process becomes so slow that this side reaction becomes very prominent and lead to very low yield. Therefore, reaction solution has to be dried very well to minimize this side reaction, especially under the catalysis of weak acids.

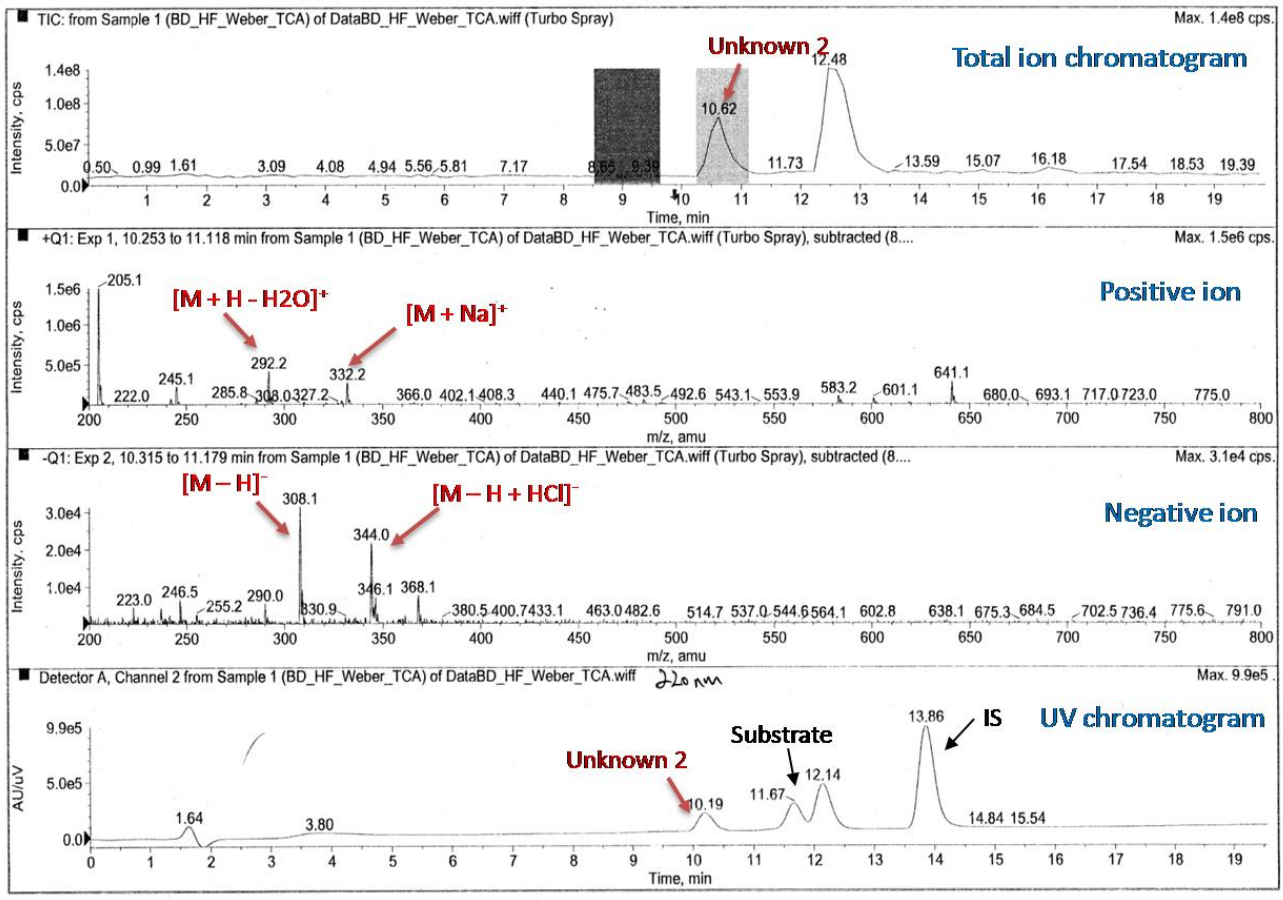

Figure 51. LC-MS studies of reaction sample catalyzed by trichloroacetic acid.

Scheme 6. Possible mechanism of Unknown 2 formation by hydration.

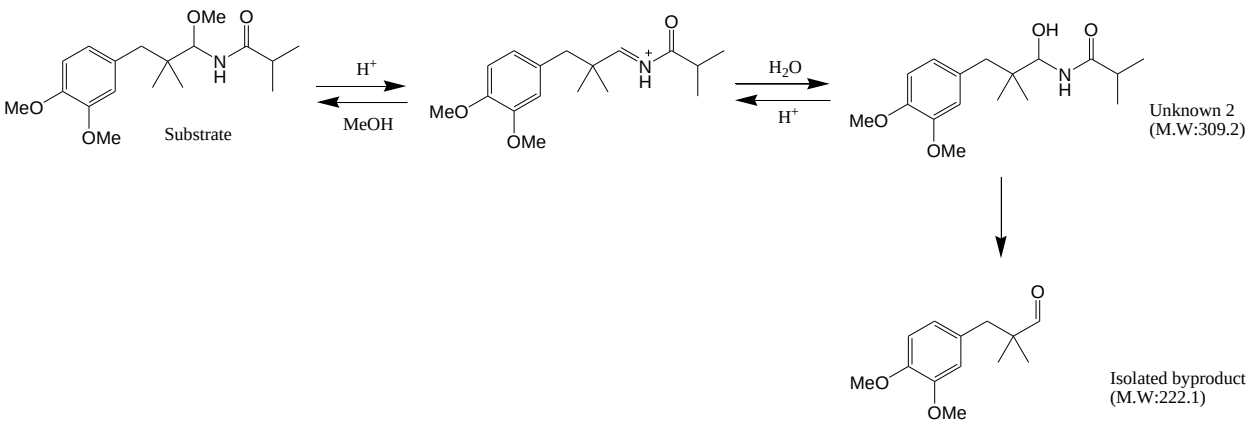

4.4 CONCLUSION

A new microreactor system integrated with UHPLC was constructed and evaluated by investigation of a novel acyliminium ion cyclization reaction. By integrating UHPLC to the microreactor, complex reaction samples can be rapidly analyzed with excellent resolution and reproducibility. The screening of acid catalysts was carried out in the microreactor in a continuous-flow, high throughput mode. Fifty four reactions were studied in a single run of 6 h which corresponds to a screening rate of nine reactions per hour. Yield and conversion determined by UHPLC showed that Lewis acids mediated reactions have better product selectivity than Brønsted acids, especially at relatively lower temperature. Among Lewis acids, lanthanide series compounds show best yield and selectivity at ambient temperature. The analysis of byproducts by GC-MS and LC-MS indicates that two different side reaction pathways probably exist and compete with the cyclization process. Water plays a key role in the formation of these byproducts. In principle, the removal of water can lessen side reactions and increase the yield and selectivity to certain extent.

BIBLIOGRAPHY

1. Yi, J. P.; Fan, Z. G.; Jiang, Z. W.; Li, W. S.; Zhou, X. P., High-throughput parallel reactor system for propylene oxidation catalyst investigation. *J. Comb. Chem.* **2007,** 9, 1053-1059.

2. Shi, G.; Hong, F.; Liang, Q.; Fang, H.; Nelson, S.; Weber, S. G., Capillary-based, serial-loading, parallel microreactor for catalyst screening. *Anal. Chem.* **2006,** 78, 1972-1979.

3. Anspach, J. A.; Maloney, T. D.; Colon, L. A., Ultrahigh-pressure liquid chromatography using a 1-mm id column packed with 1.5-micro m porous particles. *J. Sep. Sci.* **2007,** 30, 1207-1213.

4. Chesnut, S. M.; Salisbury, J. J., The role of UHPLC in pharmaceutical development. *J. Sep. Sci.* **2007,** 30, 1183-1190.

5. Dong, M. W., Ultrahigh-pressure LC in pharmaceutical analysis: performance and practical issues. *LCGC North Am.* **2007**, (Suppl.), 89-98.

6. Heinisch, S.; Desmet, G.; Clicq, D.; Rocca, J.-L., Kinetic plot equations for evaluating the real performance of the combined use of high temperature and ultra-high pressure in liquid chromatography. *J. Chromatogr., A* **2008,** 1203, 124-136.

7. Soliev, A.; Quiming, N. S.; Ohta, H.; Saito, Y.; Jinno, K., Separation of ginsenosides at elevated temperature by ultra high pressure liquid chromatography. *J. Liq. Chromatogr. Relat. Technol.* **2007,** 30, 2835-2849.

8. Wu, N.; Clausen, A.; Wright, L.; Vogel, K.; Bernardoni, F., Fast UHPLC using sub-2 micro m particles and elevated pressures for pharmaceutical process development. *Am. Pharm. Rev.* **2008,** 11, 24, 26, 28, 31-33.

9. Wu, N.; Liu, Y.; Lee, M. L., Sub-2micro m porous and nonporous particles for fast separation in reversed-phase high performance liquid chromatography. *J. Chromatogr., A* **2006,** 1131, 142-150.

10. Xiao, Q.; Floreancig, P. E., One-pot synthesis of bicyclic beta-Alkoxy amides from cyanohydrin ethers. *Org. Lett.* **2008,** 10, 1139-1142.

11. Probstein, R. F., *Physicochemical Hydrodynamics: An Introduction, 2nd Edition*. 2003; p 416.

12. Kobayashi, S.; Sugiura, M.; Kitagawa, H.; Lam, W. W. L., Rare-earth metal triflates in organic synthesis. *Chem. Rev.* **2002,** 102, 2227-2302.

13. Ritter, J. J.; Kalish, J., A new reaction of nitriles; synthesis of *t*-carbinamines. *J. Am. Chem. Soc.* **1948,** 70, 4048-50.

14. Ritter, J. J.; Minieri, P. P., A new reaction of nitriles; amides from alkenes and mononitriles. *J. Am. Chem. Soc.* **1948,** 70, 4045-8.

APPENDIX A

SAMPLING PROGRAM OF HPLC AUTOSAMPLER (HP1050) FOR CATALYST LOADING AND 6-PORT INJECTOR TRIGGERING

10 Utility Contact 1 off

20 Utility Contact 2 on // 6-port injector: switch to load position

30 Wait 0.01 min

40 Utility Contact 2 off

50 Utility Valve bypass

60 Eject max sample into seat at max speed // prepare sample loading

70 Draw 25 µL sample from vial at max speed // Sample withdrawal

80 Eject max sample into seat at speed 15 µL/min // Sample loading into 6-port injector, speed equal to the syringe pump for equal mixing with reagent.

90 Utility Contact 1 on // 6-port injector: switch to inject position

100 Wait 0.01 min

110 Utility Contact 1 off

120 Wait 3.0 min // 6-port injector: injection time into the microreactor

130 Utility Contact 2 on // 6-port injector: switch to load position

140 Wait 0.01 min

150 Utility Control 2 off

160 Utility Valve mainpass // washing pump to clean the autosampler

APPENDIX B

MICROREACTOR PARTS AND SPECIFICATIONS

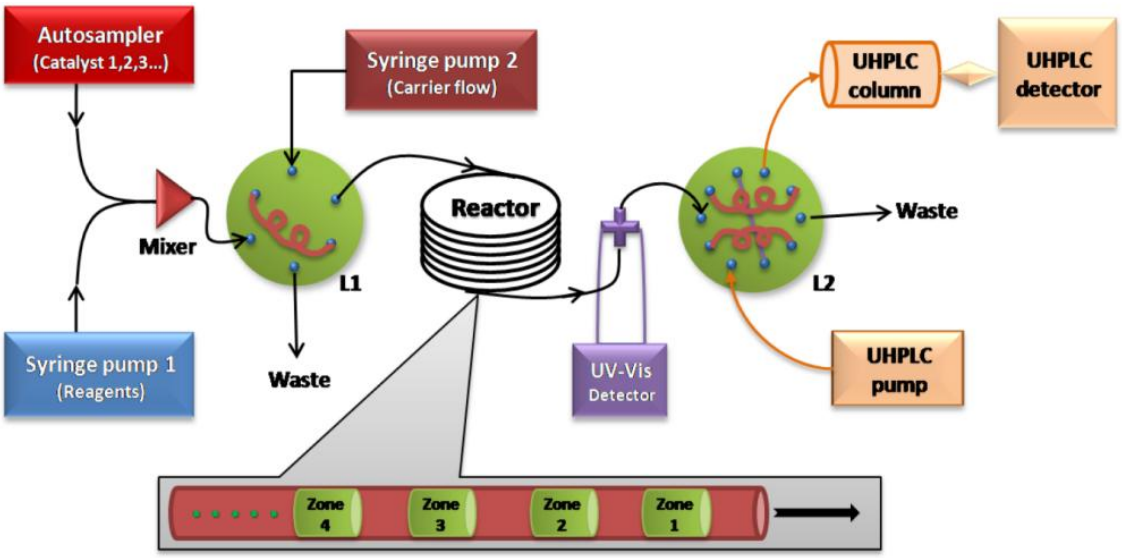

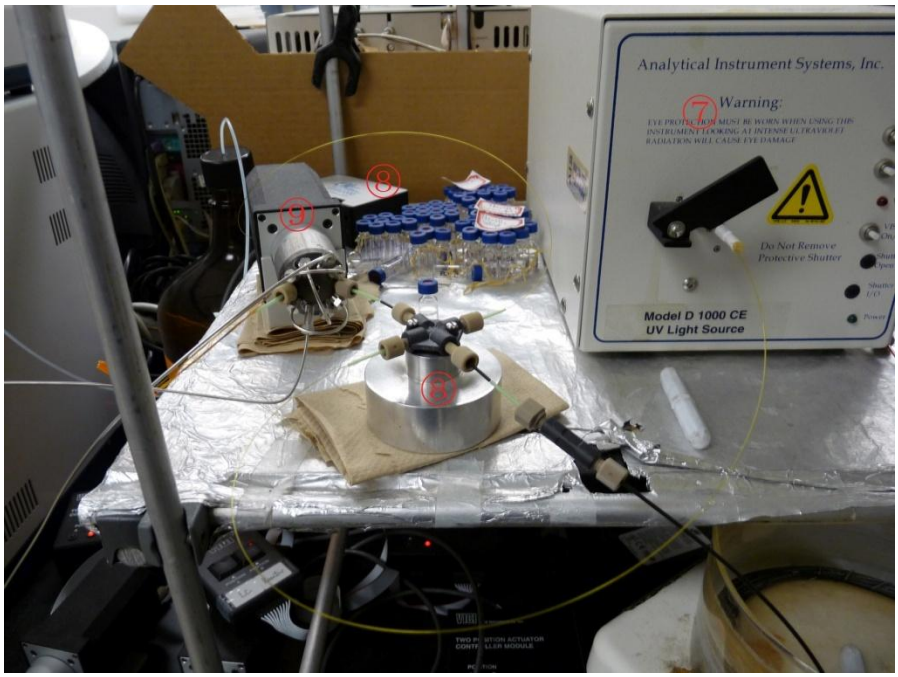

(1) Washing pump: clean the autosampler tubes and injection needle.

Waters 515 HPLC Pump (115-230 V), Isocratic pump, Pulse free solvent delivery, Flow rate range 0.001 to 10.000 mL/min.

(2) Autosampler: load catalysts from vials.

HP 1050 autosampler, 21-position sample tray, programmable, injection volumes 0.1 — 100 µl.

(3) 6-port microinjector: load and inject reaction samples into reaction capillary.

6 port valve – Model CN2, nanovolume - 5,000 psi - 1/32" Cheminert fittings, 0.10 mm ports (.004"). With standard electric actuator E60 (included in CN2-4346E): Standard two position electric actuators- 110 VAC. 60 degree, closeout.

(4) Syringe pump 2: deliver carrier flow (solvent) into the reactor capillary.

Harvard Pump 11 plus, standard infusion only, single syringe pump, flow rate 0.0014 µl/hr to 26.56 ml/min, syringe size 0.5 µL to 60 mL.

(5) Syringe pump 1: deliver carrier flow (solvent) into the reactor capillary.

Harvard Pump 11 plus, standard infusion only, single syringe pump, flow rate 0.0014 μl/hr to 26.56 ml/min, syringe size 0.5 μL to 60 mL.

(6) Reactor capillary: immersed into a water batch on a heating plate.

Teflon FEP tubing, 100 μm i.d., 1/16" o.d.

(7) UV-Vis light source: emit UV light to the flow cell (cross) via a fiber optic

DT-1000, dual fiber optic UV/Vis Source, wavelength range 190 to 850 nm

(8) Fiber optic UV-Vis detector: detect UV response of reaction zones

USB2000 Plug-and-Play Miniature Fiber Optic Spectrometer; Computer interface: USB-to-PC; Detector: 2048-element linear silicon CCD array; Wavelength range: 200-1100 nm.

(9) 10-port microinjector: load and inject reaction zones into UHPLC.

UHPLC 10-port 15,000 psi nanobore valve – Model C72X - 1/16" Valco fittings, 0.15 mm ports (.006"). With microelectric actuator EH (included in C72X-6694EH), two position, high speed.

(10) UHPLC: analyze reaction products.

Jasco X-LC (15,000 psi), dual wavelength UV-Vis detector (190 nm— 650 nm).

APPENDIX C

The aldol product:4-Hydroxy-4-phenyl-butan-2-one (^{1}H NMR 300 MHz, $CDCl_3$)

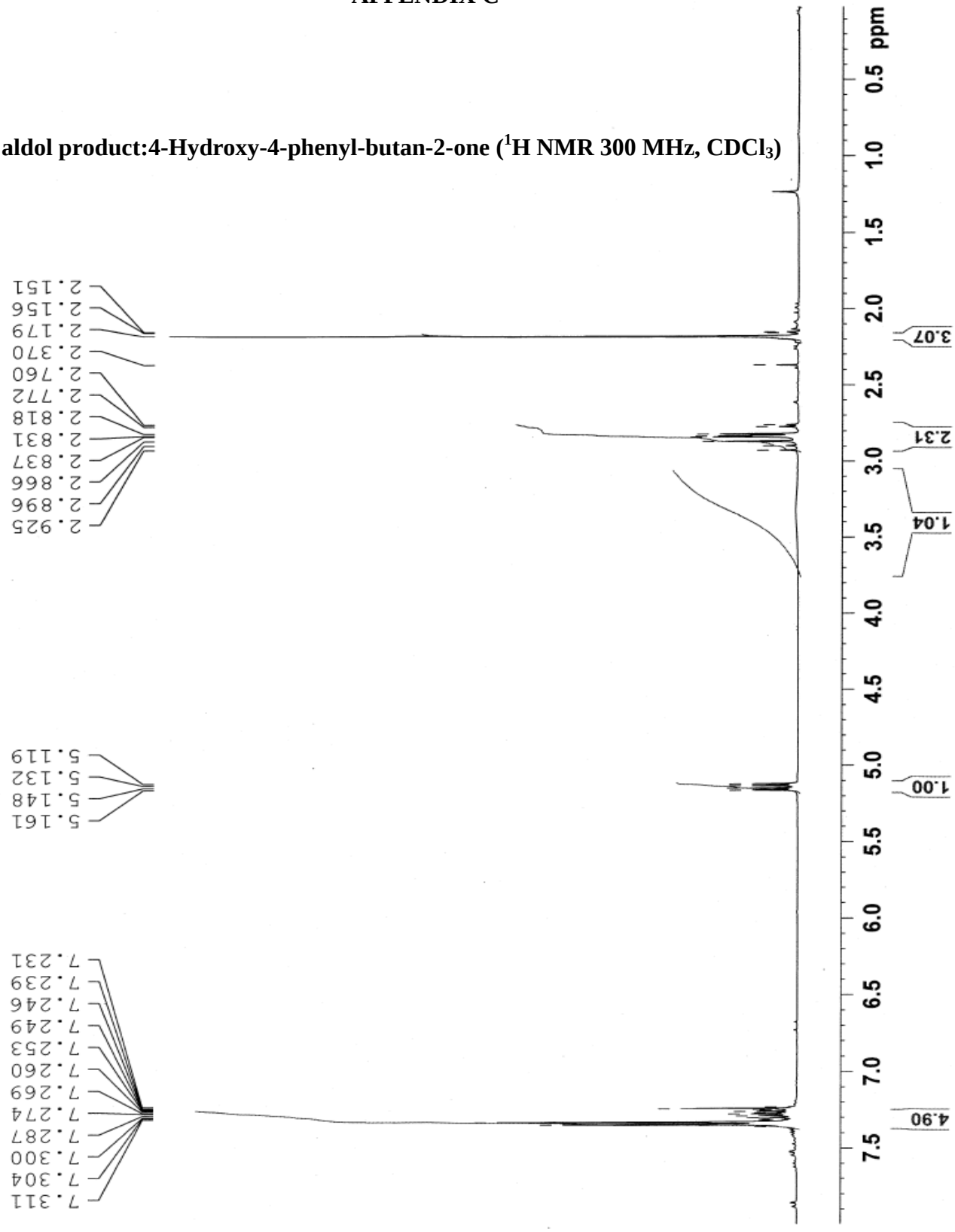

The aldol product: 4-Hydroxy-4-(4'-nitrophenyl)-butan-2-one (^{1}H NMR 300 MHz, $CDCl_3$)